

AD-A188 873

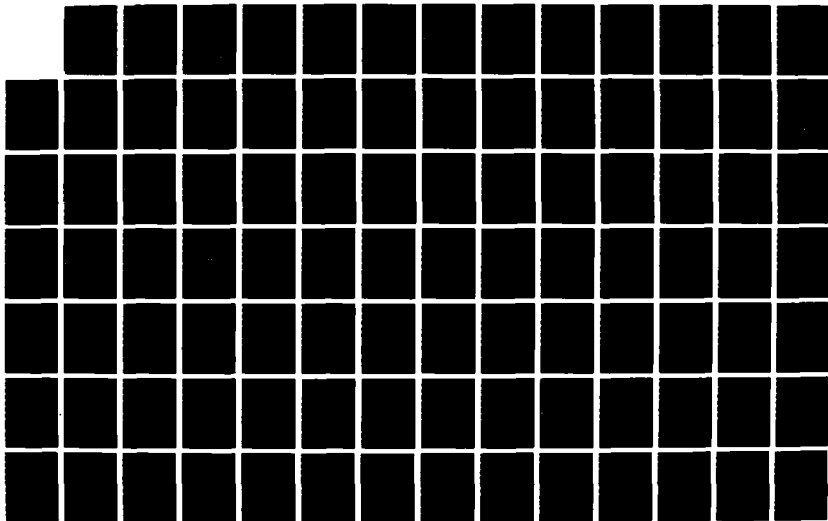
REALTIME PILOT MODEL PARAMETER IDENTIFICATION(U) AIR  
FORCE INST OF TECH WRIGHT-PATTERSON AFB OH  
H R ROSENBLEETH DEC 87 AFIT/GAE/AA/87D-19

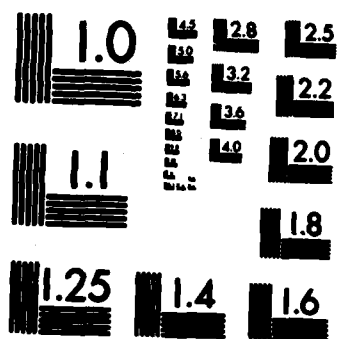
1/2

UNCLASSIFIED

F/G 1/3.3

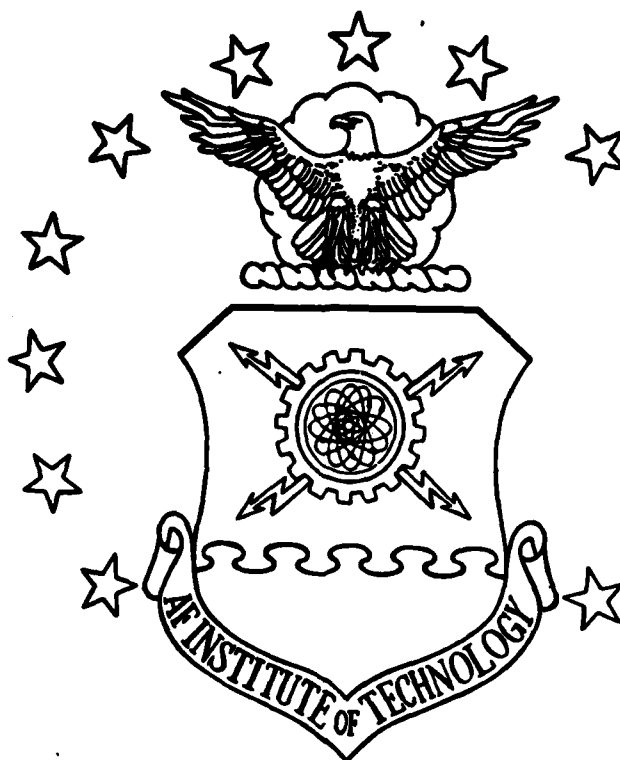
ML





MICROCOPY RESOLUTION TEST CHART  
NATIONAL BUREAU OF STANDARDS-1963-A

AD-A188 873



DTIC FILE COPY

DTIC  
ELECTE  
FEB 03 1988  
S H D

REALTIME PILOT MODEL PARAMETER  
IDENTIFICATION  
THESIS

Michael J. Rosenbleeth  
Captain, USAF  
AFIT/GAE/AA/87D-19

DEPARTMENT OF THE AIR FORCE  
AIR UNIVERSITY  
**AIR FORCE INSTITUTE OF TECHNOLOGY**

Wright-Patterson Air Force Base, Ohio

**DISTRIBUTION STATEMENT A**

Approved for public release;  
Distribution Unlimited

88 2 03 060

1

**REALTIME PILOT MODEL PARAMETER  
IDENTIFICATION**

**THESIS**

**Michael J. Rosenbleeth  
Captain, USAF  
AFIT/GAE/AA/87D-19**

**DTIC  
ELECTE  
FEB 08 1988  
S a H D**

**DISTRIBUTION STATEMENT A**

**Approved for public release;  
Distribution Unlimited**

REALTIME PILOT MODEL PARAMETER IDENTIFICATION

THESIS

Presented to the Faculty of the School of Engineering  
of the Air Force Institute of Technology

Air University

In Partial Fulfillment of the  
Requirements for the Degree of  
Master of Science in Aeronautical Engineering

Michael J. Rosenbleeth, B.S.  
Captain, USAF

December 1987

76  
COPY  
INFORMATION

Accession For	
NTIS GRA&I	<input checked="checked" type="checkbox"/>
DTIC TAB	<input type="checkbox"/>
Unannounced	<input type="checkbox"/>
Justification	
By	
Distribution/	
Availability Codes	
Dist	Avail and/or Special
A-1	

## Preface

This report summarizes the work I did in identification of pilot model parameters using the Recursive Least Squares algorithm. It is my sincere hope that the results of this investigation will contribute to the understanding and future study of the realtime identification of pilot model parameters.

I would like to thank my advisor, Major Daniel Gleason, for his contributions to this work. Major Gleason's guidance and many hours of help are greatly appreciated.

I would like to give special thanks to my wife, Kathy, whose sacrifice made this thesis possible.

Michael J. Rosenbleeth

## Table of Contents

	<u>Page</u>
Preface . . . . .	ii
List of Figures . . . . .	v
List of Tables . . . . .	viii
List of Symbols . . . . .	ix
Abstract . . . . .	xi
I. Introduction . . . . .	1
Background . . . . .	1
Problem . . . . .	2
Objectives . . . . .	3
Approach . . . . .	4
II. Technical Background . . . . .	6
Data Acquisition . . . . .	6
The Pilot Model . . . . .	14
Time Delay . . . . .	18
Discretization Techniques . . . . .	20
Least Squares . . . . .	23
Neal-Smith Theory . . . . .	27
III. Closed Loop Simulation . . . . .	32
Characteristics of the RLS Algorithm . . . . .	32
Optimum Pilot Model . . . . .	38
Discretization of Pilot Model with Time Delay . . . . .	42
Discretization of the F-15 Model Using the Matrix Exponential Function . . . . .	47

	<u>Page</u>
Digital Simulation . . . . .	48
Identification of Pilot Model Parameters. .	49
IV.    Discretization of Pilot Models . . . . .	51
Discretization of Pilot Model 2 . . . . .	77
Discretization of Pilot Model 4 . . . . .	80
V.    Neal Smith Theory . . . . .	94
VI.   Identification . . . . .	98
Analysis . . . . .	98
Identifications . . . . .	101
Discussion of Results . . . . .	120
Pilot Comments . . . . .	122
VII.  Conclusions and Recommendations . . . . .	124
Conclusions . . . . .	124
Recommendations . . . . .	124
Appendix A . . . . .	126
Appendix B . . . . .	152
Vita . . . . .	162



## List of Figures

<u>Figure</u>	<u>Page</u>
1. Target Light Configuration . . . . .	7
2. Cooper-Harper Rating Scale . . . . .	10
3. Head-Up-Display (HUD) . . . . .	12
4. Pipper Symbology . . . . .	13
5. Closed Loop System . . . . .	16
6. Neal-Smith Standard of Performance . . . . .	28
7. Nichols Chart with Performance Standards Defined . . . . .	31
8. Closed-Loop System with Error Bias and Pilot Remnant Included . . . . .	33
9. Discretized Command Input . . . . .	35
10. Nichols Chart for Optimum Pilot/ Aircraft System . . . . .	43
11. Bode Plot for Optimum Pilot/ Aircraft System . . . . .	44
12. Bode Plot for Optimal $G_{P_1}$ (no time delay) . . . . .	54
13. Bode Plot for Optimal $G_{P_2}$ (numerator time delay) . . . . .	55
14. Bode Plot for Optimal $G_{P_3}$ (denominator time delay) . . . . .	56
15. Bode Plot for Optimal $G_{P_4}$ (Padé approximation to time delay) . . . . .	57

<u>Figure</u>	<u>Page</u>
16. Step Response of Optimal $G_{P_1}(S)/$ Aircraft System (continuous) . . . . .	60
17. Step Response of Optimal $G_{P_1}(Z)/$ Aircraft System (Discretized by the backward rectangular rule) . . . . .	61
18. Step Response of Optimal $G_{P_1}(Z)/$ Aircraft System (discretized by Tustin's bilinear rule) . . . . .	62
19. Step Response of Optimal $G_{P_1}(Z)/$ Aircraft System (zero-order hold approximation) . . . . .	63
20. Step Response of Optimal $G_{P_2}(S)/$ Aircraft System (continuous) . . . . .	64
21. Step Response of Optimal $G_{P_2}(Z)/$ Aircraft System (discretized by the backward rectangular rule) . . . . .	65
22. Step Response of Optimal $G_{P_2}(Z)/$ Aircraft system (discretized by Tustin's bilinear rule) . . . . .	66
23. Step Response of Optimal $G_{P_2}(Z)/$ Aircraft System (zero-order hold approximation) . . . . .	67
24. Step Response of Optimal $G_{P_4}(S)/$ Aircraft System (continuous) . . . . .	68

<b>Figure</b>	<b>Page</b>
25. Step Response of Optimal $G_{P_4}(z)/$ Aircraft System (discretized by the backward rectangular rule) . . . . .	69
26. Step Response of Optimal $G_{P_4}(z)/$ Aircraft System (discretized by Tustin's bilinear rule) . . . . .	70
27. Step Response of Optimal $G_{P_2}(z)/$ Aircraft System (zero-order hold approximation) . . . . .	71
28. Nichols Chart for Bandwidth of 2.5 radians per second . . . . .	95
29. Nichols Chart for Bandwidth of 3.0 radians per second . . . . .	96
30. Target Light Configuration . . . . .	99
31. Longitudinal Control Stick Deflection Run 1 . . . . .	103
32. Longitudinal Pipper Error Run 1 . . . . .	104
33. Longitudinal Control Stick Deflection Run 2 . . . . .	105
34. Longitudinal Pipper Error Run 2 . . . . .	106
35. Longitudinal Control Stick Deflection Run 4 . . . . .	107
36. Longitudinal Pipper Error Run 4 . . . . .	108
37. Longitudinal Control Stick Deflection Run 5 . . . . .	109
38. Longitudinal Pipper Error Run 5 . . . . .	110

## List of Tables

<u>Table</u>	<u>Page</u>
Table 1. Pipper Symbology . . . . .	12
Table 2. Closed Loop Pilot Model Parameters Identified . . . . .	37
Table 3. Optimum Pilot Models Calculated Over a Range of Bandwidth Criterion . . . . .	97
Table 4. Description of Test Runs . . . . .	98
Table 5. Pilot Model Parameters Identified for Run 1 and Run 4 (Segment 1) . . . . .	110
Table 6. Pilot Model Parameters Identified for Run 1 and Run 4 (Segment 2) . . . . .	111
Table 7. Pilot Model Parameters Identified for Run 1 and Run 4 (Segment 3) . . . . .	112
Table 8. Pilot Model Parameters Identified for Run 2 and Run 5 (Segment 1) . . . . .	113
Table 9. Pilot Model Parameters Identified for Run 2 and Run 5 (Segment 2) . . . . .	114
Table 10. Pilot Model Parameters Identified for Run 2 and Run 5 (Segment 3) . . . . .	115
Table 11. Pilot Model Parameters Identified Using Model 2 for Run 1 and Run 2 . . . . .	116
Table 12. Pilot Model Parameters Identified Using Model 3 for Run 1 . . . . .	117
Table 13. Pilot Model Parameters Identified Using Pilot Model 3 for Run 2 . . . . .	118

# List of Symbols

<u>Symbol</u>		<u>Units</u>
$\delta$	longitudinal stick deflection	in
$e$	longitudinal pipper error	milli-radian
$K_p$	pilot gain	in
$\tau_1$	pilot lead	1/S
$\tau_2$	pilot lag	1/S
$\tau_3$	pilot delay	1/S
$S$	Laplace operator	S
$G(S)$	pilot transfer function	in/milli-rad
$\delta_r$	pilot remnant	in
$G_1(S)$	pilot transfer function no time delay	in/milli-rad
$G_2(S)$	pilot transfer function numerator time delay	in/milli-rad
$G_3(S)$	pilot transfer function denominator time delay	in/milli-rad
$G_4(S)$	pilot transfer function Pade time delay	in/milli-rad
$Z$	Z-transform operator	-
$T$	sampling frequency	S
$H_{ho}(Z)$	zero order representation of discrete transfer function	-
$H(S)$	continuous transfer function	-
$G(Z)$	discretized pilot model	in/milli-rad
$N_1$	numerator coefficient of discretized transfer function	in/milli-rad

$d_1$	denominator coefficient of discretized transfer function	-
$m$	order of numerator (discretized transfer function)	-
$n$	order of denominator (discretized transfer function)	-
$\theta$	vector of coefficients of discrete transfer functions	-
$X$	matrix of input and output data	
$Y$	vector of output data	in
$\alpha$	angle of attack	deg.
$\theta$	pitch angle	deg.
$\theta_c$	pitch command input	deg.
$B$	simulated noise signal	deg.
$\delta_p$	output of pilot model	in
$\omega$	frequency	rad/sec
$\theta_e$	pitch input error	deg

Abstract

↘ An air to ground test technique was simulated on the Flight Dynamics Laboratory's LAMARS simulation system. Data was recorded on longitudinal stick deflection and longitudinal pipper errors. The data was used to identify pilot model parameters using the Recursive Least Squares (RLS) Algorithm. Several different pilot models and discretization techniques are used to determine which method is best suited to this task. Neal-Smith Theory is used to predict a range of pilot model parameters to be expected from RLS identification. Pilot model parameters are identified using three aircraft with different time delays. The identified pilot model parameters and pilot ratings are compared to see if a correlation exist. The specific values of pilot model parameters predicted by Neal-Smith Theory were not identified. However, trends in the pilot model parameters predicted by Neal-Smith Theory, for aircraft of increasing time delay, can be observed in the identifications. (Theses).

# REALTIME PILOT MODEL PARAMETER IDENTIFICATION

## I. Introduction

### Background

During the months of March and April 1987, a joint simulation was conducted by the German Flight Test Organization (DFVLR) and the Air Force Wright Aeronautical Laboratory, Flight Dynamics Laboratory, Flight Controls Division (AFWAL/FIG). The objectives of the joint program were to introduce the flying qualities personnel and simulation personnel to a flight test method for pilot/aircraft analysis [1]. The method was simulated on the Large Amplitude Multimode Aerospace Research Simulator System (LAMARS). The objective of the testing was to analyze the pilot/aircraft system in the ground attack mode. The testing technique employed by DFVLR uses the Ground Attack Test Equipment (GRATE). The GRATE system is a series of lights placed in a pattern on the ground to serve as targets. In the ground attack mode the pilot must continuously align the target sight in his head-up-display (HUD) with the target on the ground. The lights are switched forcing the pilot to react to pipper errors in his HUD. The light switching and realignment action by the pilot excites the pilot/aircraft system over



the wide range of frequencies necessary for system identification. The terrain board was modified with lights similar to the ones used by DFVLR in flight testing for the purpose of conducting a simulation to determine the system's suitability for the analysis of flying qualities. Two aircraft were used in the simulation. Both DFVLR and AFWAL/FIGC provided an aircraft model and a test pilot for the simulation. Both aircraft models were linearized transfer function models. The German model was called Aircraft A and had dynamics similar to a German Alpha-Jet. The model provided by the flying qualities group (AFWAL/FIGC) was called Aircraft B and had dynamics similar to an F-15. Both aircraft models and light bank software were integrated into the LAMARS Simulation System by the author. Test runs were flown at the target lights by each pilot in each aircraft. Simulation variables and pilot ratings were recorded for each run. Pilot comments were recorded and pilot ratings were given using the Cooper-Harper rating scale [2].

### Problem

The problem is to identify a transfer function model of human pilot dynamics. A simplification of the Neal-Smith pilot model will be used. The parameters to be identified are the pilot gain, lead, lag and time delay. In order to identify a transfer function you must have

recorded time histories of the input and output of the transfer function. The data collected in the joint AFWAL/DFVLR simulation is suitable for this purpose. Of particular interest to the identification of pilot model parameters are the recorded time histories of control stick deflection (output) and pipper errors (input). A Recursive Least Squares (RLS) algorithm can be used to identify pilot model parameters from the recorded time histories of control stick deflection and pipper errors. The more pilot compensation that is required the worse the Cooper-Harper ratings should become. Once the pilot model parameters are identified they will be compared to Cooper-Harper ratings to see if a correlation exists. A correlation with Cooper-Harper ratings would serve as validation that the pilot model parameters identified by (RLS) are accurate.

### Objectives

The objectives of this research are to: 1) assess the ability of the recursive least squares algorithm (RLS) to identify pilot model parameters from operating records obtained from the joint AFWAL/DFVLR simulation. 2) Provide a test of the sensitivity of the established (RLS) algorithm to noise, strategy changes, biases and reduced order models. 3) Analyze the effects of loop-closures and time delays and assess the value of

continued research using operating records from flight test experiments. 4) To determine if it is feasible to identify pilot delay as well as pilot lead, lag and gain. It is also an objective of this research to determine the best method of discretization for the task of identifying pilot model parameters.

#### Approach

In order to become familiar with the operation of the RLS algorithm and to be able to apply it with confidence to a model of unknown form, it will first be applied to data generated synthetically. An open-loop simulation will be performed to generate synthetic data from a pilot model with known parameters. Once comfortable with identification in the open loop case an aircraft model will be placed in series with pilot and the pilot will close the loop. Identification will then be accomplished for the closed loop case. Biased error signals and pilot remnants are then added to the simulation and the identification repeated. The results are compared to the results of the uncorrupted data to assess their effects on the identification.

Neal-Smith Theory can be used to determine a pilot model for a given aircraft and bandwidth criterion that meets specified standards of performance. The pilot model parameters predicted by Neal-Smith Theory is highly

dependent on the selection of a bandwidth criteria. Pilot model parameters will be calculated for a number of bandwidths to determine a range of pilot model parameters to be expected from identification of the operating records obtained in simulation.

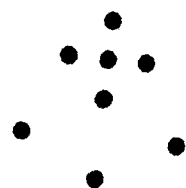
In examining the pilot models it was found that there are several methods to approximate the pilot time delay. Four different methods for the approximation of the pilot time delay are used and the results are compared. Several different methods are available for the discretization of the pilot models. Four methods were used. They are the forward rectangular rule, backward rectangular rule, Tustin's bilinear rule, and the zero order hold approximation. Each method to approximate the time delay is used giving four different pilot models to be investigated. Each pilot model is discretized using all four methods for discretization yielding 16 separate representations. These will be compared to see which yields the most accurate results.

All identifications will be done using the batch least squares and the recursive least squares features of  $MATRIX_x$ . Pilot model parameters identified by  $MATRIX_x$  will be compared to the pilot comments and Cooper-Harper ratings obtained during simulation to see if a correlation exists.

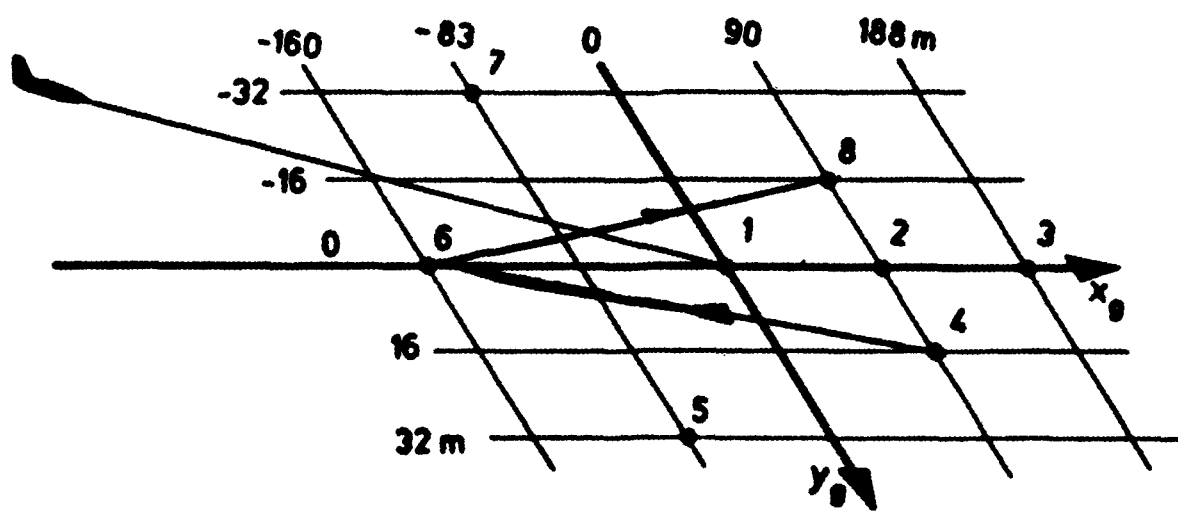
## II. Technical Background

### Data Acquisition

To use the RLS algorithm to identify a transfer function it is necessary to have time histories of the input and output of the transfer function. This work attempts to identify a transfer function of the human pilot from time histories of his input and output obtained from a realtime pilot-in-the-loop simulation. The task simulated was ground attack. The ground attack task was simulated by an array of lights situated in a 8-pin pattern on the ground. The array of lights is shown in Figure 1. The lights are numbered from one to eight. The arrow in Figure 1 indicates the switching of the lights. In order to obtain an accurate identification of a transfer function, the transfer function must be persistently excited over a wide range of frequencies. This is a well known fact from system identification theory. This persistent excitation is accomplished by the array of lights. When in ground attack, the the test pilot attempts to align the pipper in his Head Up Display (HUD) with the lamp that is currently illuminated. In other words, the pilot attempts to minimize pipper errors. After a specified period of time the lamp which is currently illuminated is turned off and another lamp is



View of Ground Targets  
from the Cockpit



Target Light Configuration  
Figure 1

turned on. This serves as a step input in pipper error to the pilot aircraft system. The lights are switched at specified intervals in order to obtain the persistent excitation over a wide range of frequencies required for identification. For identification of the human pilot model, the input is the longitudinal pipper error and the output is the longitudinal stick deflection. Both variables were recorded during the realtime simulations and will be used for this purpose.

Much work was done by the author in preparing the simulation for use at the Flight Dynamics Lab, Flight Controls Division, Simulation Integration Branch, LAMARS Simulation Facility. For the purpose of identification of pilot model parameters it is necessary to have accurate time histories of the input (pipper errors) and output (stick deflections). However, so that the reader will better understand how the data was collected I will present an overview of the simulation. Two areas that are of particular interest to the collection of data for the purpose of identification of pilot model parameters are the HUD and the aircraft model.

The aircraft model used in the simulation was a fighter aircraft with dynamics similar to that of the F-15. The transfer functions for the longitudinal short period dynamics are as follows:

$$\frac{\theta(s)}{\delta(s)} = \frac{.60 (1.585s + 1.896)}{s(s^2 + 4.2s + 9.0)} \quad (1)$$

$$\frac{\alpha(s)}{\delta(s)} = \frac{.46 (.043s + 1.935)}{(s^2 + 4.2s + 9.0)} \quad (2)$$

It is generally recognized that an aircraft will receive progressively lower pilot ratings as its response to pilot input is delayed. To simulate aircraft of different flying qualities a time delay was used. The transfer functions for the time delays were developed by cascading a first order Padé approximation. The Padé approximation for the time delay is given as

$$e^{-TS} \approx \frac{1 - (T/2)s}{1 + (T/2)s} \quad (3)$$

The Padé approximations for different time delays are given as follows:

$$T = 100 \text{ ms} \rightarrow e^{-TS} \approx - \frac{(s-20)}{(s+20)} \quad (4)$$

$$T = 200 \text{ ms} \rightarrow e^{-TS} \approx - \frac{(s-10)}{(s+10)} \quad (5)$$

$$T = 300 \text{ ms} \rightarrow e^{-TS} \approx - \frac{(s-6.67)}{(s+6.67)} \quad (6)$$

Equations 1 and 2 were multiplied by Equations 4, 5 and 6. These equations together with the undelayed equations give four different aircraft to be evaluated. During testing the pilot was asked to fly each aircraft in the ground attack task. During each run, pipper errors and stick deflections were recorded. At the end of several



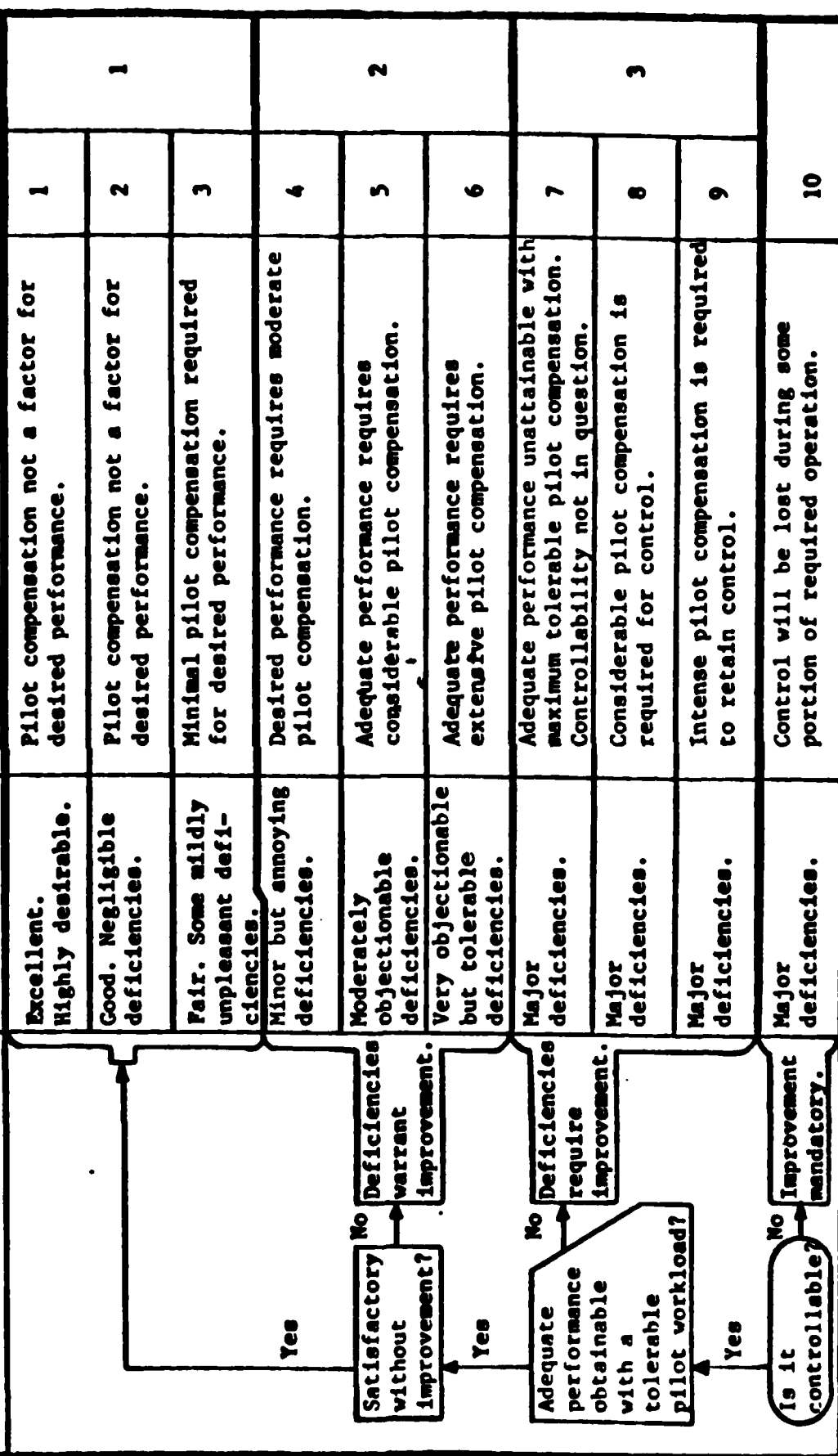
ADEQUACY FOR SELECTED TASK OR REQUIRED OPERATION	AIRCRAFT CHARACTERISTICS	DEMANDS ON THE PILOT IN SELECTED TASK OR REQUIRED OPERATION	PILOT RATING	FLYING QUALITY LEVELS
 <pre> graph TD     Start([Start]) --&gt; Q1{Satisfactory without improvement?}     Q1 -- Yes --&gt; R1[1]     Q1 -- No --&gt; Q2{Deficiencies warrant improvement?}     Q2 -- Yes --&gt; R2[2]     Q2 -- No --&gt; Q3{Adequate performance obtainable with a tolerable pilot workload?}     Q3 -- Yes --&gt; R3[3]     Q3 -- No --&gt; Q4{Deficiencies require improvement?}     Q4 -- Yes --&gt; R4[4]     Q4 -- No --&gt; Q5{Is it controllable?}     Q5 -- Yes --&gt; R5[5]     Q5 -- No --&gt; R6[6] </pre>	Excellent. Highly desirable.	Pilot compensation not a factor for desired performance.	1	1
	Good. Negligible deficiencies.	Pilot compensation not a factor for desired performance.	2	
	Fair. Some mildly unpleasant deficiencies.	Minimal pilot compensation required for desired performance.	3	
	Minor but annoying deficiencies.	Desired performance requires moderate pilot compensation.	4	2
	Moderately objectionable deficiencies.	Adequate performance requires considerable pilot compensation.	5	
	Very objectionable but tolerable deficiencies.	Adequate performance requires extensive pilot compensation.	6	
	Major deficiencies.	Adequate performance unattainable with maximum tolerable pilot compensation. Controllability not in question.	7	3
	Major deficiencies.	Considerable pilot compensation is required for control.	8	
	Major deficiencies.	Intense pilot compensation is required to retain control.	9	
	Major deficiencies.	Control will be lost during some portion of required operation.	10	

Figure 2 Cooper-Harper Pilot Opinion Rating Scale

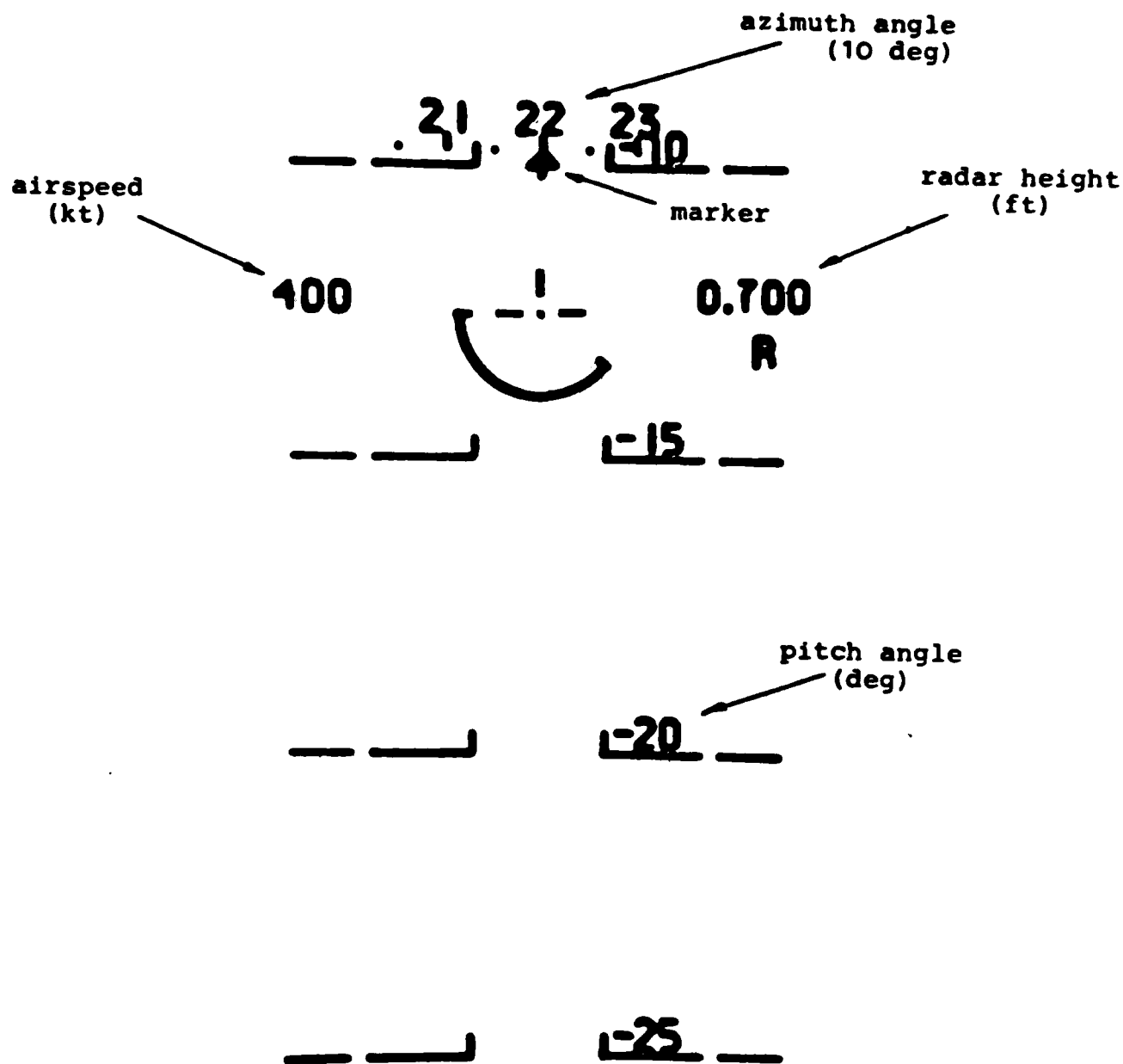
runs for which the pilot flew the same aircraft he was asked to evaluate it. The evaluations were made using the Cooper-Harper rating scale (Figure 2). In all, 71 runs were made and time histories and pilot comments were recorded.

The HUD used in the simulation is representative of the HUD used in the German Alpha-Jet (Figure 3). The major components of the display are airspeed, azimuth angle, radar height, and pitch angle. Of particular importance to the ground attack task is the pipper centered between the -10 degree and -15 degree pitch markings. The pipper symbol changes depending upon which stage of the attack you are in. The appearance of the pipper during each stage of the attack is shown in Figure 4. The symbols are displayed as follows shown in Table 1.

Symbol 1	in distance ( $X > 1900\text{m}$ )
Symbol 2	in range ( $X=1900\text{m}$ )
Symbol 3	in firing range ( $X=1750\text{m}$ )
Symbol 4	at the end ( $X=750\text{m}$ )
	the cross flashes on/off every 1/3 sec.

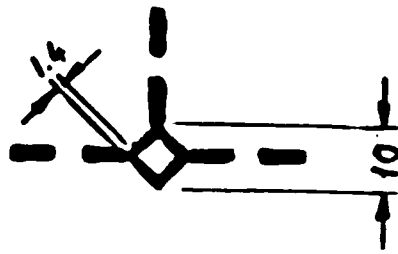
#### Pipper Symbolology

Table 1

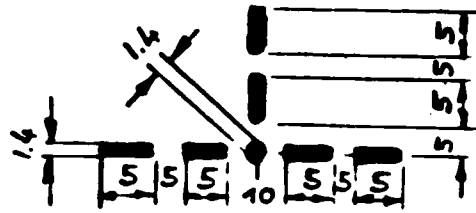


Head Up Display

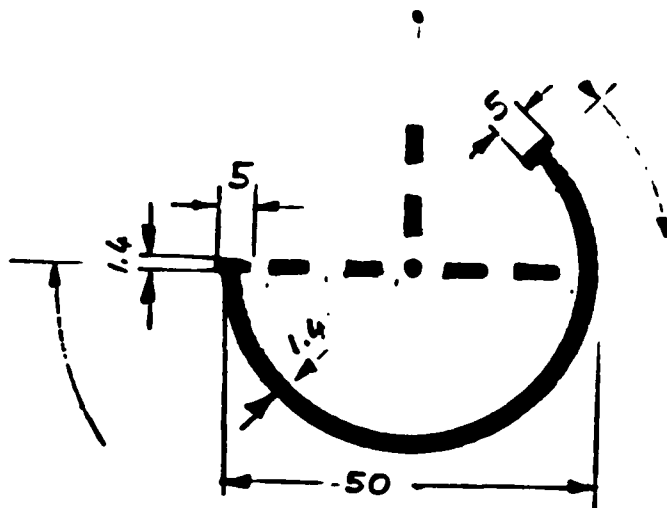
Figure 3



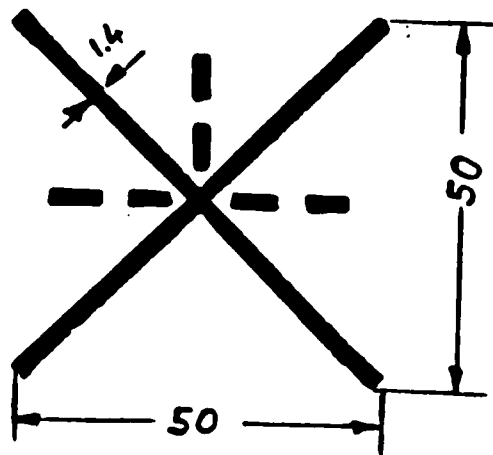
Symbol 1



Symbol 2



Symbol 3



Symbol 4

Pipper Symbolology  
Figure 4

The pipper is fixed in the lateral direction, however, it may move in the longitudinal direction. Two effects are taken into account when calculating the longitudinal pipper location. The first effect is caused by a change in target location in the HUD as the aircraft approaches it on a fixed trajectory. This effect is called trajectory shift and is readily calculated from the geometry of the attack. A second but less significant effect is the effect of drag and gravity on the bullets. This effect is called gravity drop. Even though these effects were taken into account, the pipper usually remained in the upper half of the HUD and did not move more than approximately 75 milli-radians.

All data collected during the simulation effort was stored in standard AFWAL/FIGD binary format. It was required to convert the data to ASCII format and put in a form that can be loaded into MATRIX<sub>x</sub>.

#### The Pilot Model

The pilot model under study is a simplification of the classical Neal-Smith model. The basic definitions of the pilot model parameters are:

$$G(s) = \frac{\delta(s)}{e(s)} = K_p \exp^{-\tau_3 s} \frac{\tau_1 s + 1}{\tau_2 s + 1} \quad (7)$$

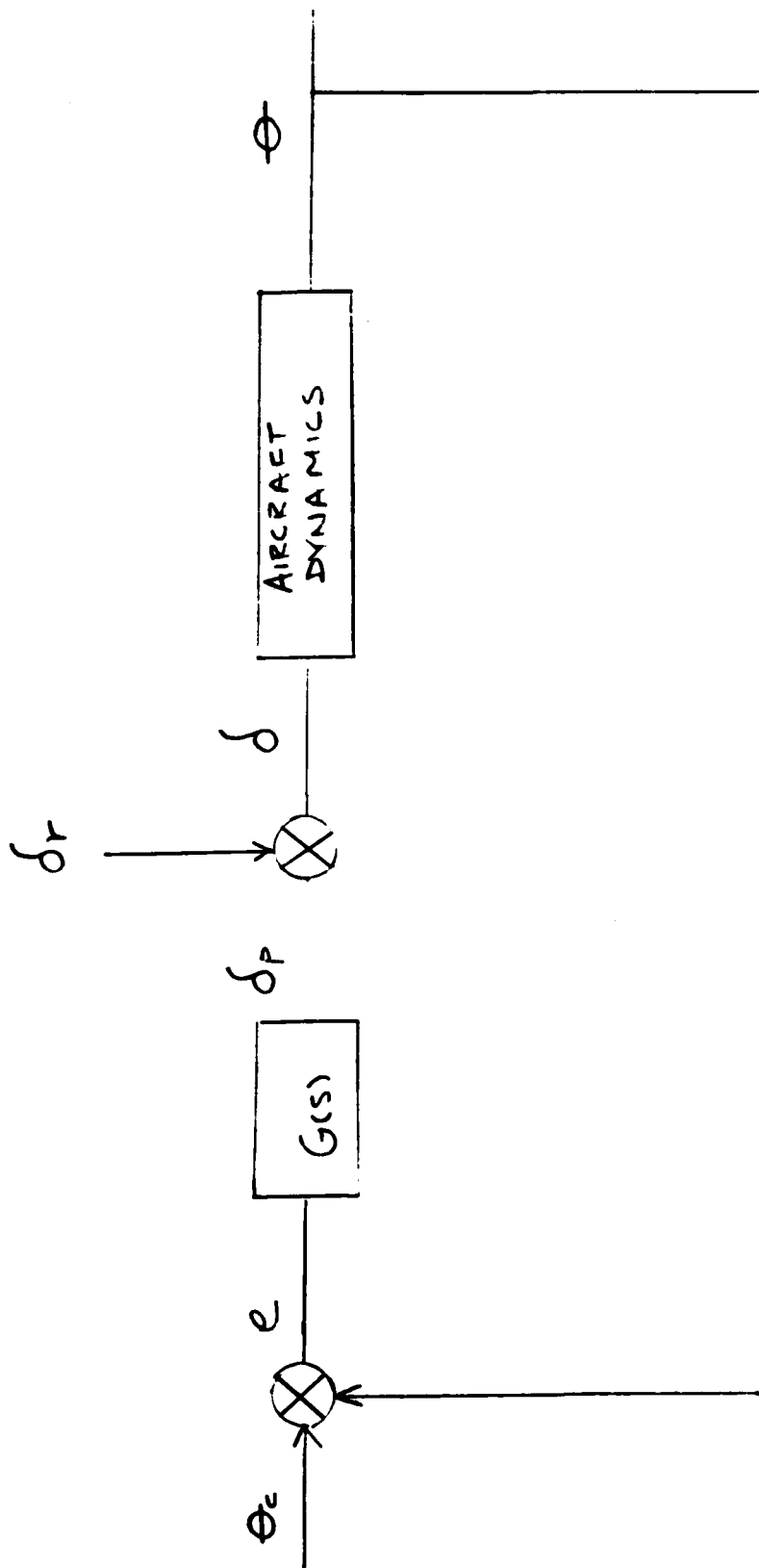
$\delta$  = longitudinal stick deflection , in

$e$  = longitudinal pipper error , milli-radians

$K_p$	= pilot gain	, in
$\tau_1$	= pilot lead	, secs
$\tau_2$	= pilot lag	, secs
$\tau_3$	= pilot delay	, secs

The objective of this work is to identify the pilot model parameters  $K_p$ ,  $\tau_1$ ,  $\tau_2$ ,  $\tau_3$  from the time histories of  $\delta$  and  $e$  obtained from the simulation. The pilot model given in Equation 1 is acting as part of a feedback control system (Figure 5). There are some basic assumptions involved in using the above pilot model. It is assumed the pilot behaves like a good servo-controller. That is to say he provides a specified command-response relationship. It is assumed that the pilot suppresses unwanted inputs and disturbances and concentrates solely on the desired control of the aircraft. It is also assumed that he reduces the effects of variations and uncertainties in elements of the control loop (4).

The describing function of the human pilot is a linear model. This a good assumption for short periods of time. However, the human controller is very non-linear. The non-linear portion of the human pilot is called the pilot remnant and is the difference between the output of the describing function and actual pilot output. The pilot remnant will not be identified in this work. It will be assumed however that any differences between the output of the pilot model and the actual time histories



Closed Loop System

Figure 5

recorded in simulation will be attributable, at least in part, to the unmodeled pilot remnant.

There are several restrictions on the use of Equation 7 for pilot modeling. The input to the pilot must be random. The pilot should not become sufficiently familiar with the task so as to be able to anticipate the forcing function. He must react to the forcing function with no prior knowledge of what the function will do. This was accomplished in simulation by switching the lights at different time intervals  $\Delta t$ . Where

$$2.25 \leq \Delta t \leq 3.15$$

Different sequences of lights were also used. Because the sequence of lights and the time interval between switching was varied the pilot was unable to become familiar with the sequence. He was not able to anticipate which light would turn on and when.

The input to the pilot is an error signal. In the case of ground attack the error is displayed on the HUD. The primary input to the pilot is the longitudinal distance between the center of the aiming reticle and the target light as seen through the HUD. This is the pipper error. The system is compensatory in that only the error and not the error rate is displayed. The pilot attempts to minimize the error in minimum time through control stick deflections.



Pilot compensation is very sensitive to aircraft dynamics. A small perturbation model which is linearized about a nominal operating point should be used. It is essential that the pilots attention be focused on his primary task, minimization of pilpex errors in minimum time. His attention should not be diverted to side tasks.

The pilot should be a trained and motivated operator. He should be familiar with the dynamics of the aircraft and the task to be accomplished. He should be motivated in the sense that his maximum effort is being given to the task. Should his attention be diverted or he gives less than his maximum effort to the task, the data he generates will be poor and the identification of his dynamics as represented by the pilot model parameters will be questionable.

### Time Delay

From Equation 7 it can be seen that the pilot model contains an exponential term.

$$\exp^{-\tau_3 s} \quad (8)$$

This term models the pilot delay due to neuro-muscular lag. It is also called the transportation lag or dead time. In order to identify the pilot model parameters of Equation 7 using the algorithm RLS it is necessary to discretize the equation. This will be shown in more detail in a later section. In discretizing Equation 7 it was found that the transportation lag given by Equation 8

was not easily discretized. It was necessary to use an approximation to the pilot delay.

Several approximations to Equation 8 will be used. The Padé approximation to the time delay given in Equation 3 will be used. Two other methods will also be used. These methods are not as accurate as the Padé approximation but are simpler to implement.

If  $\tau_3$  is very small, then the pilot delay may be approximated by

$$\exp^{-\tau_3 S} = 1 - \tau_3 S \quad (9)$$

$$\exp^{-\tau_3 S} = \frac{1}{1 + \tau_3 S} \quad (10)$$

Such approximations are good if  $\tau_3$  is very small and, the input time function  $f(t)$  to the pilot delay term is a smooth and continuous one. This means that the second - and higher order derivatives of  $f(t)$  are small (5).

In addition to the two representations shown above, another representation to the time delay was used. It is the well-known Padé approximation for time delay and is given by

$$\exp^{-\tau_3 S} = \frac{1 - (\tau_3/2)S}{1 + (\tau_3/2)S} \quad (11)$$

It is not known which of these representations for pilot time delay is best suited for the task of pilot model parameter identification. It is desired to try all three methods as well as neglecting the pilot time delay

altogether. This gives rise to four distinct representations of the pilot model  $G(s)$ .

$$G_1(s) = K_p \frac{(\tau_1 s + 1)}{(\tau_2 s + 1)} \quad (12)$$

$$G_2(s) = K_p (1 - \tau_3 s) \frac{(\tau_1 s + 1)}{(\tau_2 s + 1)} \quad (13)$$

$$G_3(s) = \frac{K_p}{(1 + \tau_3 s)} \frac{(\tau_1 s + 1)}{(\tau_2 s + 1)} \quad (14)$$

$$G_4(s) = K_p \frac{(1 - (\tau_3/2)s)}{(1 + (\tau_3/2)s)} \frac{(\tau_1 s + 1)}{(\tau_2 s + 1)} \quad (15)$$

Bode plots of magnitude and phase shift give a good indication of which approximation to pilot delay most closely approximates the actual delay. This will be examined more closely in Chapter 4.

### Discretization Techniques

In order to apply the recursive least squares (RLS) feature of  $MATRIX_x$  it is necessary to discretize the pilot models of Equations 12 through 15. This is necessary because the RLS algorithm in  $MATRIX_x$  identifies the coefficients of the discrete transfer function not the continuous. In order to discretize the equations one must have a relationship between the  $s$  domain and the  $z$  domain. There are a number of such relationships available. Each represents a discrete approximation to a continuous

system. Three different methods for discretization are used. They are shown as follows:

$$s = \frac{z-1}{T} \quad (16)$$

$$s = \frac{z-1}{Tz} \quad (17)$$

$$s = \frac{2}{T} \frac{z-1}{z+1} \quad (18)$$

The above approximations to  $s$  are substituted into the pilot models of Equations 12 through 15. The discrete time variable  $z$  is equivalent to the advance of one time step.

$$zy(KT) = y(KT+T) \quad (19)$$

Equations 16 through 18 are different ways of approximating the process of differentiation in the  $z$  - domain. Equation 16 is called forward integration and is equivalent to estimating the rate by looking forward over the time interval.

$$\frac{y(KT+T) - y(KT)}{T} = y(KT) \frac{(z-1)}{T} \quad (20)$$

Equation 17 is called backward integration and is equivalent to estimating the rate by looking backward over the time interval

$$\frac{y(KT) - y(KT-T)}{T} = y(KT) \frac{(z-1)}{Tz} \quad (21)$$

The approximation given by Equation 18 is the trapezoid rule or Tustin's bilinear rule, found by approximating the average rate over the interval. An

additional method is also used. It is called Hold Equivalence or Zero Order Hold. The concept behind this technique is that the output of the discretized transfer function is equivalent to the output of its corresponding continuous transfer function with the exception that the output is constant or held over the interval. The discretized transfer function is formed from the continuous transfer function from the following relationship (6).

$$H_{ho}(z) = (1 - z^{-1}) \mathcal{Z} \left[ \frac{H(s)}{s} \right] \quad (22)$$

The script  $\mathcal{Z}$  denotes Z-transformation, which is the Z-domain equivalent to Laplace transformation.

Each of the four methods of discretization described above are used to discretize the 4 pilot models given in Equations 12 through 15. This will yield 16 different discrete representations of Equation 7. Each of these representations will be used to identify the pilot model parameters and a determination of which one is best suited to the task of pilot model parameter identification will be made.

The general form of the discretized pilot model is shown as follows:

$$G(z) = \frac{N_0 z^m + N_1 z^{m-1} + \dots + N_m}{d_0 z^n + d_1 z^{n-1} + \dots + d_n} \quad (23)$$

The order of the numerator and denominator are  $m$  and  $n$ , respectively. They will vary depending on the discretization technique used. In all cases,

$$n \geq m \quad (24)$$

and the coefficients

$$N_0, N_1, \dots, N_m$$

and

$$d_0, d_1, \dots, d_n$$

are identified by the RLS algorithm. Algebraic expressions for the coefficients are obtained when the pilot models are discretized. In all cases they are functions of the pilot model parameters.

$$\begin{aligned} N_0 &= f(K_p, \tau_1, \tau_2, \tau_3) \\ &\cdot \\ &\cdot \\ &\cdot \\ &\cdot \\ d_n &= f(K_p, \tau_1, \tau_2, \tau_3) \end{aligned} \quad (25)$$

The identification involves solving these equations for  $K_p, \tau_1, \tau_2, \tau_3$ . In some cases these equations are non-linear and do not yield unique solutions. These equations are developed in more detail in Chapter 4.

### Least Squares

Both Batch Least Squares (BLS) and the Recursive Least Squares (RLS) are used for identification. Both

algorithms are well established and have been in use extensively in system identification.

Batch least squares is a very popular approach that goes back to Gauss and Legendre in the early 19th Century. Recursive identification algorithms update parameters at every sample, as opposed to batch methods which operate on an entire time history of data all at once. Recursive algorithms are characterized by finite non-increasing storage requirements. They are typically well-suited for real-time on-line identification with modest processors [8].

Both algorithms form least squares estimates of the coefficients from the following equation:

$$\theta' = (X^T X)^{-1} X^T Y \quad (26)$$

where

$\theta' = [N_0, N_1, \dots, N_m, d_0, d_1, \dots, d_n]$   
the Least Squares estimate of  
coefficients.

$X$  = Matrix formed from input and  
output data

$Y$  = output vector

The above equation is a simplification presented only for background information. In order to understand and use the BLS and RLS features of MATRIX<sub>x</sub> and be confident of the results it returns, it was necessary to understand the algorithms in greater detail. For a detailed derivation and discussion of the batch and recursive least squares algorithms refer to reference [6].

An example best serves to illustrate the use of  $\text{MATRIX}_x$  for identification of the coefficients of a discrete transfer function. Given the following discrete transfer function:

$$H(Z) = \frac{\delta(Z)}{e(Z)} = \frac{a_0 Z + a_1}{Z - b_1}$$

This can be rewritten as:

$$\frac{\delta(Z)}{e(Z)} = \frac{a_0 Z + a_1}{Z - b_1} \frac{Z^{-1}}{Z^{-1}} = \frac{a_0 + a_1 Z^{-1}}{1 - b_1 Z^{-1}} \quad (27)$$

The difference equation can then be written as:

$$\begin{aligned} \delta(Z) (1 - b_1 Z^{-1}) &= e(Z) (a_0 + a_1 Z^{-1}) \\ \delta(K) &= a_0 e(K) + a_1 e(K-1) + b_1 \delta(K-1) \end{aligned} \quad (28)$$

The discrete time histories of  $e$  and  $\delta$  from  $t=1$  to  $t=N$  would yield the following set:

$$\begin{aligned} \delta(1) &= a_0 e(1) + a_1 e(0) + b_1 \delta(0) \\ \delta(2) &= a_1 e(2) + a_1 e(1) + b_1 \delta(1) \\ \delta(3) &= a_0 e(3) + a_1 e(2) + b_1 \delta(2) \\ &\vdots \\ \delta(N) &= a_0 e(N) + a_1 e(N-1) + b_1 \delta(N) \end{aligned} \quad (29)$$

This can be written in  $\text{MATRIX}_x$  format as:

$$Y = X\theta' \quad (30)$$

where

$$Y = [\delta(1), \delta(2), \delta(3), \dots, \delta(N)] \quad (31)$$

$$\theta' = [a_0, a_1, b_1] \quad (32)$$



and

$$X = \begin{bmatrix} e(1) & e(0) & \delta(0) \\ e(2) & e(1) & \delta(1) \\ e(3) & e(2) & \delta(2) \\ . & . & . \\ . & . & . \\ . & . & . \\ e(N) & e(N-1) & \delta(N-1) \end{bmatrix} \quad (33)$$

The Batch Least Squares solution to  $\theta'$  may be found by typing into MATRIX<sub>x</sub>:

$$\theta' = X \backslash Y$$

MATRIX<sub>x</sub> will internally solve Equation 30.

To solve the problem using the recursive algorithm is considerably more simple when using MATRIX<sub>x</sub>. One need only provide the algorithm with an initial guess at the coefficients  $[a_0, a_1, b_1]$ , the initial covariance which defaults to  $10^5$ , and the time histories of input and output. In this case one would input:

$Y = [\delta(1), \delta(2), \delta(3), \dots, \delta(N)]$

$U = [e(1), e(2), e(3), \dots, e(N)]$

$NUM0 = [0 \ 0]$

$DEN0 = [1 \ 0]$

$[NUM, DEN, FITERR] = RLS(Y, U, NUM0, DEN0, P0)$

Where NUM0, DEN0 are the initial guesses at the coefficients. The program will return;

$$\text{NUM} = \{a_0, a_1\}$$

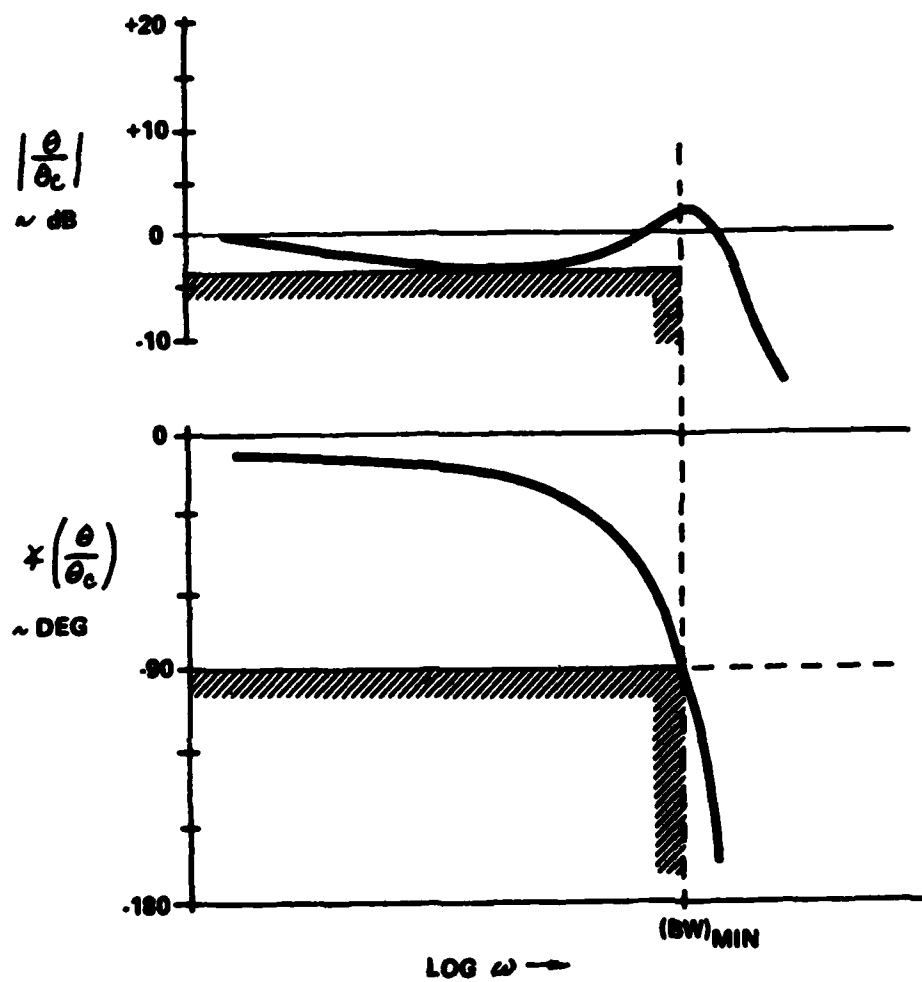
$$\text{DEN} = \{1, b_1\}$$

The FITERR parameter is defined as the sum of the squared residuals and gives an indication of the goodness of fit.

The preceding was done for the discrete transfer function of Equation 27, but may be extended easily to a discrete transfer function of any order.

### Neal-Smith Theory

Neal-Smith Theory is a means of predicting what compensation the pilot is likely to apply and relating the compensation to pilot opinion. The pilot is represented by Equation 7. The pilot is viewed as a good servo-controller that adapts himself to the control system/aircraft combination by providing the compensation required to achieve the desired performance. The pilot is trying to achieve certain performance standards. The work done by Neal-Smith examines pilot performance for the pitch-tracking task. The pilot's view of good tracking is that he be able to "acquire the target quickly and predictably." In the frequency domain this is equivalent to minimizing the bandwidth. The pilot is also trying to achieve two other other things. He tries to minimize the low frequency droop and at the same time he tries to minimize the resonant peak. These parameters are illustrated in Figure 6. Standards for these parameters



Neal-Smith Standards of Performance  
Figure 6

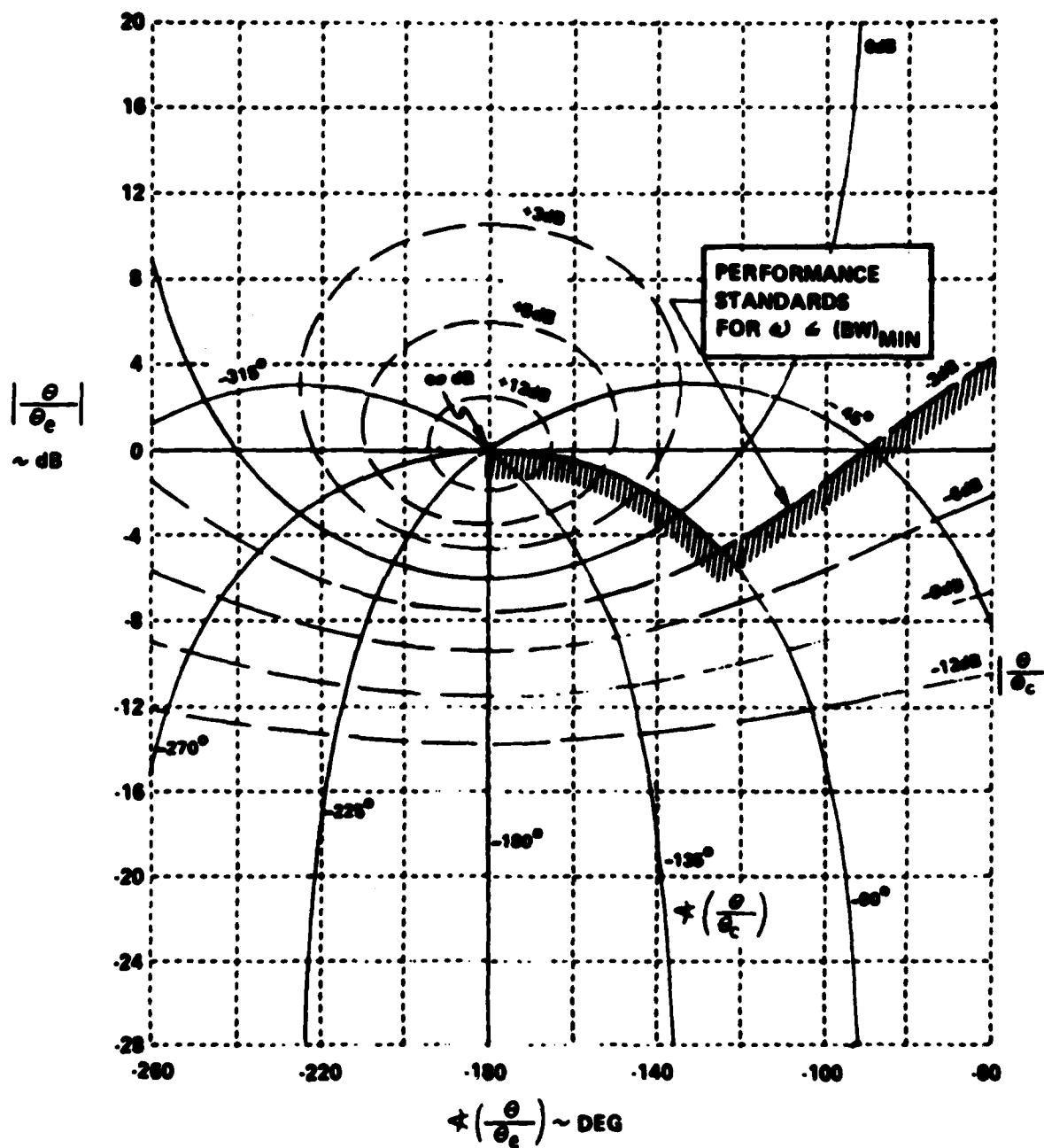
have been established by Neal-Smith. For most configurations the minimum bandwidth is 3.5 rad/sec. The low frequency droop was determined to be -3db. Both standards of performance were determined somewhat arbitrarily. In this work the minimum bandwidth will be varied to examine its effect on optimal pilot compensation. When using Neal-Smith theory to calculate optimal pilot compensation, pilot time delay is assumed to be constant and equal to .3. The theory is then used to calculate the optimal values of  $\tau_1$  and  $\tau_2$ .

In order to obtain closed-loop characteristics from the open-loop system a Nichols chart will be used. The Nichols chart has the performance standards defined on it as in Figure 7. This provides a graphical means to determine if the closed loop pilot/aircraft system meets the desired standards of performance. The Nichols chart is also useful for determining the resonant peak.

Neal-Smith showed that there is a relationship between pilot compensation and pilot ratings. Closed-loop resonance is plotted versus total pilot-compensation. In general, the lower the closed-loop resonance and the closer to zero the total pilot compensation the better the pilot rating.

In this work Neal-Smith theory will be used to predict what values of  $K_p$ ,  $\tau_1$ ,  $\tau_2$  are to be expected from

pilot model identification of the operating records obtained from the simulation. Optimal pilot models will be calculated over a range of bandwidth criterion to determine a range of pilot model parameters to be expected. Closed-loop resonance will be plotted versus the pilot model parameters obtained from identification to see if a correlation exists with the pilot ratings [3].



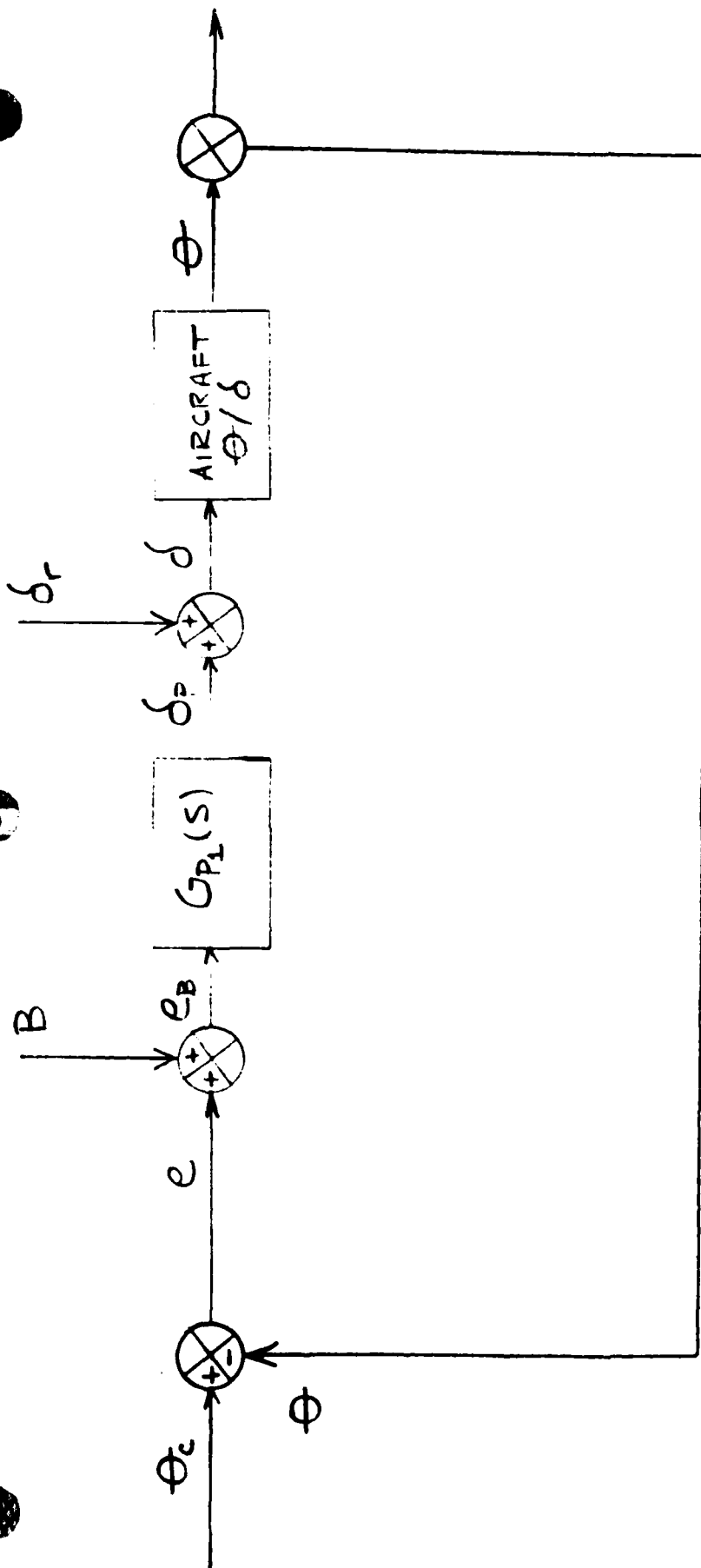
Standards of Performance Defined on Nichols Chart  
Figure 7

### III. Closed-Loop Simulation

#### Characteristics of the RLS Algorithm

The purpose of this section is to investigate the characteristics of the RLS algorithm. The algorithm will be used to identify pilot model parameters in the closed loop case. In order to close the loop around the pilot model it is necessary to simulate the aircraft pitch response to control stick deflections generated by the pilot model. A stick to pitch transfer function was chosen that is representative of a generic fighter-type aircraft in the ground attack mode. A discretized input signal found useful in system identification is then applied to the pilot/aircraft system and time histories of input and output are recorded. These time histories are then used to identify the pilot model parameters. The ability of the algorithm to identify pilot model parameters when the system is corrupted by noise is also investigated.

The system under study is the closed loop system shown in Figure 8. The pilot model actually represents the linear portion of the human pilot. The additional term  $\delta_z$  is added to account for nonlinear human pilot effects. The term  $\delta_z$  is the pilot remnant and is the



Closed-Loop System with Error  
Bias and Pilot Remnant. Included

Figure 8



difference between the output of the pilot model and the actual control deflection.

Two pilot models will be identified. The first model is representative of a pilot using excessive lead compensation and is implemented with:

$$\begin{aligned}K_p &= 2.0 \\ \tau_1 &= .8 \\ \tau_2 &= .2\end{aligned}$$

The second pilot model is representative of a pilot using excessive lag compensation and is implemented with:

$$\begin{aligned}K_p &= 1.0 \\ \tau_1 &= .2 \\ \tau_2 &= .8\end{aligned}$$

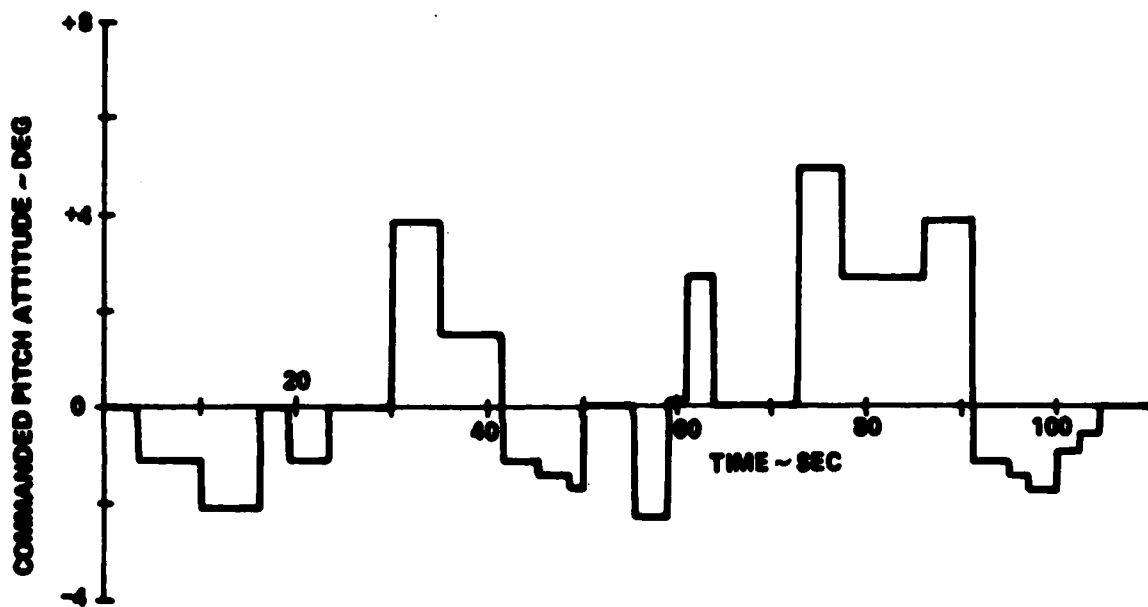
The aircraft stick to pitch transfer function used is representative of a German alpha-jet and is given as follows:

$$\frac{\theta(s)}{\delta(s)} = \frac{b_0 s + b_1}{s^3 + a_2 s^2 + a_1 s + a_0} \quad (34)$$

Where

$$\begin{aligned}b_0 &= 1.406 & a_0 &= .0985 \\ b_1 &= 2.38 & a_1 &= 23.5 \\ & & a_2 &= 5.67\end{aligned}$$

The RLS identification is not dependent on the aircraft model used. The optimum pilot model and the closed loop simulation both use the F-15 model. The discretized pitch input command;  $\theta_c$  is shown in Figure 9. In order to



Discrete - Error Pitch - Attitude Command Signal

Figure 9

implement the pilot model, the pitch response to stick input and the command input had to be discretized. The command input was easily discretized because it is already in a discrete form as can be seen in Figure 9. The pilot and aircraft model were not so trivially discretized. The pilot and aircraft models were both discretized using the forward integration rule.

The pilot model may be written in discretized form as:

$$G_{p1}(z) = \frac{\delta(z)}{e(z)} = \frac{A_1 z + A_0}{z + B_0} \quad (35)$$

Where

$$B_0 = - \frac{(\tau_2/T)}{(\tau_1/T + 1)} \quad (35a)$$

$$A_0 = - \frac{(K_D \tau_1)}{(\tau_2/T + 1)} \quad (35b)$$

$$A_1 = \frac{(K_D \tau_1/T + K_D)}{(\tau_2/T + 1)} \quad (35c)$$

Where  $A_0$ ,  $A_1$ ,  $B_0$  can be identified by the RLS algorithm.

The aircraft model can be written in discretized form as:

$$\frac{\theta(z)}{\delta(z)} = \frac{D_1 z + D_0}{z^3 + C_2 z^2 + C_1 z + C_0} \quad (36)$$

Where

$$C_2 = \frac{(-3/T^3 - 2a_2/T^2 - a_1/T)}{(1/T^3 + a_2/T^2 + a_1/T + a_0)} \quad (37a)$$

$$C_1 = \frac{(3/T^3 + a_2/T^2)}{(1/T^3 + a_2/T^2 + a_1/T + a_0)} \quad (37b)$$

$$C_0 = - \frac{(1/T^3)}{(1/T^3 + a_2/T^2 + a_1/T + a_0)} \quad (37c)$$

$$D_1 = \frac{(b_1/T + b_0)}{(1/T^3 + a_2/T^2 + a_1/T + a_0)} \quad (37d)$$

$$D_0 = \frac{-b_1/T}{(1/T^3 + a_2/T^2 + a_1/T + a_0)} \quad (37e)$$

In order to evaluate the recursive least squares algorithm data was generated for several cases. Constant and sinusiodal biases were added to corrupt the data. The following signals were used:

$$e_n = \theta_c - \theta + .1 \quad \text{Constant Bias} \quad (38)$$

$$e_n = \theta_c - \theta + .1 \sin \omega t. \quad \text{Sinusiodal Bias} \quad (39)$$

Where  $\omega = 1/25$

The unbiased error signal was applied to the pilot model so the bias would be unmodeled. The bias was then added to the error signal before application of the recursive least squares algorithm.

A similar procedure was used to model the pilot remnant.

$$\delta_r = .1 \quad \text{Constant Remnant} \quad (40)$$

$$\delta_r = .1 \sin \omega t. \quad \text{Sinusiodal Remnant} \quad (41)$$

The remnant was added to the output of the pilot model and used in identification.

The remnants and bias were tested on both pilot models providing 10 separate identifications.

Table 2 contains the results of the 10 identifications.

Data Type	First Pilot			Second Pilot		
	$K_p$	$\tau_1$	$\tau_2$	$K_p$	$\tau_1$	$\tau_2$
Actual	2.0	.8	.2	1.0	.2	.8
No Bias	2.000	.8001	.2000	.9999	.2000	.8000
eBias/Const	1.0467	1.9199	.2541	1.0429	.2264	.9225
eBias/Sin	1.3862	1.3437	.2346	1.008	.2110	.8425
Rem/Const	1.5879	1.1101	.2209	1.031	.2139	.8708
Rem/Sin	1.8324	.9131	.2097	1.031	.2139	.8708

Table 2. Closed Loop Pilot Model Parameters Identified

The second pilot model did not seem to be very sensitive to noise and remnants. The first pilot model was more sensitive to noise and remnants. The identifications of  $\tau_2$  was fairly accurate but large differences exist in  $K_p$  and  $\tau_1$ . In general the algorithm seems to be fairly sensitive to both the constant and sinusoidal biases and remnants.

#### Optimum Pilot Model

There are two objectives to this section. The first objective is to calculate an optimum pilot model for the F-15. A Neal-Smith analysis was done on the F-15 to obtain the optimum pilot compensation. In the Neal-Smith analysis a Padé approximation was used to represent the

pilot time delay. The optimum pilot model, including the Padé approximation to the time delay are discretized using the backward integration discretization technique. The F-15 is discretized by putting the model in phase variable canonical form and using the approximation to the matrix exponential function. Both models are then used to simulate the closed loop pilot/aircraft system. The simulation was used to generate time histories of the input and output of the optimum pilot model. The second objective of this section is to identify pilot model parameters including the time delay. The batch least squares and recursive least squares algorithms in Matrix<sub>x</sub> along with the time histories generated in the simulation will be used for the identification.

The aircraft model used in this work is the stick to pitch transfer function for an F-15 shown below as

$$\frac{\theta(s)}{\delta(s)} = \frac{.60(1.58s + 1.896)}{s(s^2 + 4.2s + 9.0)} \quad (42)$$

The optimal pilot model is calculated for the F-15 because it is the aircraft used in the realtime simulation. The optimal pilot model parameters may then be compared to the results obtained from RLS identification of the simulation data.

In order to calculate an optimum pilot model you must plot the open loop pilot/aircraft transfer function on a Nichols chart. In general, the transfer function is

$$\frac{\theta}{\theta_c} = \frac{\delta}{\theta_c} \cdot \frac{\theta}{\delta}$$

where

$$\frac{\delta}{\theta_c} = K_p \exp(-.3s) \frac{\tau_1 s + 1}{\tau_2 s + 1}$$

and the Padé approximation to  $e^{(-.3s)}$  is used and is given as

$$\exp(-.3s) \approx \frac{1 - .15s}{1 + .15s}$$

The first step is to plot only the time delay multiplied by the aircraft transfer function and adjust the gain until the magnitude at  $\omega = 3.0$  is approximately -5dB, then add lead or lag compensation as required. In this section it will be assumed that the pilot delay is equal to 300 milli-seconds. The Padé approximation to the time delay, multiplied by the aircraft transfer function, is given as follows

$$\frac{\theta(s)}{\theta_c(s)} = \left[ \frac{1 - .15s}{1 + .15s} \right] \left[ \frac{.60(1.58s + 1.896)}{s(s^2 + 4.2s + 9.0)} \right]$$

After multiplying through by the Padé approximation the transfer function becomes

$$\frac{\theta(s)}{\theta_c(s)} = \frac{-.1422s^2 + .7774s + 1.376}{.15s^4 + 1.63s^3 + 5.55s^2 + 9.0s}$$

In order to use the above equation in a Nichols plot program it was necessary to substitute  $s=j\omega$  in for  $s$  and reduce the above transfer function to the following form

$$\frac{\theta(j\omega)}{\theta_c} = \frac{(.1422\omega^2 + 1.1376) + .7774\omega j}{(.15\omega^4 - 5.55\omega^2) + (-1.63\omega^3 + 9.0\omega)j} = \frac{A+Bj}{C+Dj}$$

where

$$A = .1422\omega^2 + 1.1376$$

$$B = .7774\omega$$

$$C = .15\omega^4 - 5.55\omega^2$$

$$D = -1.63\omega^3 + 9.0\omega$$

A,B,C,D were programmed in a Nichols chart program and a plot was generated. From the plot it was evident that 10dB of gain was needed to raise the plot to the correct level and that lead compensation would be needed. A bandwidth of  $\omega_{BW} = 3$  was chosen as the design point. At  $\omega_{BW} = 3$  the phase angle should equal -130 degrees (3). But at  $\omega_{BW} = 3$  the phase is -160 degrees. Therefore the pilot model should contribute 30 degrees of phase lead at  $\omega_{BW} = 3$ . We have

$$\tau_1\omega = .60 \text{ at } \omega = 3.0$$

$$\tau_1 = \frac{.60}{3.0} = .200 \text{ sec}$$

This gives the following pilot model

$$K_p(\tau_1 s + 1) = 10(.2s + 1)$$

which represents pure lead compensation. The following represents the optimal pilot/aircraft system.

$$\frac{\theta(s)}{\theta_c(s)} = 10(.2s + 1) \left[ \frac{1 - .15s}{1 + .15s} \right] \left[ \frac{.948s + 1.1376}{s(s^2 + 4.2s + 9.0)} \right]$$



The system requires further adjustment in order to meet the standards of performance. After several iterations of adjusting the lead and gain, the following system was determined to be optimal and a Nichols chart is presented in Figure 10.

$$\frac{\theta}{\theta_c} = 7.4728(.1933s + 1) \left[ \frac{1 - .15s}{1 + .15s} \right] \left[ \frac{.948s + 1.1376}{s(s^2 + 4.2s + 9.0)} \right]$$

Also shown in Figure 11 is a Bode plot of the closed loop system for comparison with the Nichols chart. The plots of Figure 11 show a system where the low frequency drop is -3dB with a closed loop peak of zero dB. This is exactly as is seen in the simulation results that follow. The optimum pilot model calculated indicates level 1 flying qualities because it requires minimum pilot compensation and has a low closed loop resonance.

#### Discretization of Pilot Model with Time Delay

The full pilot model with time delay is defined as

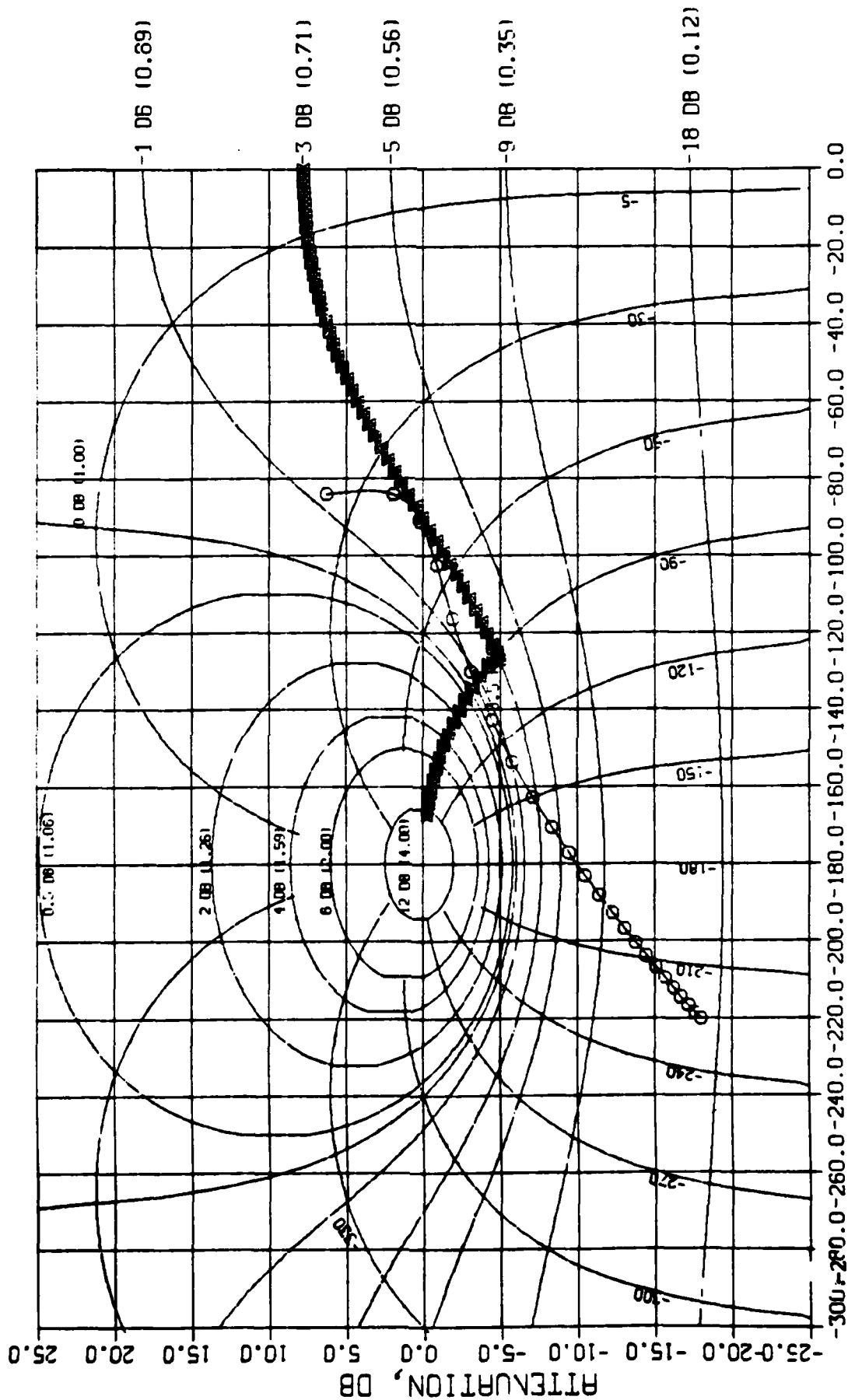
$$\frac{\delta(s)}{e(s)} = K_p \frac{1 - (T/2)s}{1 + (T/2)s} \frac{\tau_1 s + 1}{\tau_2 s + 1}$$

Let  $T/2$  equal  $\tau_3$  and you have

$$\frac{\delta(s)}{e(s)} = K_p \frac{1 - \tau_3 s}{1 + \tau_3 s} \frac{\tau_1 s + 1}{\tau_2 s + 1}$$

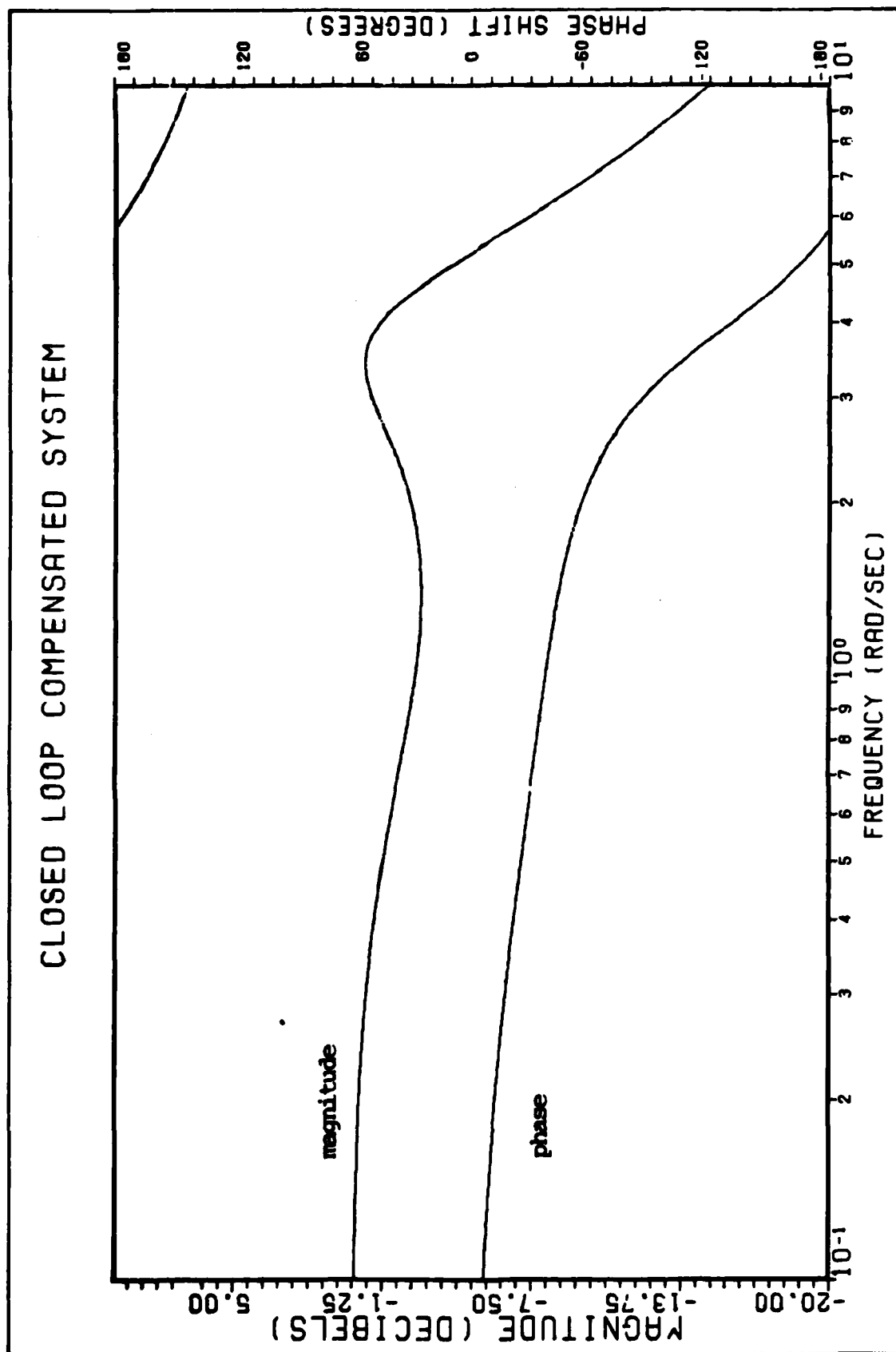
After multiplying out and rearranging terms, the above can be expressed as

# NICHOLS CHART



Nichols Chart for Optimum Pilot/Aircraft System

Figure 10



Bode Plot for Optimum Pilot/Aircraft

Figure 11

$$\frac{\delta(s)}{e(s)} = \frac{a_2 s^2 + a_1 s + a_0}{s^2 + b_1 s + b_0} \quad (43)$$

where

$$a_2 = \frac{-K_D \tau_1 \tau_3}{\tau_2 \tau_3} \quad (44a)$$

$$a_1 = \frac{K_D (\tau_1 - \tau_3)}{\tau_2 \tau_3} \quad (44b)$$

$$a_0 = \frac{K_D}{\tau_2 \tau_3} \quad (44c)$$

$$b_1 = \frac{\tau_2 + \tau_3}{\tau_2 \tau_3} \quad (44d)$$

$$b_0 = \frac{1}{\tau_2 \tau_3} \quad (44e)$$

Equation 43 was discretized using the backward integration rule given by Equation 17. This approximation for  $s$  was substituted into Equation 43. After multiplication and rearranging terms, Equation 43 becomes

$$\frac{\delta(z)}{e(z)} = \frac{\Lambda_0 z^2 + \Lambda_1 z + \Lambda_2}{z^2 + B_1 z + B_2} \quad (45)$$

where

$$\Delta = \frac{1}{T^2} + \frac{b_1}{T} + b_0$$

$$\Lambda_0 = \frac{\frac{a_2}{T^2} + \frac{a_1}{T} + a_0}{\Delta} \quad (46a)$$

$$\Lambda_1 = \frac{\frac{-2a_2}{T^2} - \frac{a_1}{T}}{\Delta} \quad (46b)$$

$$A_2 = \frac{\frac{a_2}{T^2}}{\Delta} \quad (46c)$$

$$B_1 = \frac{-\frac{2}{T^2} - \frac{b_1}{T}}{\Delta} \quad (46d)$$

$$B_2 = \frac{\frac{1}{T^2}}{\Delta} \quad (46e)$$

When using the least squares algorithm it is  $A_0$ ,  $A_1$ ,  $A_2$ ,  $B_1$ , and  $B_2$  that are identified. The problem then is to relate these to  $K_p$ ,  $\tau_1$ ,  $\tau_2$ ,  $\tau_3$ . Given  $A_0$  through  $B_2$  from the RLS algorithm the following set of algebraic equations relates them to the pilot model parameters.

$$b_0 = \frac{B_1 + B_2 - 1}{T^2 B_2}$$

$$b_1 = -\frac{1}{T} \left[ \frac{B_1}{B_2} + 2 \right]$$

$$a_2 = A_2 T^2 \Delta$$

$$a_1 = \frac{A_1 T^2 + 2A_2}{-T}$$

$$a_0 = A_0 T^2 \Delta - a_2 - a_1 T$$

$$K_p = \frac{a_0}{b_0}$$

$$\tau_3 = \frac{-a_1 + \sqrt{(a_1^2 - 4a_0a_2)}}{2a_0}$$

$$\tau_1 = \frac{-a_2}{a_0 T}$$

$$\tau_2 = \frac{b_1 - b_0 \tau_3}{b_0}$$

In the calculation of  $\tau_3$  the positive square root was chosen to insure that  $\tau_3$  remains positive.

#### Discretization of the F-15 Model Using the Matrix Exponential Function

The transfer function for the F-15 model is given in Equation 42. After transforming this system to phase variable canonical form we have

$$\begin{bmatrix} \dot{x}_1 \\ \dot{x}_2 \\ \dot{x}_3 \end{bmatrix} = \begin{bmatrix} 0 & 1 & 0 \\ 0 & 0 & 1 \\ 0 & -9 & -4.2 \end{bmatrix} \begin{bmatrix} x_1 \\ x_2 \\ x_3 \end{bmatrix} + \begin{bmatrix} 0 \\ 0 \\ 1 \end{bmatrix} \delta \quad (47)$$

$$\phi(t) = \begin{bmatrix} 1.1376 & .948 & 0 \end{bmatrix} \begin{bmatrix} x_1 \\ x_2 \\ x_3 \end{bmatrix} \quad (48)$$

The corresponding discrete system is

$$XT(K) = AT * XT(K-1) + BT * UT(K-1) \quad (49)$$

$$YT(K) = CT * XT(K) \quad (50)$$

where

$$AT = I + AT + \frac{A^2 T^2}{2!} \quad (51)$$

$$BT = IT + \frac{AT^2}{2!} + \frac{A^2T^3}{3!} \quad (52)$$

$$CT = C \quad (53)$$

MATRIX<sub>x</sub> was used to calculate AT and BT with T = .1. The following matrices were calculated.

$$AT = \begin{bmatrix} 1 & .0985 & .0043 \\ 0 & -.9613 & .0804 \\ 0 & -.7240 & .6235 \end{bmatrix}$$

$$BT = \begin{bmatrix} .0001677 \\ .0043 \\ .0804 \end{bmatrix}$$

An eigenvalue analysis was done on "AT" to determine if all of the roots are inside the unit circle. The roots are

$$\begin{aligned} &1.0 \\ &.7924 + .1723j \\ &.7924 - .1723j \end{aligned}$$

The root at 1.0 was changed to .9998 to insure stability. The above equations were programmed in FORTRAN and implemented in the simulation as subroutine F15.

#### Digital Simulation

The digital simulation used to generate the time histories for identification is the same as the simulation program used in the previous simulation with the exception of the pilot and aircraft models. The program was modified with the new pilot model that includes time delays. The aircraft model was replaced with subroutine F15. A listing of this program is contained in Appendix A. The simulation was run for 110 seconds and tabulated

data for  $e$ ,  $\delta_p$ ,  $\theta$ , and  $\theta_c$  is also contained in Appendix A. It can be seen from the tabulated data that THETA approaches THETAC without overshooting as would be indicated by the Bode plot in Figure 11. The Bode plot of Figure 8 serves to validate what is seen in the data.

#### Identification of Pilot Model Parameters

In order for the optimum pilot model calculated from the Neal-Smith theory to fit the format of the discretized general pilot model it was necessary to add a lag term. The lag term that was added is  $(.01 * s + 1)$ . It was determined that this term adds no amplitude and negligible phase lag. It was included only so the form of the optimum pilot model would match the form of the discretized model. This would make identification of pilot lag possible.

The data generated by the simulation is converted to a format usable by MATRIX<sub>x</sub> by program CONVERT. Given  $K_p$ ,  $\tau_1$ ,  $\tau_2$ ,  $\tau_3$ , from the optimum pilot model, and the equations for the coefficients of the discretized pilot model, the coefficients may be calculated as

$$\begin{aligned} A_0 &= -.1568 \\ A_1 &= .5741 \\ A_2 &= -.3102 \\ B_1 &= .6909 \\ B_2 &= -.0545 \end{aligned}$$



The MATRIX<sub>x</sub> diary is contained in Appendix B. The coefficients as identified by MATRIX<sub>x</sub> from the time histories are

$$\begin{aligned}A_0 &= -.1569 \\A_1 &= .5741 \\A_2 &= -.3104 \\B_1 &= .6913 \\B_2 &= -.0545\end{aligned}$$

This is a good identification as can be seen by the closeness of the numbers. The fiterr of .2446 is the sum of the squared residuals from the RLS algorithm. A fiterr of .2446 is very low by comparison to much larger values of fiterr obtained on runs where there was not a good identification.

#### IV. Discretization of Pilot Models

It is desirable to determine which of the approximations to the pilot time delay most accurately approximates the actual time delay. This can be done by comparing the frequency response of the pilot model with the actual time delay to the frequency response of the pilot models with the approximations to the time delays. The frequency range of interest for human pilot dynamics is from .1 to 10 radians per second [3]. In order to generate frequency response plots for the pilot models it is necessary to have values for the pilot model parameters. The optimal pilot model parameters determined from the Neal-Smith analysis of the previous section will be used for this purpose. The optimal pilot model parameters are

$$K_p = 7.47$$

$$\tau_1 = .19$$

$$\tau_2 = .01$$

$$\tau_3 = .15$$

These values of the optimal pilot model parameters are substituted into the pilot models of Equation 7 and Equations 12 through Equation 15. The resulting pilot models are given in Equations 55 through 59.

$$G_p(s) = 7.47 \frac{(.19s+1)}{(.01s+1)} \exp^{(-.38)} \quad (55)$$

$$G_{P_1} = 7.47 \frac{(.19s+1)}{(.01s+1)} \quad (56)$$

$$G_{P_2} = 7.47 (1-.3s) \frac{(.19s+1)}{(.01s+1)} \quad (57)$$

$$G_{P_3} = 7.47 \frac{1}{(1+.3s)} \frac{(.19s+1)}{(.01s+1)} \quad (58)$$

$$G_{P_4} = 7.47 \frac{(1-.15s)}{(1+.15s)} \frac{(.19s+1)}{(.01s+1)} \quad (59)$$

Bode plots for  $G_{P_1}$  through  $G_{P_4}$  were generated using the interactive software package TOTAL (13). A Bode plot for Equation 55 cannot be generated using TOTAL because of the complex exponential term representing the time delay. Equation 55 must be solved numerically. In order to generate a solution let  $s=j\omega$  and substitute into Equation 55.

$$7.47 \frac{1+.19(j\omega)}{1+.01(j\omega)} \exp^{-.3(j\omega)}$$

The magnitude and phase angle for the above expression can be given as

$$\text{Mag} = 7.47 \sqrt{\frac{1 + (.19)^2 \omega^2}{1 + (.01)^2 \omega^2}}$$

$$\phi = \tan^{-1} (.19\omega) - \tan^{-1} (.01\omega) - (.3\omega)$$

The above equations for magnitude and phase angle are programmed in FORTRAN program BASE. The frequency is varied from 0 to 10 radians per second by .1 radians per second. Tabular data for the magnitude and phase angle along with program BASE are contained in Appendix B. Bode

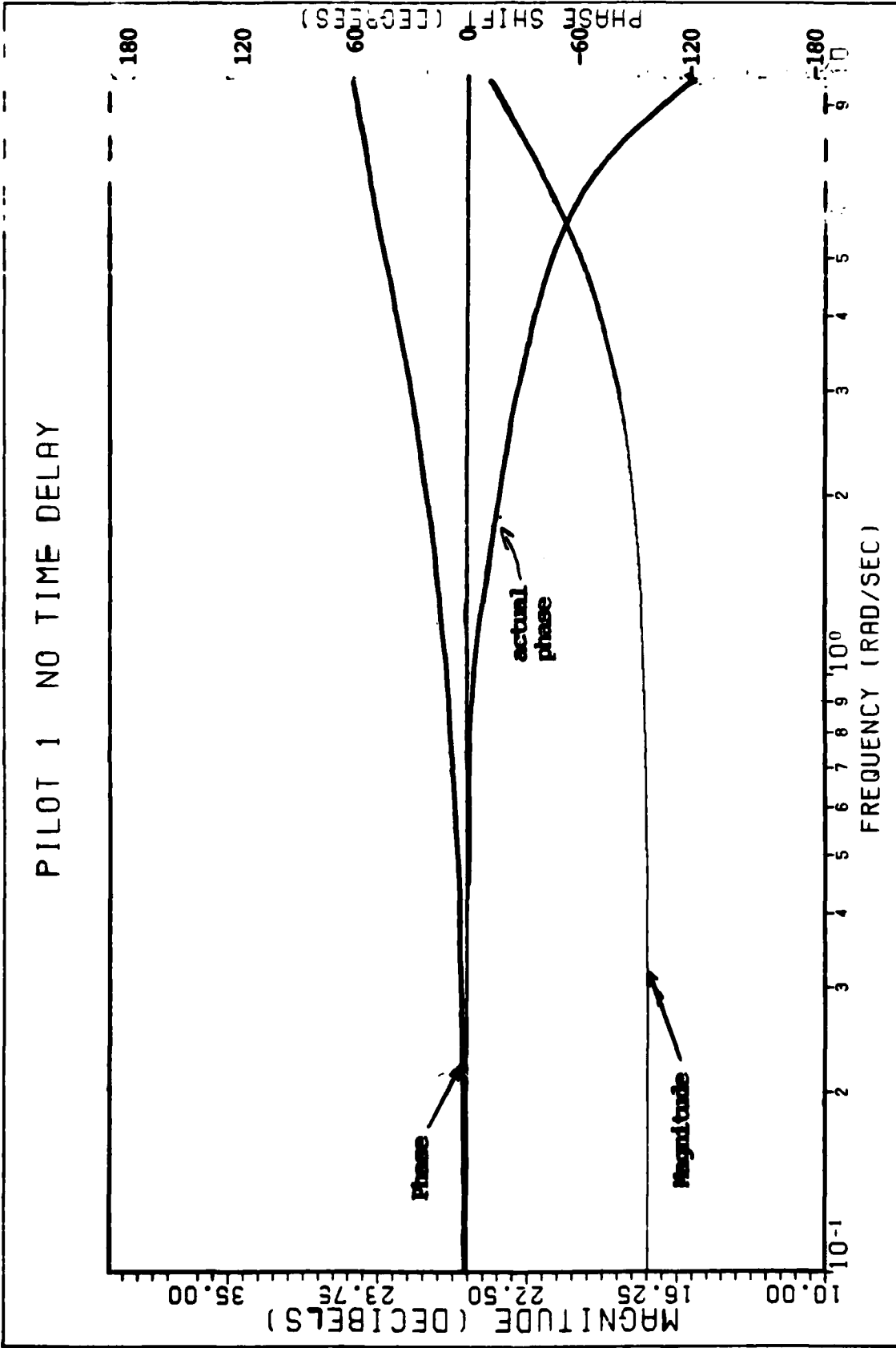
plots for  $G_{p_1}$  through  $G_{p_4}$  are presented in Figure 12 through 15 for comparison.

The plots of Figure 12 through Figure 15 contain the actual phase and magnitude calculated from the above expressions for phase and magnitude. The actual phase and magnitude can then be compared to the approximate phase and magnitude given by Equations 56 through 59.

From Figure 12 it can be seen that the magnitude of  $G_{p_1}$  is identical to the magnitude of  $G_p$ . The phase angle of  $G_{p_1}$  closely approximates the phase angle of  $G_p$  for frequencies less than 1 radian per second. For frequencies greater than 1 they start to diverge. At a frequency of 10 radians per second there is approximately 180 degrees difference in the phase angle of  $G_p$  and  $G_{p_1}$ .  $G_p$  is the pilot model with the time delay unmodeled. Figure 12 shows that for unmodeled time delay the output of the pilot model will lead the actual output by 180 degrees.

Figure 13 is a Bode plot of  $G_{p_2}$ . There is some magnitude distortion at the higher frequencies as would be expected when adding the numerator term as the approximation to the delay. At a frequency of 10 radians per second the magnitude of  $G_{p_2}$  is approximately 12db greater than the magnitude of  $G_p$ . The phase angle of  $G_{p_2}$  is relatively constant, dropping to only -15 degrees at 10 radians per second. This leads the actual phase angle by

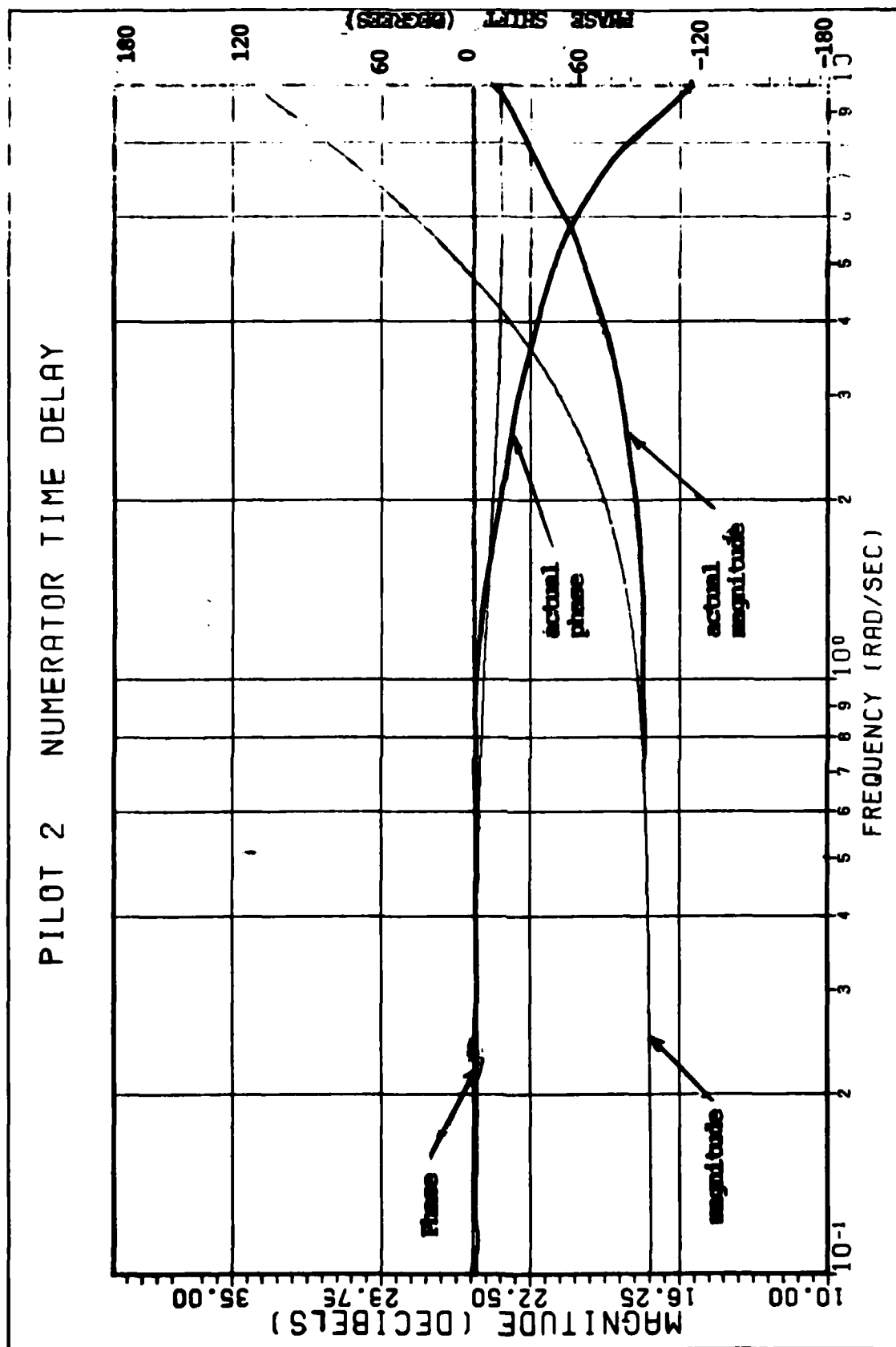
# PILOT 1 NO TIME DELAY



Bode Plot for Optimal  $G_{p1}$  (No time delay)

Figure 12

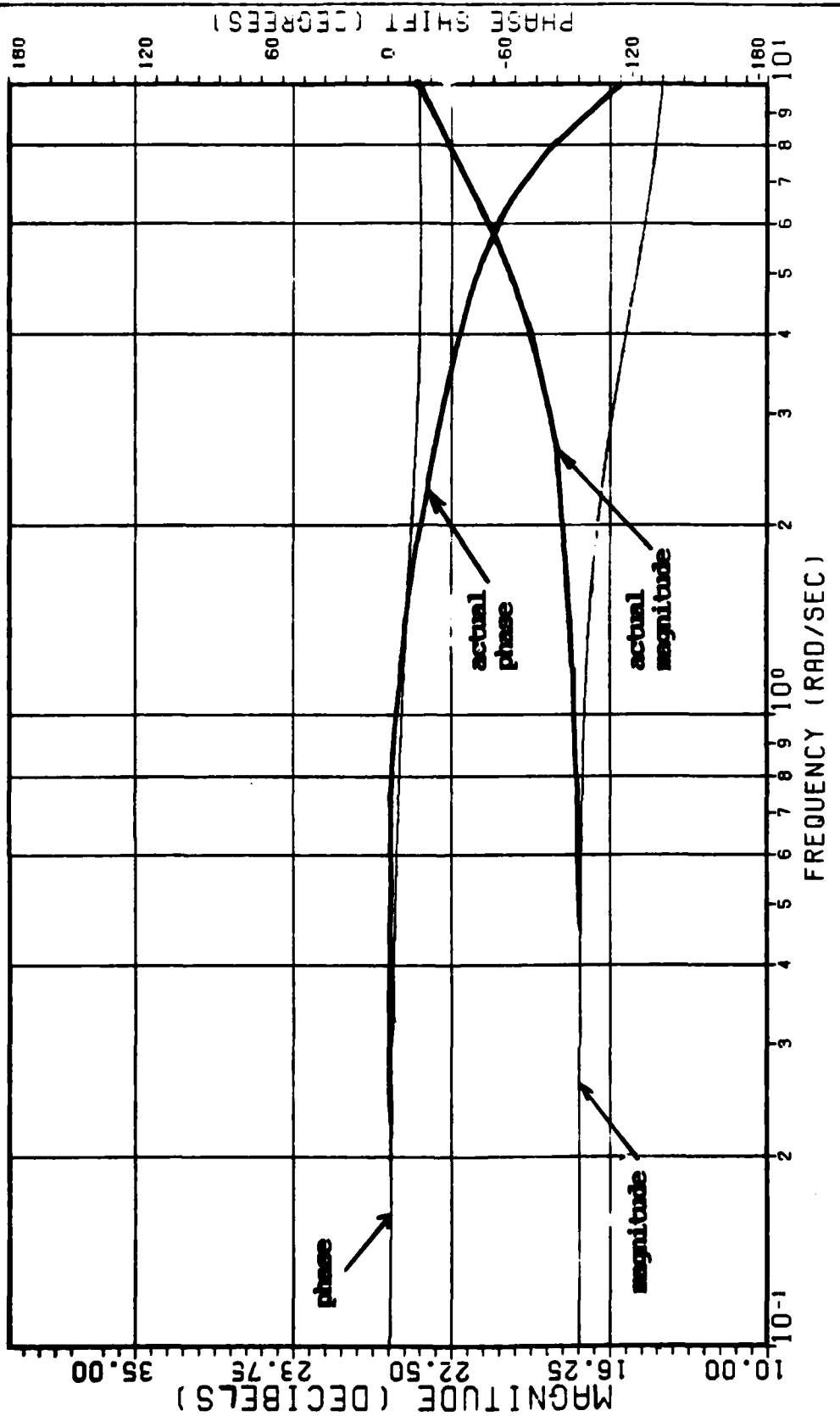
# PILOT 2 NUMERATOR TIME DELAY



Bode Plot for Optimal  $G_{p2}$  (numerator time delay)

Figure 13

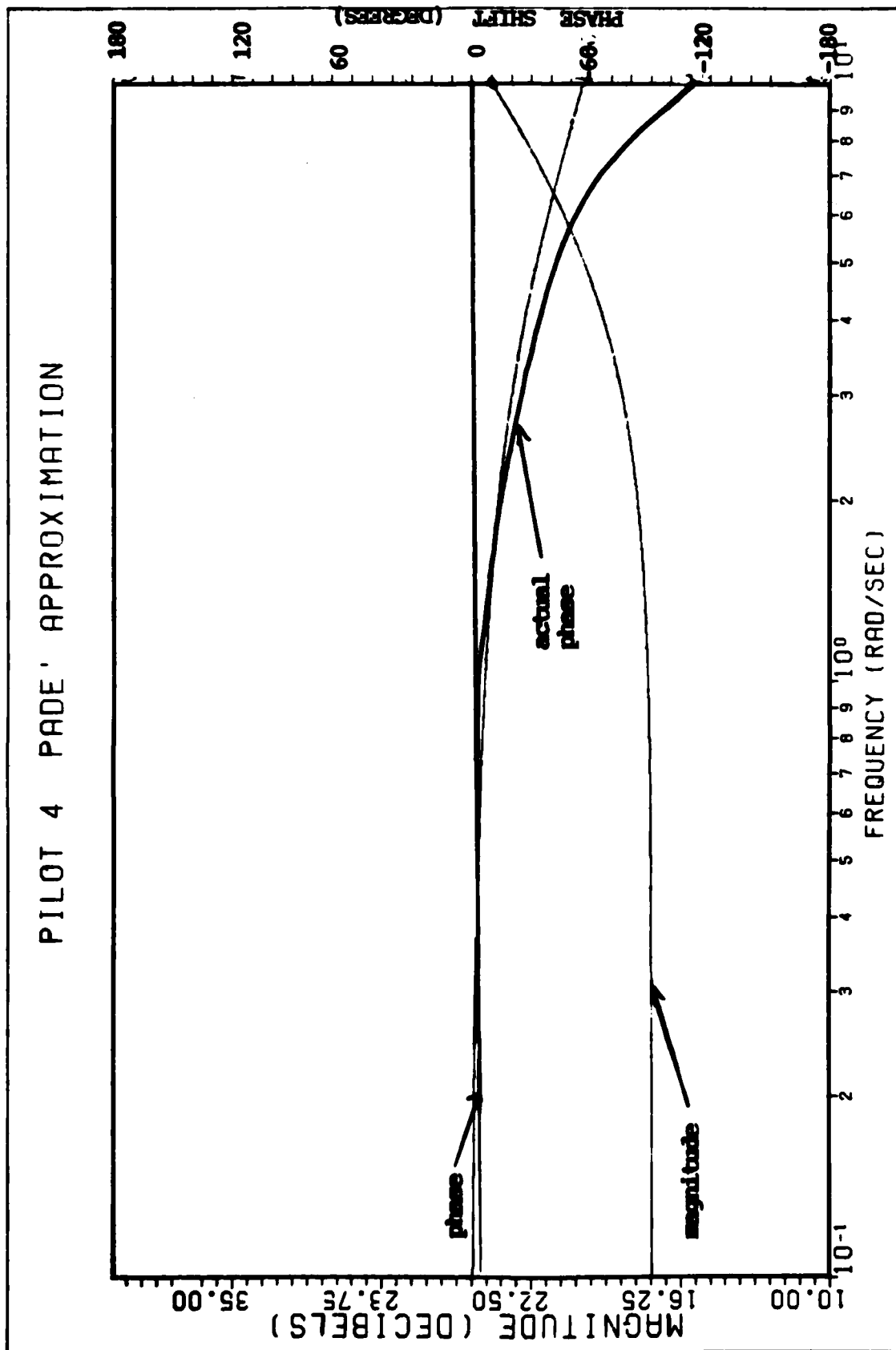
# PILOT 3 DENOMINATOR TIME DELAY



Bode Plot for Optimal  $G_{p3}$  (denominator time delay)

Figure 14

# PILOT 4 PADE' APPROXIMATION



Bode Plot for Optimal  $G_{p4}$  (Padé approximation to time delay)

Figure 15



approximately 100 degrees at 10 radians per second. This is a large phase lead but it is an improvement over the 180 degrees lead of  $G_{p_1}$ .

Figure 14 is a Bode plot of  $G_{p_3}$ . The magnitude of  $G_{p_3}$  is 10db less than the magnitude of  $G_p$  at 10 radians per second. The phase angle of  $G_{p_3}$  is similar to the phase angle of  $G_{p_2}$  and also leads the actual phase angle by approximately 100 degrees.

Figure 15 is a Bode plot of  $G_{p_4}$ . The magnitude of  $G_{p_4}$  is exactly the same as the magnitude of  $G_p$ . This is expected because the Pade approximation to the time delay will not introduce any distortion in magnitude. The Pade approximation to the time delay will only introduce a phase shift. The phase angle of  $G_{p_4}$  is equal to approximately -55 degrees at a frequency of 10 radians per second.  $G_{p_4}$  leads  $G_p$  by 60 degrees at this frequency.

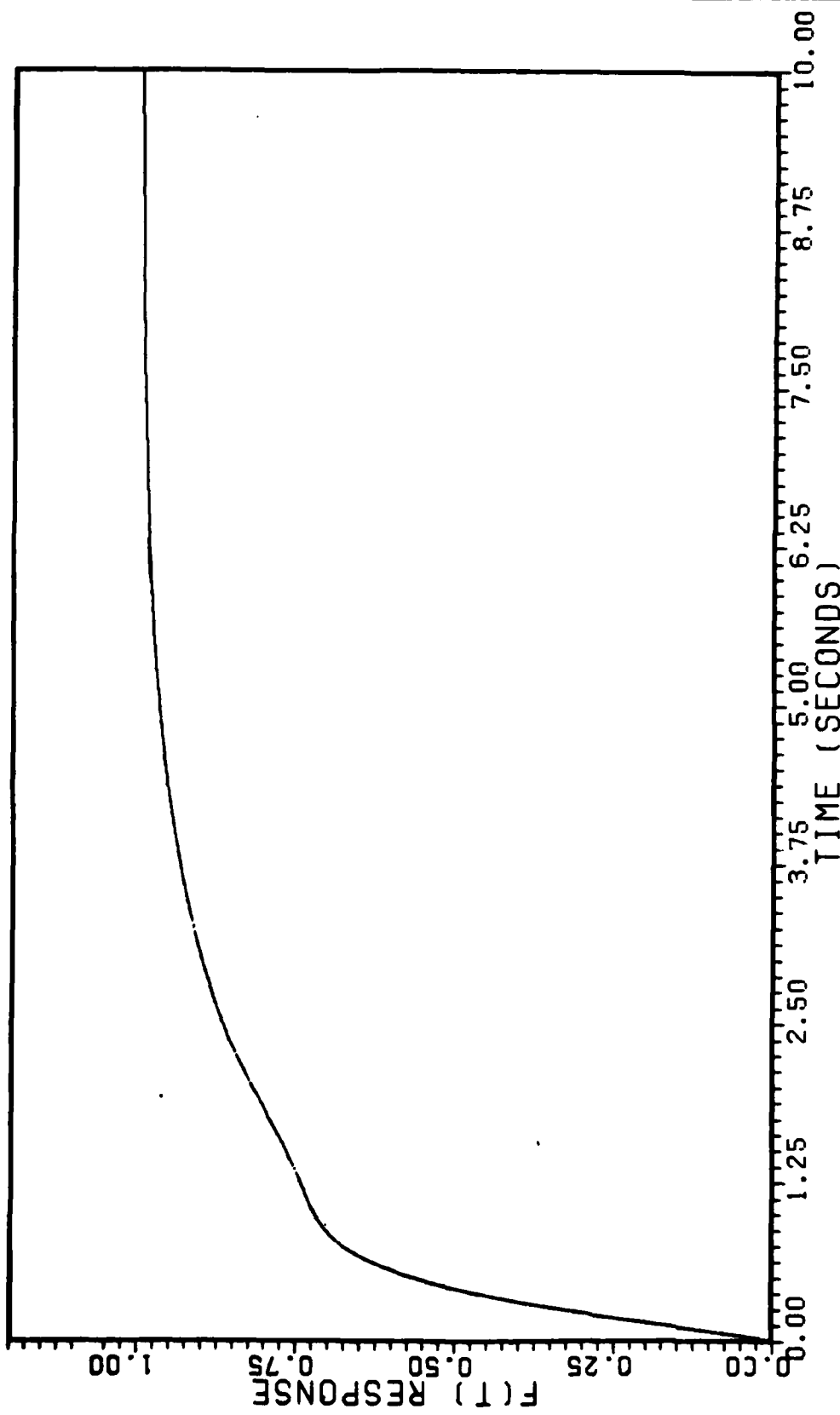
The 180 degrees lead introduced in  $G_{p_1}$  by not modeling the pilot delay, is the worst of the 4 cases.  $G_{p_2}$  and  $G_{p_3}$  provide similar responses in phase shift and are both off by about the same amount in magnitude. The 60 degrees phase lead  $G_{p_4}$  is the best of the 4 cases. Since the responses of  $G_{p_2}$  and  $G_{p_3}$  provide equivalent amounts of accuracy,  $G_{p_3}$  is eliminated from further consideration.

The step responses of the closed-loop optimal pilot/aircraft systems are examined to determine how well

the different discretization techniques approximate the continuous responses. The pilot models of Equations 56, 57 and 59 and the aircraft model of Equation 1 are used to form the close loop system. The closed loop responses are calculated and plotted using TOTAL. Three different discretization techniques are used. They are the backward rectangular rule, the Tustin's bilinear rule and the zero-order hold approximation.  $G_{P_1}$ ,  $G_{P_2}$ ,  $G_{P_4}$  are each discretized using each method giving a total of 9 plots for comparison. A plot of the continuous system is also presented for comparison with the discrete plots. The plots are presented in Figures 16 through 24. The sampling rate or time period for these plot is .1 second. A time period of .1 was chosen because this is the sampling rate used in the realtime simulation. In each case the discretization technique provides a time response that is an adequate approximation to the continuous. The most accurate discretization technique is the zero-order hold approximation. The zero-order hold approximation is essentially equivalent to the continuous with the exception that the output is held constant over the time interval.

In this section I will present the discretization of the pilot models by the 4 methods previously discussed. The discretization methods are as follows:

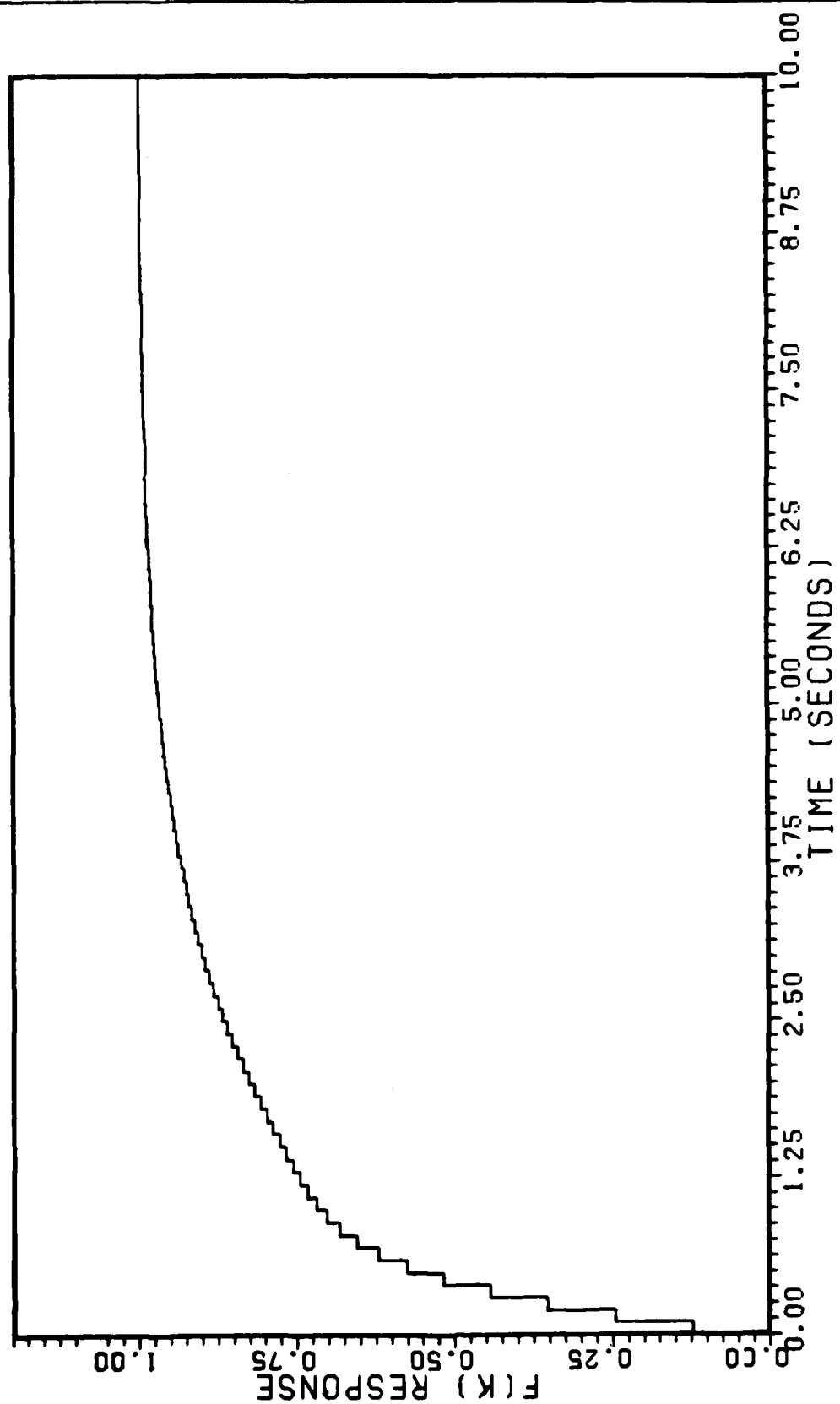
# OPTIMAL PILOT/AIRCRAFT SYSTEM CONTINUOUS



Step Response of Optimal  $G_{P1}(s)$ /Aircraft System (continuous)

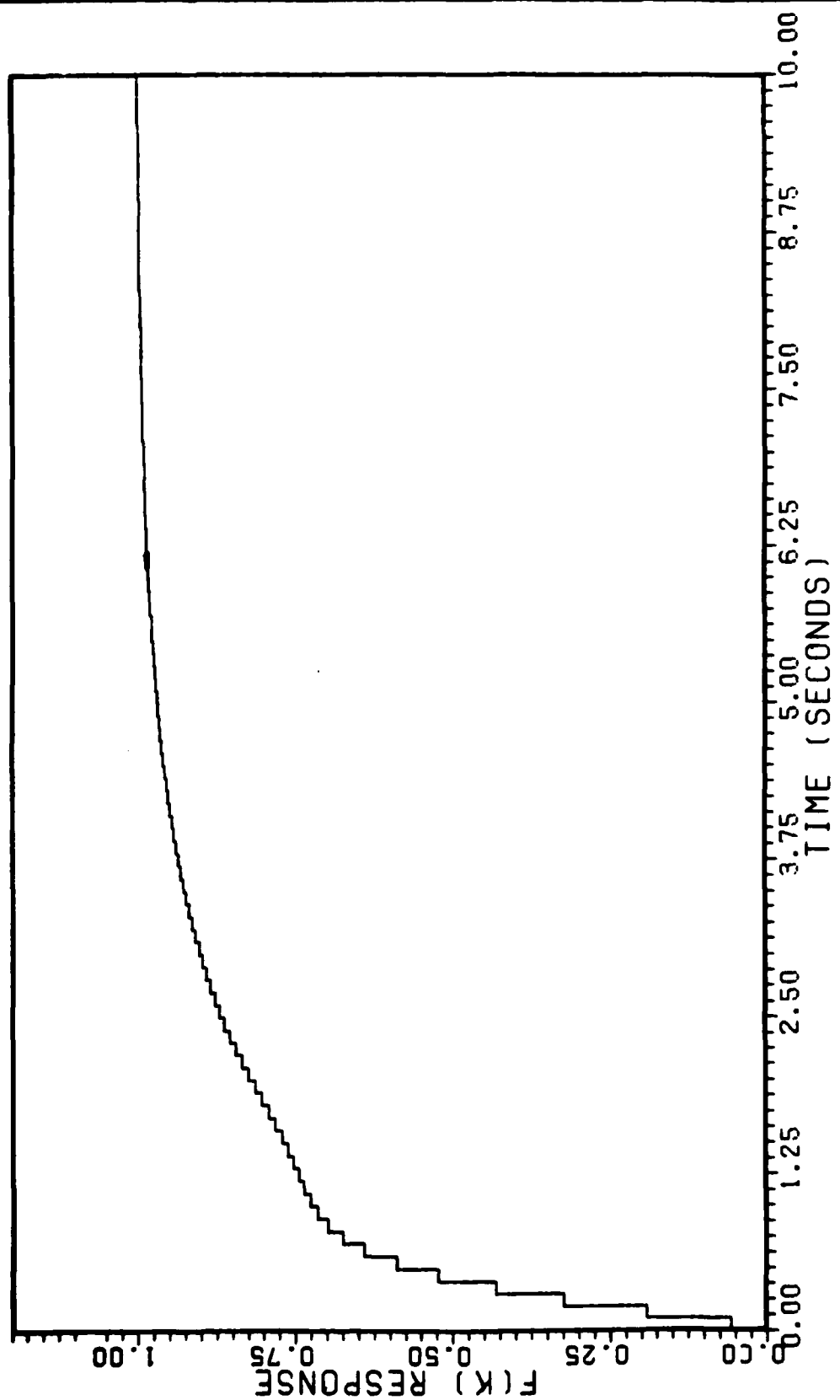
Figure 16

# OPTIMAL PILOT/AIRCRAFT SYSTEM DISCRETE BRR



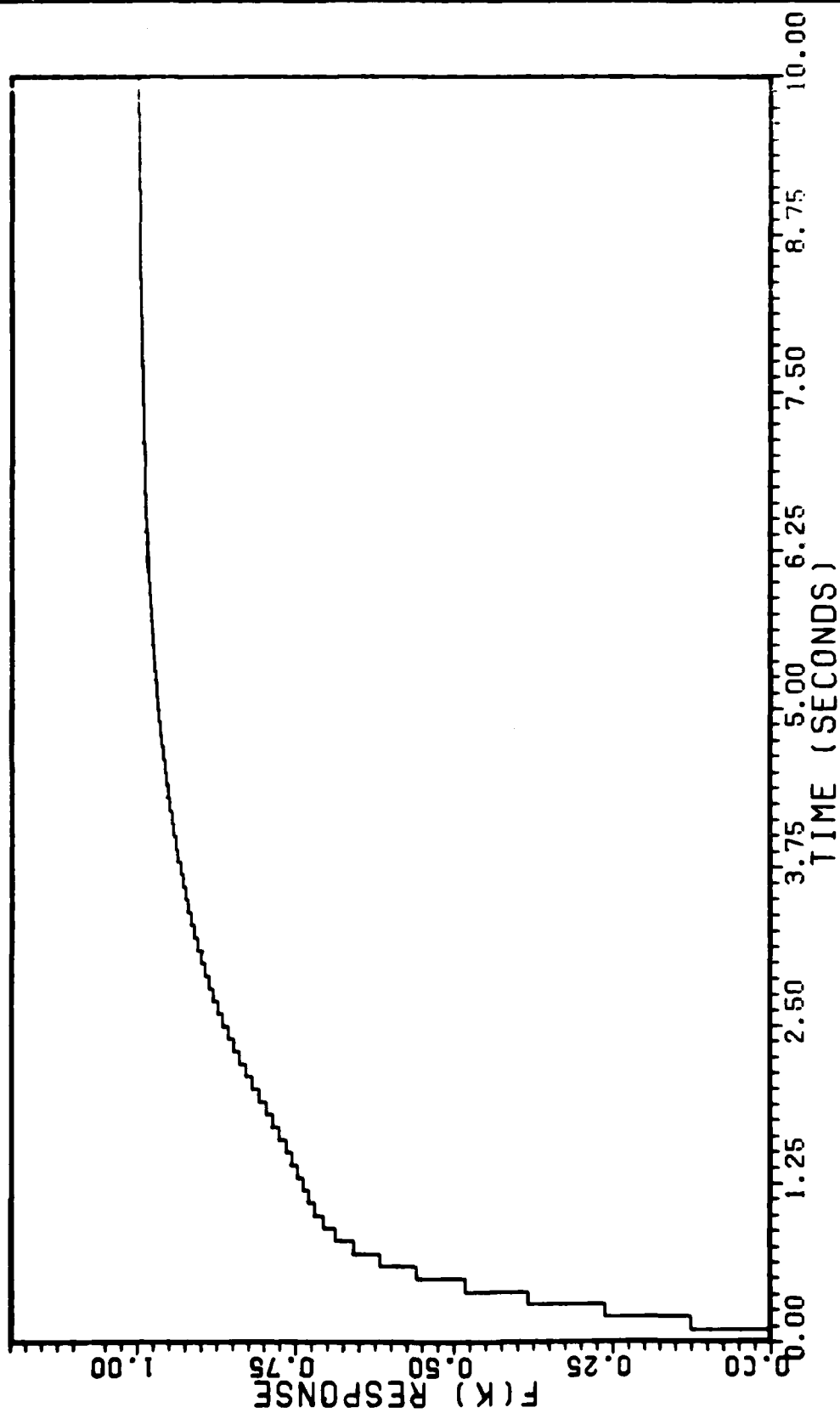
Step Response of Optimal  $G_p(z)/\text{Aircraft System}$   
(discretized by backward rectangular rule)  
Figure 17

# OPTIMAL PILOT/AIRCRAFT SYSTEM DISCRETE TUSTIN



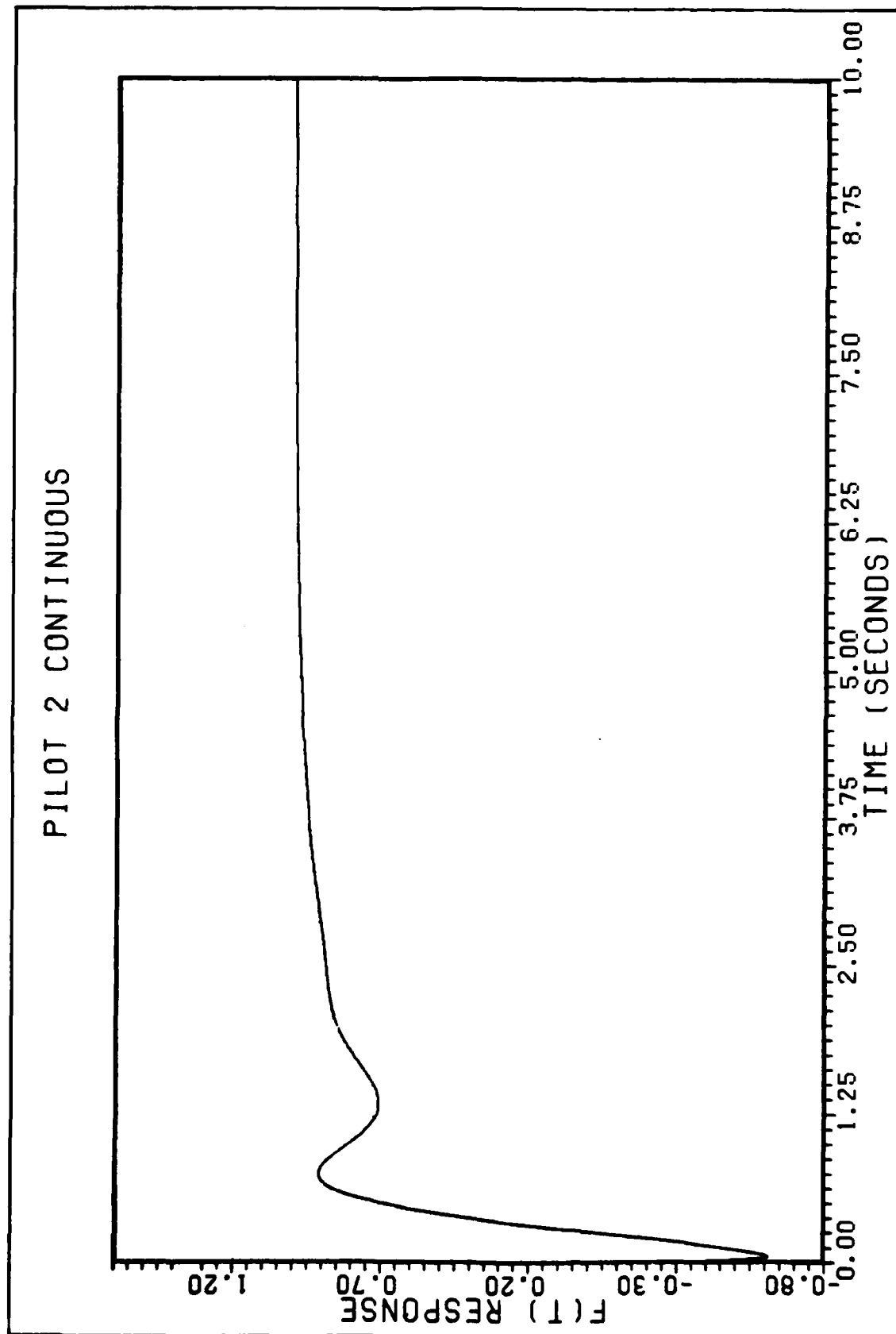
Step Response of Optimal  $G_{p1}(z)$ /Aircraft System  
(discretized by tustins bilinear rule)  
Figure 18

# PILOT 1 ZERO ORDER HOLD



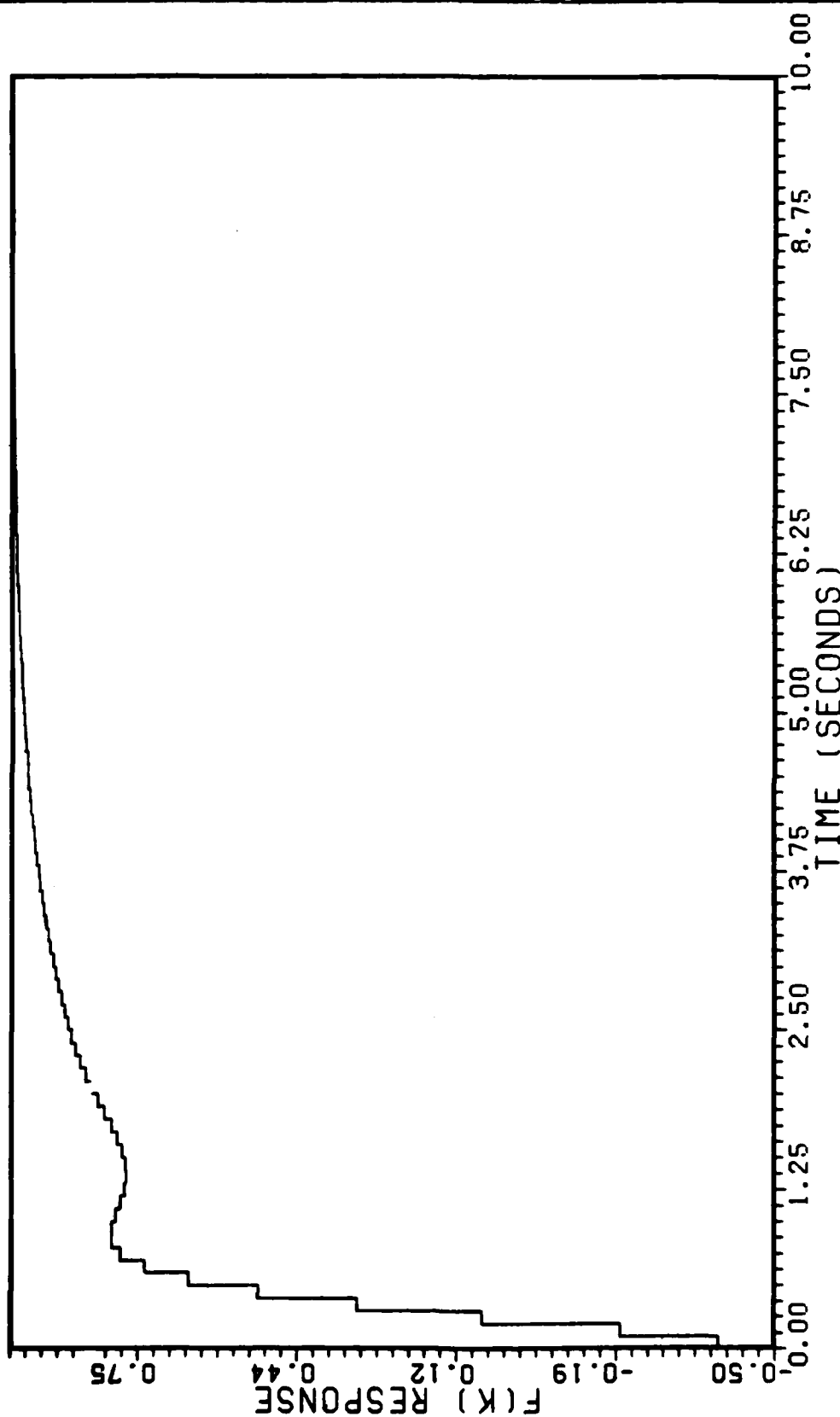
Step Response of Optimal  $G_p(z)/\text{Aircraft System}$   
(zero-order hold approximation)  
Figure 19

PILOT 2 CONTINUOUS



Step Response of Optimal  $G_{p2}(S)$ /Aircraft System  
(continuous)  
Figure 20

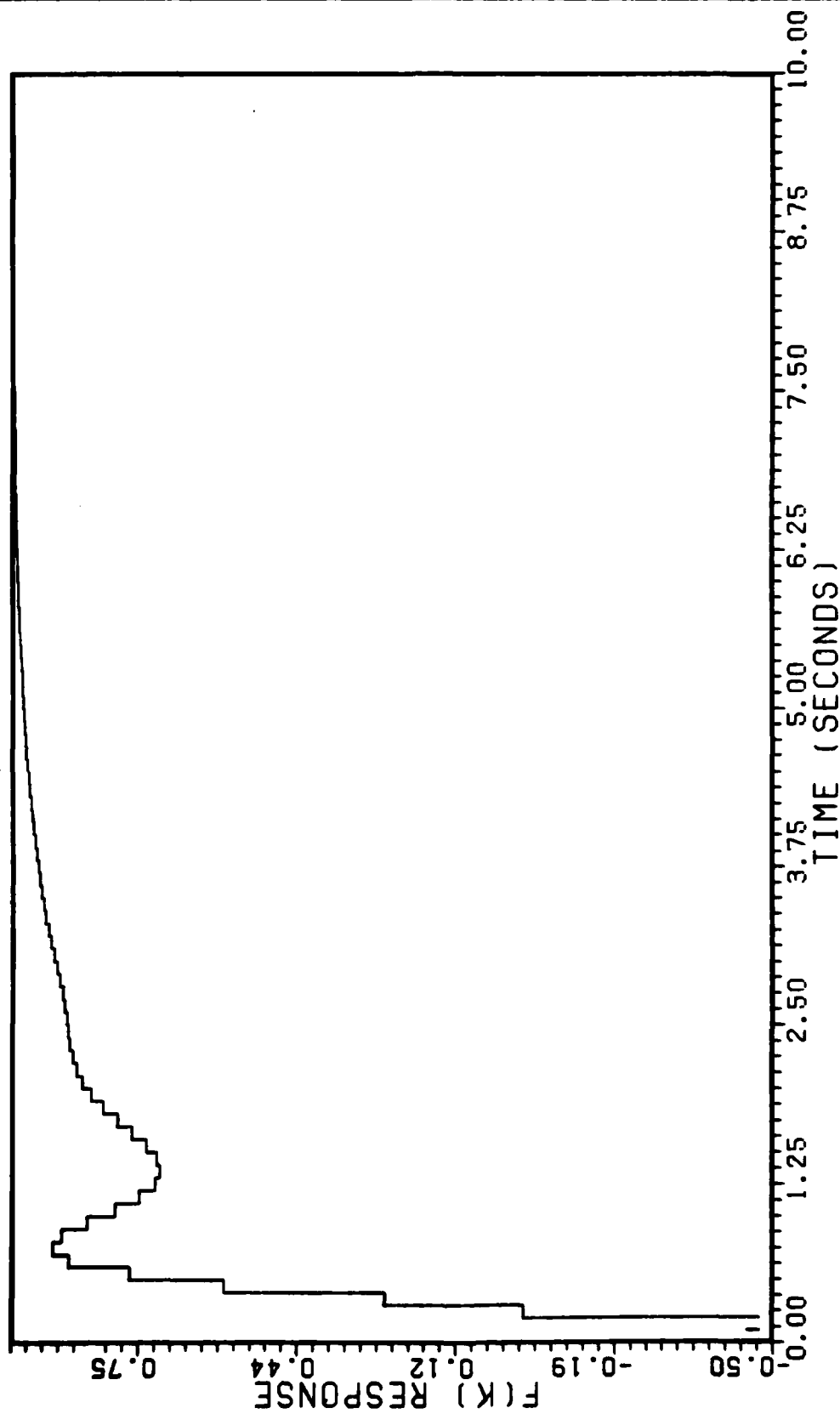
# PILOT 2 DISCRETE BRR



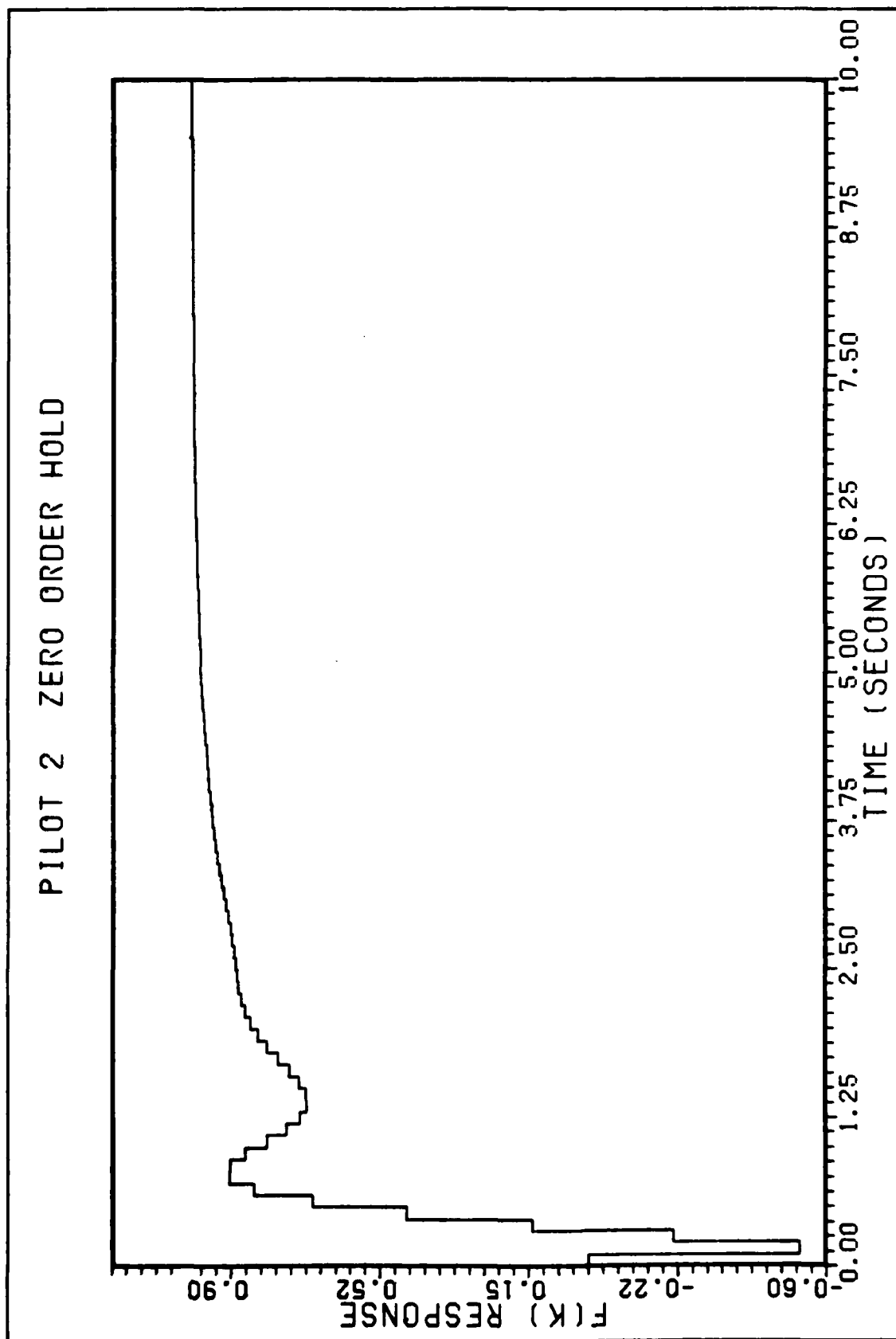
Step Response of Optimal  $G_{p2}(z)$ /Aircraft System  
(discretized by the backward rectangular rule)  
Figure 21



# PILOT 2 DISCRETE TUSTIN

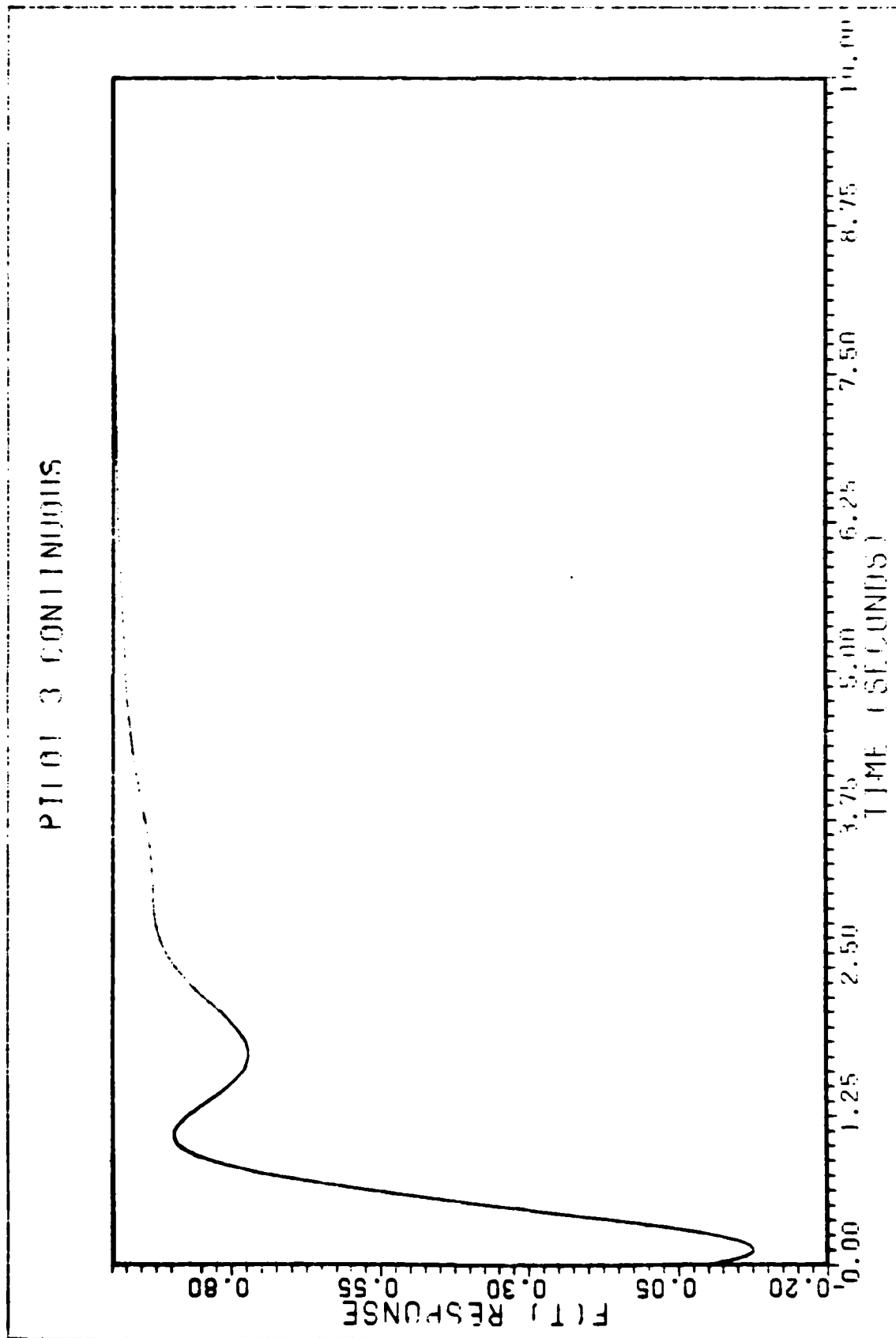


Step Response of Optimal  $Gp_2(z)$ /Aircraft System  
(discretized by tustins bilinear rule)  
Figure 22



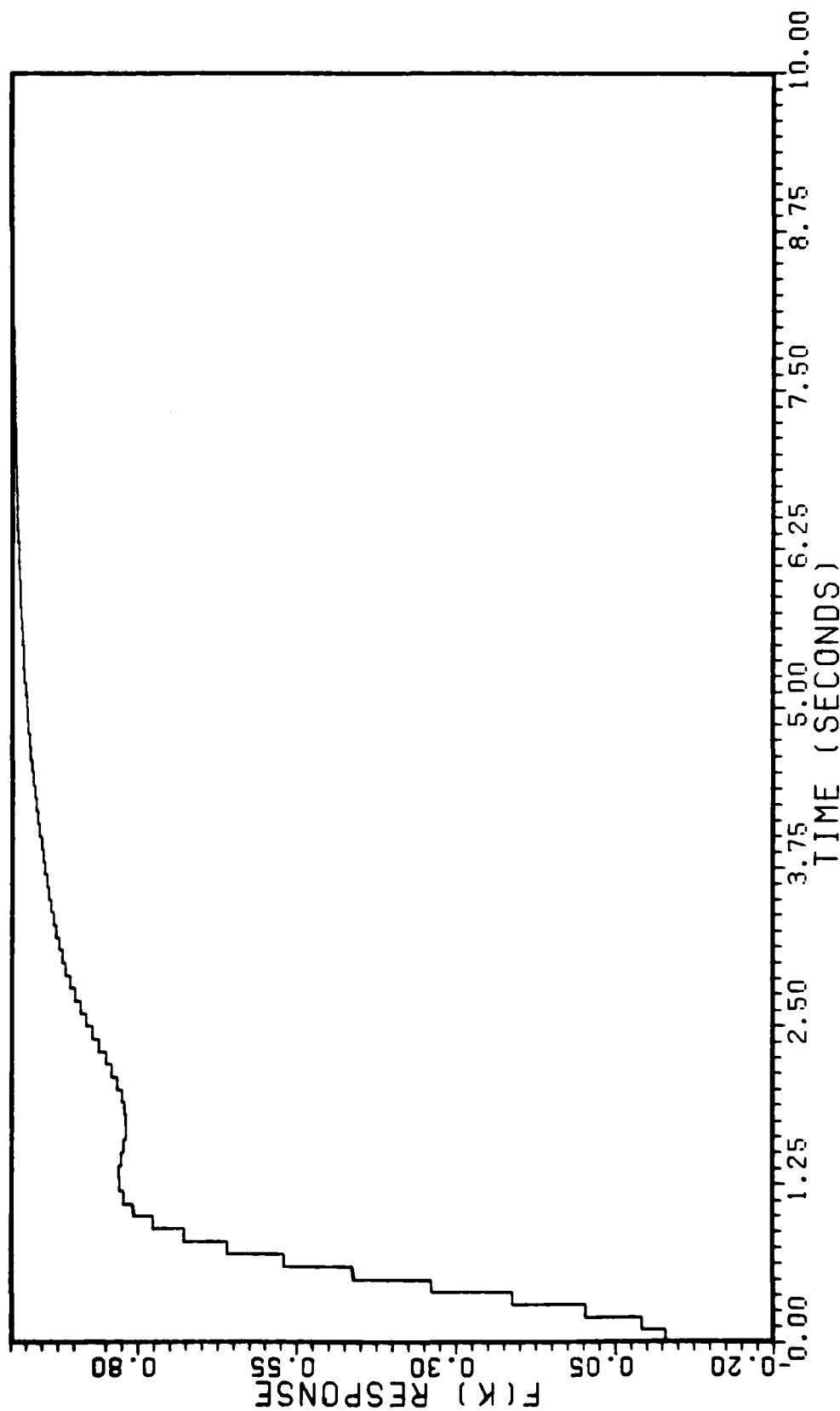
Step Response of Optimal  $G_{p2}(z)$ /Aircraft System  
(zero-order hold approximation)  
Figure 23

# Pilot 3 Continuous



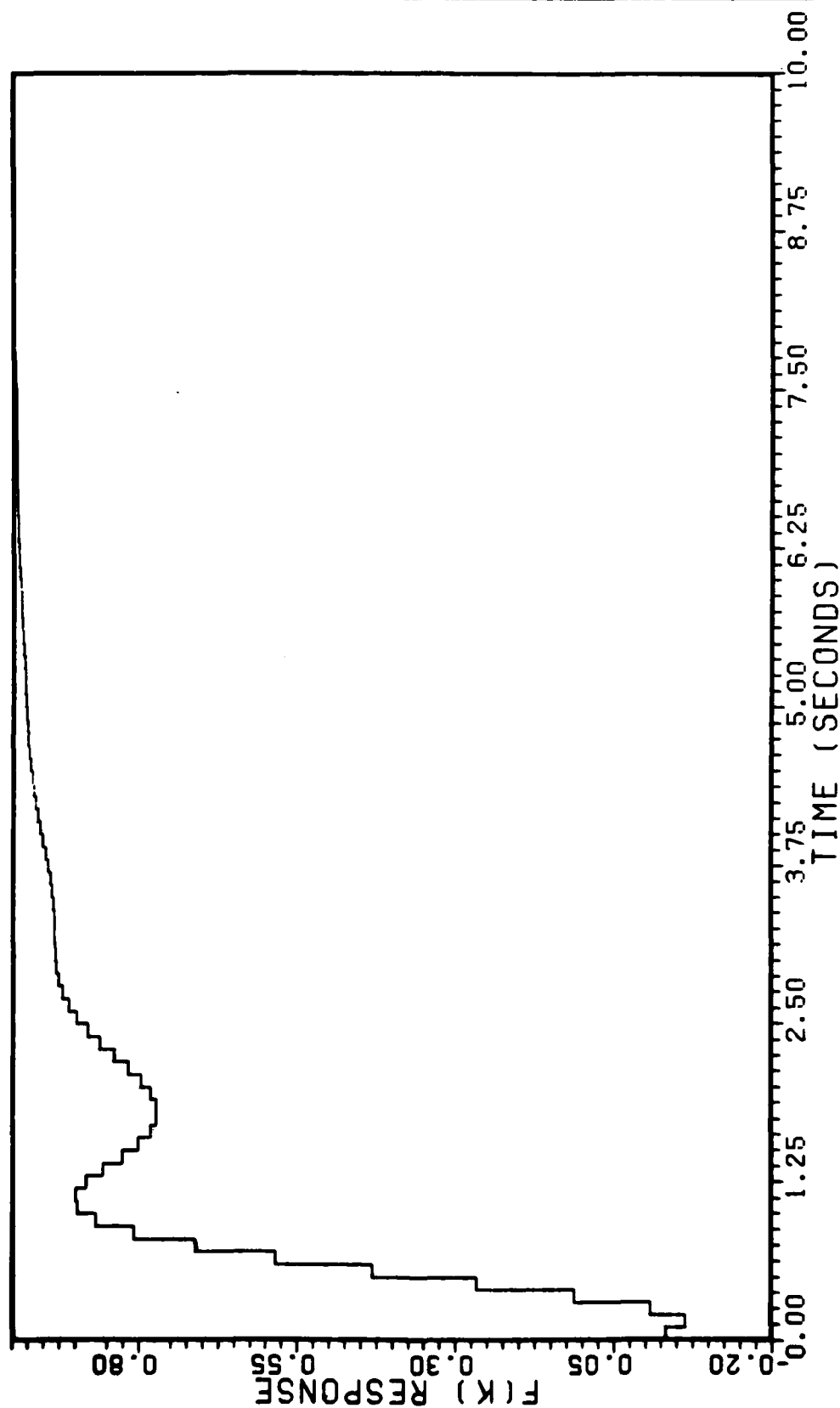
Step Response of Optimal  $Gp_4(s)$ /Aircraft System  
(continuous)  
Figure 24

# PILOT 3 DISCRETIZED BRR



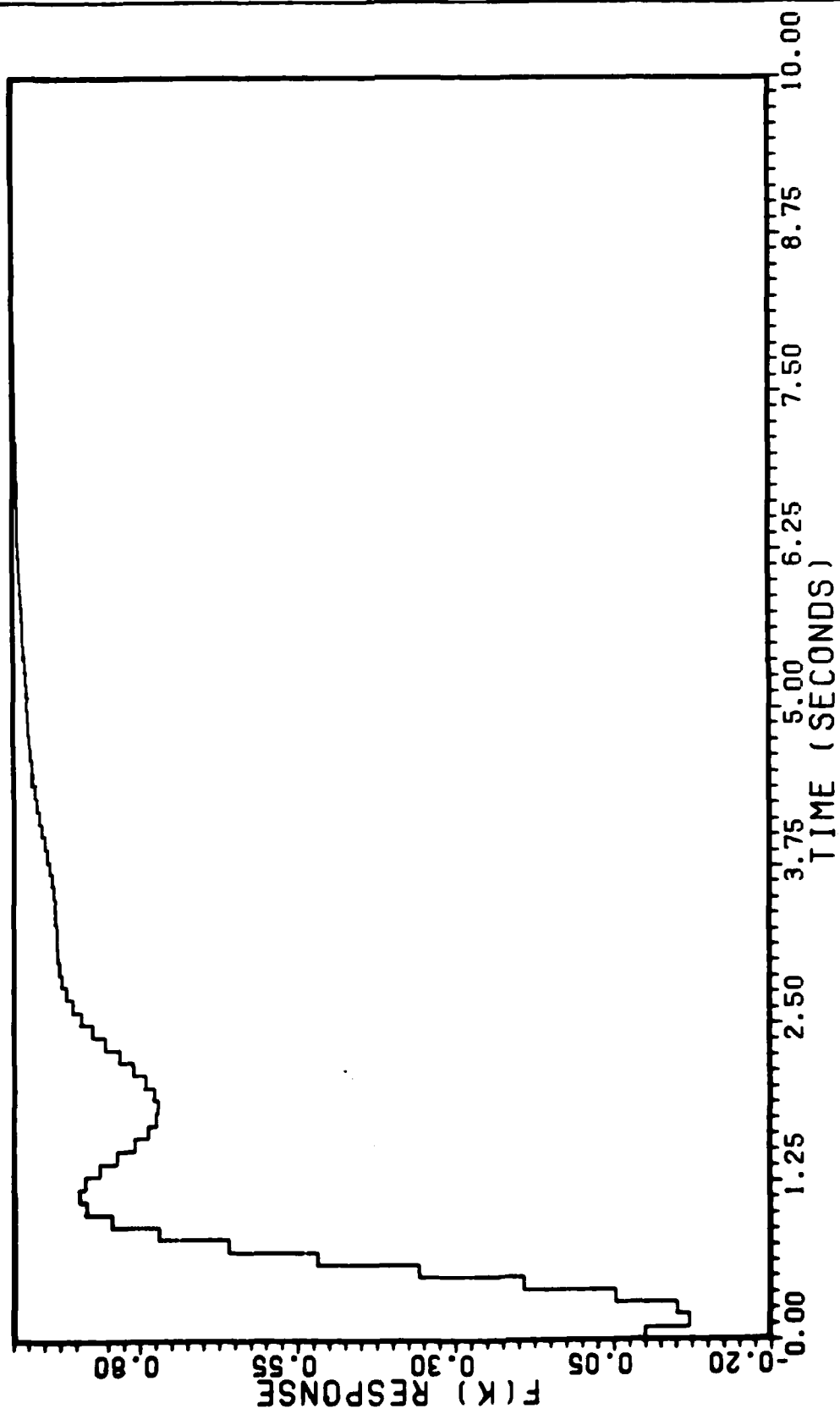
Step Response of Optimal  $Gp_4(z)/\text{Aircraft System}$   
(discretized by the backward rectangular rule)  
Figure 25

# PILOT 3 DISCRETIZED TUSTIN



Step Response of Optimal  $Gp_4(z)/\text{Aircraft}$  System  
(discretized by tustins bi-linear rule)  
Figure 26

PILOT 3 ZERO ORDER HOLD



Step Response of Optimal  $Gp_2(z)$ /Aircraft System  
(zero-order hold approximation)

Figure 27

1. Forward Rectangular Rule

$$s = \frac{Z-1}{T}$$

2. Backward Rectangular Rule

$$s = \frac{Z-1}{TZ}$$

3. Tustin's Bilinear Rule

$$s = \frac{2}{T} \frac{Z-1}{Z+1}$$

4. Zero Order Hold

$$H_{ho}(Z) = (1-Z^{-1}) \mathcal{Z} \left[ \frac{H(s)}{s} \right]$$

First I will discretize  $G_{p_1}$  using each of the 4 methods.

In order to make the discretization process easier I will put the pilot model in a convenient form.

$$G_{p_1}(s) = K_p \frac{\tau_1 s + 1}{\tau_2 s + 1} \quad (60)$$

$$= \frac{K_p \tau_1 s + K_p}{\tau_2 s + 1} \quad (60a)$$

$$= \frac{a_1 s + a_0}{b_1 s + b_0} \quad (60b)$$

Where

$$a_1 = K_p \tau_1 \quad (61a)$$

$$a_0 = K_p \quad (61b)$$

$$b_1 = \tau_2 \quad (61c)$$

$$b_0 = 1 \quad (61d)$$

Making the substitution for  $S$  given by the forward rectangular rule into Equation 60b and rearranging terms leads to the discrete transfer function given below as.

$$G_{p_1}(z) = \frac{\Lambda_1 z + \Lambda_0}{z + B_0} \quad (62)$$

Where

$$\Lambda_1 = \frac{a_1}{b_1} \quad (63a)$$

$$\Lambda_0 = \frac{(a_0 T - a_1)}{b_1} \quad (63b)$$

$$B_0 = \frac{(b_0 T - b_1)}{b_1} \quad (63c)$$

The coefficients  $\Lambda_1$ ,  $\Lambda_0$ ,  $B_0$  are identified by the RLS algorithm. It is necessary to use the values of  $\Lambda_0$ ,  $\Lambda_0$ ,  $B_0$  and Equations 61 and 63 in order to solve for  $K_p$ ,  $\tau_1$ , and  $\tau_2$ . The following set of equations solves for the pilot model parameters from Equations 61 and 63.

$$a_0 = \frac{\Lambda_0 + \Lambda_1}{1 + B_0} \quad (64a)$$

$$a_1 = \frac{\Lambda_1 T}{1 + B_0} \quad (64b)$$

$$b_1 = \frac{T}{1 + B_0} \quad (64c)$$

And

$$K_p = a_0 \quad (65a)$$

$$\tau_2 = b_1 \quad (65b)$$

$$\tau_1 = \frac{a_1}{a_0} \quad (65c)$$



The above equations are for the forward rectangular rule.  
 Making the substitution for  $S$  given by the backward  
 rectangular rule yields.

$$A_1 = \frac{a_1 + a_0 T}{b_1 + b_0 T} \quad (66a)$$

$$A_0 = \frac{-a_1}{b_1 + b_0 T} \quad (66b)$$

$$B_0 = \frac{-b_1}{b_1 + b_0 T} \quad (66c)$$

$$a_0 = \frac{A_0 + A_1}{B_0 + 1} \quad (67d)$$

$$a_1 = -\frac{TA_0}{B_0 + 1} \quad (67e)$$

$$b_1 = -\frac{TB_0}{B_0 + 1} \quad (67f)$$

The Tustin's bilinear rule yields.

$$A_1 = \frac{2a_1 + a_0 T}{2b_1 + b_0 T} \quad (68a)$$

$$A_0 = \frac{-2a_1 + a_0 T}{2b_1 + b_0 T} \quad (68a)$$

$$B_0 = \frac{-2b_1 + b_0 T}{2b_1 + b_0 T} \quad (68c)$$

$$a_0 = \frac{A_0 + A_1}{B_0 + 1} \quad (69a)$$

$$a_1 = \frac{T}{2} \frac{A_1 - A_0}{B_0 + 1} \quad (69b)$$

$$b_1 = -\frac{T}{2} \frac{(B_0 - 1)}{(B_0 + 1)} \quad (69c)$$

Equation sets 64, 67, and 69 can all be related to the pilot model parameters through equation set 65.

For the zero order hold approximation the pilot model of Equation 1a is first put in the following form.

$$G_p(s) = K_p \frac{\tau_1 s + 1}{\tau_2 s + 1} \quad (60a)$$

$$G_{p1}(s) = \left[ (K_p) \frac{\tau_1}{\tau_2} \right] \left[ \frac{s + 1/\tau_1}{s + 1/\tau_2} \right] \quad (70a)$$

$$= K \frac{(s + a)}{(s + b)} \quad (70b)$$

Where

$$K = K_p \frac{\tau_1}{\tau_2} \quad (71a)$$

$$a = 1/\tau_1 \quad (71b)$$

$$b = 1/\tau_2 \quad (71c)$$

The zero order hold approximation to  $G_{p1}$  is given by Equation 22.

Where

$$\frac{H(s)}{s} = \frac{K(s + a)}{s(s + b)} \quad (72)$$

It is convenient to use partial fraction expansion

$$\frac{K(s+a)}{s(s+b)} = \frac{r_1}{s} + \frac{r_2}{s+b} \quad (73)$$

Where

$$r_1 = K \frac{a}{b} \quad (74a)$$

$$r_2 = K \frac{(-b+a)}{-b} \quad (74b)$$

The Z-transform of Equation 73 is

$$H(Z) = \frac{r_1 Z}{Z-1} + \frac{r_2 Z}{Z-r_3} \quad (75)$$

Where

$$r_3 = \exp^{-bT} \quad (74c)$$

The zero order hold approximation is given by

$$H_{ho}(Z) = \frac{A_1 Z + A_0}{Z + B_0} \quad (76)$$

Where

$$A_1 = r_1 + r_2 \quad (77a)$$

$$A_0 = -r_2 - r_1 r_3 \quad (77b)$$

$$B_0 = -r_3 \quad (77c)$$

The zero order hold approximation was checked by using known values for  $K_p$ ,  $\tau_1$ ,  $\tau_2$  and calculating  $A_1$ ,  $A_0$  and  $B_0$  using Equations 71, 74 and 77. These numbers were then compared to the numbers obtained by using the discretize command found in MATRIX<sub>x</sub>. The results are identical. This serves to confirm that the required Equations 71, 74 and 77 are correct. Given  $A_0$ ,  $A_1$ , and  $B_0$  from an identification, it remains to relate these back to the pilot model parameters. The following set of equations will accomplish this.

$$r_1 = \frac{A_1 + A_0}{1 + B_0} \quad (78a)$$

$$r_2 = \frac{A_1 B_0 - A_0}{1 + B_0} \quad (78b)$$

$$r_3 = -B_0 \quad (78c)$$

$$K = r_1 + r_2 \quad (79a)$$

$$a = \frac{r_1 \ln(r_3)}{-T(r_1 + r_2)} \quad (79b)$$

$$b = \frac{\ln(r_3)}{-T} \quad (79c)$$

$$K_p = Ka/b \quad (80a)$$

$$\tau_1 = 1/a \quad (80b)$$

$$\tau_2 = 1/b \quad (80c)$$

#### Discretization of Pilot Model 2

$$\begin{aligned} G_{p_2}(s) &= K_p (1 - \tau_3 s) \frac{(\tau_1 s + 1)}{(\tau_2 s + 1)} \\ &= \frac{-K_p \tau_1 \tau_3 s^2 + K_p (\tau_1 - \tau_3) s + K_p}{\tau_2 s + 1} \end{aligned} \quad (81a)$$

$$= \frac{a_2 s^2 + a_1 s + a_0}{b_1 s + b_0} \quad (81b)$$

Where

$$a_2 = -K_p \tau_1 \tau_3 \quad (82a)$$

$$a_1 = K_p (\tau_1 - \tau_3) \quad (82b)$$

$$a_0 = K_p \quad (82c)$$

$$b_1 = \tau_2 \quad (82d)$$

$$b_0 = 1. \quad (82e)$$

Pilot model 2 was discretized using the 4 methods previously discussed. Equation 81b is an improper transfer function. After discretization it is still improper when using the forward rectangular rule, backward rectangular rule, and the zero-order-hold approximation.

When using Tustin's bilinear rule to discretize Equation 81b the result is a proper discrete transfer function. Since the RLS feature of MATRIX<sub>x</sub> can only be used with proper discrete transfer functions this will be the only technique used with pilot model 2. Using Tustins bilinear rule to discretize Equation 81b yields

$$G_{P_2}(z) = \frac{A_2 z^2 + A_1 z + A_0}{z^2 + B_1 z + B_0} \quad (83)$$

Where

$$A_2 = \frac{\frac{4a_2}{T^2} + \frac{2a_1}{T} + a_0}{\frac{2b_1}{T} + b_0} \quad (84a)$$

$$A_1 = \frac{-\frac{8a_2}{T} + 2a_0}{\frac{2b_1}{T} + b_0} \quad (84b)$$

$$A_0 = \frac{\frac{4a_2}{T} - \frac{2a_1}{T} + a_0}{\frac{2b_1}{T} + b_0} \quad (84c)$$

$$B_1 = \frac{2b_0}{\frac{2b_1}{T} + b_0} \quad (84d)$$

$$B_0 = \frac{-\frac{2b_1}{T} + b_0}{\frac{2b_1}{T} + b_0} \quad (84e)$$

The coefficients  $\Delta_2$ ,  $\Delta_1$ ,  $\Delta_0$ ,  $B_1$ ,  $B_0$  are identified by the RLS algorithm. The following set of equations relates these to the pilot model parameters.

$$b_0 = 1. \quad (85a)$$

$$b_1 = T \left[ \frac{1}{B_1} + \frac{1}{2} \right] \quad (85b)$$

Let the common denominator of Equation 84a through 84d equal.

$$\Delta_2 = \frac{2b_1}{T} + b_0 \quad (86)$$

Then from Equations 84a through 84c form the following matrix equation.

$$e_0 = T^2 \Delta_2 \Delta_0 \quad (87a)$$

$$e_1 = T^2 \Delta_2 \Delta_1 \quad (87b)$$

$$e_2 = T^2 \Delta_2 \Delta_2 \quad (87c)$$

$$\begin{bmatrix} T^2 & 2T & 4 \\ 2T^2 & 0 & -8 \\ T^2 & -2T & 4 \end{bmatrix} \begin{bmatrix} a_0 \\ a_1 \\ a_2 \end{bmatrix} = \begin{bmatrix} e_0 \\ e_1 \\ e_2 \end{bmatrix} \quad (88)$$

$$\begin{bmatrix} a_0 \\ a_1 \\ a_2 \end{bmatrix} = \begin{bmatrix} \tau^2 & 2\tau & 4 \\ 2\tau^2 & 0 & -8 \\ \tau^2 & -2\tau & 4 \end{bmatrix}^{-1} \begin{bmatrix} e_0 \\ e_1 \\ e_2 \end{bmatrix} \quad (89)$$

It is necessary to use the quadratic equation and Equations 82 to solve for the pilot model parameters.

Let

$$a = 1$$

$$b = \frac{a_1}{a_0}$$

$$c = \frac{a_2}{a_0}$$

$$\tau_3 = \frac{-b + \sqrt{b^2 - 4ac}}{2a}$$

The positive value of  $\tau_3$  is selected in each case.

$$\tau_1 = \frac{a_1}{a_0} + \tau_3$$

$$K_p = a_0$$

#### Discretization of Pilot Model 4

$$G_{p4}(s) = K_p \left[ \frac{1 - \tau_3 s}{1 + \tau_3 s} \right] \left[ \frac{\tau_1 s + 1}{\tau_2 s + 1} \right] \quad (90a)$$

$$= - \frac{K_p \tau_1 \tau_3 s^2 + K_p (\tau_1 - \tau_3) s + K_p}{\tau_2 \tau_3 s^2 + (\tau_2 + \tau_3) s + 1} \quad (90b)$$

$$= \frac{a_2 s^2 + a_1 s + a_0}{b_1 s + b_0} \quad (90c)$$

Where

$$a_2 = -K_p \tau_1 \tau_3 \quad (91c)$$

$$a_1 = K_p (\tau_1 - \tau_3) \quad (91b)$$

$$a_0 = K_p \quad (91c)$$

$$b_2 = \tau_2 \tau_3 \quad (92a)$$

$$b_1 = (\tau_2 + \tau_3) \quad (92b)$$

$$b_0 = 1 \quad (92c)$$

Since Equation 90c is a proper transfer function it is also a proper transfer function after it is discretized. Equation 90c is discretized using each of the 4 discretization methods. After discretization Equation 90c is of the following form.

$$G_{p4}(z) = \frac{\lambda_2 z^2 + \lambda_1 z + \lambda_0}{z^2 + B_1 z + B_0} \quad (93)$$

The forward rectangular rule yields

$$\lambda_2 = \frac{\frac{a_2}{\tau^2}}{\frac{b_2}{\tau^2}} \quad (94a)$$

$$\lambda_1 = \frac{-\frac{2a_2}{\tau^2} + \frac{a_1}{\tau}}{\frac{b_2}{\tau^2}} \quad (94b)$$



$$A_0 = \frac{\frac{a_2}{T^2} - \frac{a_1}{T} + a_0}{\frac{a_2}{T^2}} \quad (94c)$$

$$B_1 = \frac{-\frac{2b_2}{T^2} + \frac{b_1}{T}}{\frac{b_2}{T^2}} \quad (94d)$$

$$B_0 = \frac{\frac{b_2}{T^2} - \frac{b_1}{T} + b_0}{\frac{b_2}{T^2}} \quad (94e)$$

The following set of equations solves for  $a_0, a_1, a_2, b_0, b_1, b_2$  given  $B_0, B_1, A_0, A_1, A_2$ .

$$b_0 = 1 \quad (95a)$$

$$b_1 = \frac{-T(2 - B_1)}{(B_1 + B_2 - 1)} \quad (95b)$$

$$b_2 = \frac{-T^2}{(B_1 + B_2 - 1)} \quad (95c)$$

Let the common denominator of Equation 94a through 94c equal.

$$\Delta_3 = \frac{b_2}{T^2} \quad (96)$$

$$e_0 = T^2 \Delta_3 A_2$$

$$e_1 = T^2 \Delta_3 A_1$$

$$e_2 = T^2 \Delta_3 A_0$$

$$\begin{bmatrix} 0 & 0 & 1 \\ 0 & T & -2 \\ T^2 & -T & 1 \end{bmatrix} \begin{bmatrix} a_0 \\ a_1 \\ a_2 \end{bmatrix} = \begin{bmatrix} e_0 \\ e_1 \\ e_1 \end{bmatrix} \quad (97)$$

$$\begin{bmatrix} a_0 \\ a_1 \\ a_2 \end{bmatrix} = \begin{bmatrix} 0 & 0 & 1 \\ 0 & T & -2 \\ T^2 & -T & 1 \end{bmatrix} \begin{bmatrix} e_0 \\ e_1 \\ e_2 \end{bmatrix} \quad (98)$$

The backward rectangular rule yields

$$\lambda_2 = \frac{\frac{a_2}{T^2} + \frac{a_1}{T} + a_0}{\frac{b_2}{T^2} + \frac{b_1}{T} + b_0} \quad (99a)$$

$$\lambda_1 = \frac{\frac{-2a_2}{T^2} - \frac{a_1}{T}}{\frac{b_2}{T^2} + \frac{b_1}{T} + b_0} \quad (99b)$$

$$\lambda_0 = \frac{\frac{a_2}{T^2}}{\frac{b_2}{T^2} + \frac{b_1}{T} + b_0} \quad (99c)$$

$$B_1 = \frac{\frac{-2b_2}{T^2} - \frac{b_1}{T}}{\frac{b_2}{T^2} + \frac{b_1}{T} + b_0} \quad (99d)$$

$$B_0 = \frac{\frac{b_2}{T^2}}{\frac{b_2}{T^2} + \frac{b_1}{T} + b_0} \quad (99e)$$

AD-A198 873

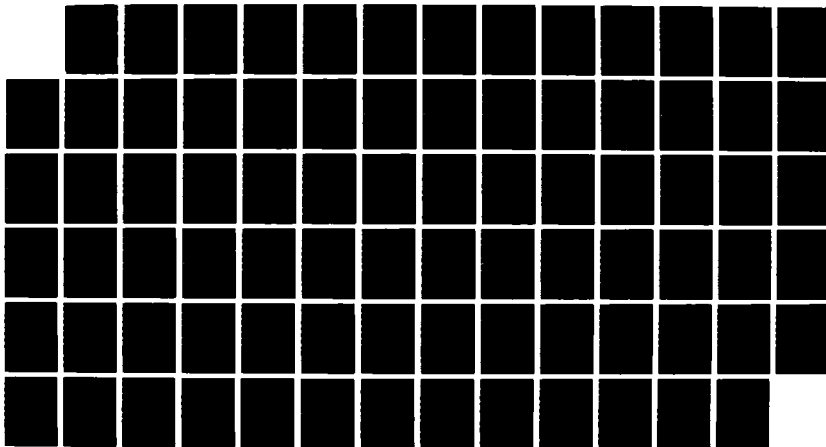
REALTIME PILOT MODEL PARAMETER IDENTIFICATION(U) AIR  
FORCE INST OF TECH WRIGHT-PATTERSON AFB OH  
M R ROSENBLEETH DEC 87 AFIT/GAE/RA/87D-19

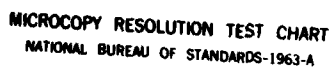
2/2

UNCLASSIFIED

F/G 1/3.3

ML





**MICROCOPY RESOLUTION TEST CHART**  
**NATIONAL BUREAU OF STANDARDS-1963-A**

The following set of equations solves for  $a_1, a_1, a_2,$   
 $b_0, b_1, b_2$  given  $B_0, B_1, \Lambda_0, \Lambda_1, \Lambda_2.$

$$b_0 = 1.$$

Let

$$e_1 = -B_0 T^2$$

$$e_2 = -B_1 T^2$$

Then  $b_1,$  and  $b_2$  can be found from the matrix equation.

$$\begin{bmatrix} B_0 T & (B_0 - 1) \\ (B_1 + 1) T & (B_1 + 2) \end{bmatrix} \begin{bmatrix} b_1 \\ b_2 \end{bmatrix} = \begin{bmatrix} e_1 \\ e_2 \end{bmatrix} \quad (100)$$

$$\begin{bmatrix} b_1 \\ b_2 \end{bmatrix} = \begin{bmatrix} B_0 T & B_0 - 1 \\ (B_1 + 1) T & B_1 + 2 \end{bmatrix}^{-1} \begin{bmatrix} e_1 \\ e_2 \end{bmatrix} \quad (101)$$

Let the common denominator of Equation 99a through  
 99c equal

$$\Delta_4 = \frac{b_2}{T^2} + \frac{b_1}{T} + b_0$$

The Equations 99a through 99c can be solved by the  
 following equations.

$$\begin{aligned} e_0 &= \Delta_4 \Lambda_2 T^2 \\ e_1 &= \Delta_4 \Lambda_1 T^2 \\ e_2 &= \Delta_4 \Lambda_0 T^2 \end{aligned}$$

$$\begin{bmatrix} T^2 & T & 1 \\ 0 & -T & -2 \\ 0 & 0 & 1 \end{bmatrix} \begin{bmatrix} a_0 \\ a_1 \\ a_2 \end{bmatrix} = \begin{bmatrix} e_0 \\ e_1 \\ e_2 \end{bmatrix} \quad (102)$$

$$\begin{bmatrix} a_0 \\ a_1 \\ a_2 \end{bmatrix} = \begin{bmatrix} T^2 & T & 1 \\ 0 & -T & -2 \\ 0 & 0 & 1 \end{bmatrix}^{-1} \begin{bmatrix} e_0 \\ e_1 \\ e_2 \end{bmatrix} \quad (103)$$

The Tustin's bilinear rule yields

$$A_2 = \frac{\frac{4a_2}{T^2} + \frac{2a_1}{T} + a_0}{\frac{4b_2}{T^2} + \frac{2b_1}{T} + b_0} \quad (104a)$$

$$A_1 = \frac{\frac{-8a_2}{T^2} + 2a_0}{\frac{4b_2}{T^2} + \frac{2b_1}{T} + b_0} \quad (104b)$$

$$A_0 = \frac{\frac{4a_2}{T^2} + \frac{2a_1}{T} + a_0}{\frac{4b_2}{T^2} + \frac{2b_1}{T} + b_0} \quad (104c)$$

$$B_1 = \frac{\frac{-8b_2}{T^2} + \frac{2b_0}{T}}{\frac{4b_2}{T^2} + \frac{2b_1}{T} + b_0} \quad (104d)$$

$$B_2 = \frac{\frac{4b_2}{T^2} - \frac{2b_1}{T} + b_0}{\frac{4b_2}{T^2} + \frac{2b_1}{T} + b_0} \quad (104e)$$

The following set of equations solves for  $a_0, a_1, a_2, b_0, b_1, b_2$  given  $B_0, B_1, A_0, A_1, A_2$

$$\begin{aligned} \text{Let } b_0 &= 1 \\ e_1 &= -T^2(B_1 + 2) \\ e_2 &= -T^2(B_2 + 1) \end{aligned}$$

Then  $b_1$  and  $b_2$  can be found from the following matrix equation.

$$\begin{bmatrix} 2B_1T & 4(B_1-2) \\ 2(B_2-1)T & 4(B_2+1) \end{bmatrix} \begin{bmatrix} b_1 \\ b_2 \end{bmatrix} = \begin{bmatrix} e_1 \\ e_2 \end{bmatrix} \quad (105)$$

$$\begin{bmatrix} b_1 \\ b_2 \end{bmatrix} = \begin{bmatrix} 2B_2T & 4(B_1-2) \\ 2(B_2-1)T & 4(B_2+1) \end{bmatrix}^{-1} \begin{bmatrix} e_1 \\ e_2 \end{bmatrix} \quad (106)$$

Let the common denominator of Equation 104a through 104c equal

$$\Delta_5 = \frac{4b_2}{T^2} + \frac{2b_1}{T} + b_0$$

The equations 104a through 104c can be solved for  $a_0, a_1, a_2$ , from the following set of equations.

$$\begin{aligned} e_0 &= T^2 \Delta_5 A_2 \\ e_1 &= T^2 \Delta_5 A_1 \\ e_2 &= T^2 \Delta_5 A_0 \end{aligned}$$

$$\begin{bmatrix} T^2 & 2T & 4 \\ 2T^2 & 0 & -8 \\ T^2 & -2T & 4 \end{bmatrix} \begin{bmatrix} a_0 \\ a_1 \\ a_2 \end{bmatrix} = \begin{bmatrix} e_0 \\ e_1 \\ e_2 \end{bmatrix} \quad (107)$$

$$\begin{bmatrix} a_0 \\ a_1 \\ a_2 \end{bmatrix} = \begin{bmatrix} T^2 & 2T & 4 \\ 2T^2 & 0 & -8 \\ T^2 & -2T & 4 \end{bmatrix}^{-1} \begin{bmatrix} e_0 \\ e_1 \\ e_2 \end{bmatrix} \quad (108)$$

For each of the discretization techniques just presented  $a_0$ ,  $a_2$ ,  $b_0$ ,  $b_2$ , and  $b_2$  are all related to  $K_p$ ,  $\tau_1$ ,  $\tau_2$ , and  $\tau_3$  through the same set of equations. Equations 91a through 92f are used to solve for the pilot model parameters once having solved for  $a_0$ ,  $a_1$ ,  $a_2$ ,  $b_0$ ,  $b_1$ ,  $b_2$ , for each of the techniques. The quadratic equation is used for solving for  $\tau_1$ .

$$K_p = a_0 \quad (109)$$

let

$$a = 1.$$

$$b = -\frac{1}{a_0}$$

$$c = \frac{a_2}{a_0}$$

then

$$\tau_1 = \frac{-b + \sqrt{b^2 - 4ac}}{2a} \quad (110)$$

the sign is chosen such that  $\tau_1$  is positive.

$$\tau_3 = \tau_1 + b \quad (111)$$

$$\tau_2 = \frac{b_2}{\tau_3} \quad (112)$$

The zero-order hold technique is also used to discretize Equation 90a. When using the zero-order hold technique



the following format is more convenient than Equation 90c.

$$G_{p_4}(s) = \frac{\Lambda_2 s^2 + a_1 s + a_0}{(s + b_1)(s + b_2)} \quad (113)$$

Where

$$a_2 = -K_p \frac{\tau_1 \tau_3}{\tau_2 \tau_3} \quad (114a)$$

$$a_1 = K_p \frac{(\tau_1 - \tau_3)}{\tau_2 \tau_3} \quad (114b)$$

$$a_0 = \frac{K_D}{\tau_2 \tau_3} \quad (114c)$$

$$b_1 = \frac{1}{\tau_2} \quad (114d)$$

$$b_2 = \frac{1}{\tau_3} \quad (114e)$$

the zero-order hold approximation to  $G_{p_4}$  is given by Equation 22 where

$$\frac{H(s)}{s} = \frac{\Lambda_2 s^2 + a_1 s + a_0}{s(s + b_1)(s + b_2)} \quad (115)$$

as before it is convenient to use partial fraction expansion.

$$\frac{H(s)}{s} = \frac{r_1}{s} + \frac{r_2}{s + b_1} + \frac{r_3}{s + b_2} \quad (116)$$

Where

$$r_1 = \frac{a_0}{b_1 b_2} \quad (117a)$$

$$r_2 = \frac{a_2 b^2 - a_1 b_1 + a_0}{-b_1 (-b_1 + b_2)} \quad (117b)$$

$$r_3 = \frac{a_2 b_2 - a_1 b_2 + a_0}{-b_1 (-b_1 + b_2)} \quad (117c)$$

The Z-transform of Equation 116 is

$$H(z) = \frac{r_1 z}{z-1} + \frac{r_2 z}{z-r_4} + \frac{r_3 z}{z-r_5} \quad (118)$$

Where  $r_4 = \exp^{-b_1 T}$  (117d)

$$r_5 = \exp^{-b_2 T} \quad (117e)$$

The zero-order hold approximation to  $G_{p_4}$  is

$$H_{ho}(z) = (1-z^{-1}) \mathcal{Z} \left[ \frac{H(s)}{s} \right] \quad (119)$$

this can be written in its simplest form as

$$H_{ho}(z) = \frac{A_2 z^2 + A_1 z + A_0}{z^2 + B_1 z + B_0} \quad (120)$$

Where

$$A_2 = r_1 + r_2 + r_3 \quad (121a)$$

$$A_1 = r_1(-r_4-r_5) + r_2(-1-r_5) + r_3(-1-r_4) \quad (121b)$$

$$A_0 = r_1 r_4 r_5 + r_2 r_5 + r_3 r_4 \quad (121c)$$

$$B_1 = -r_4 - r_5 \quad (121d)$$

$$B_0 = r_4 r_5 \quad (121e)$$

The zero order hold approximation for  $G_{p4}$  was checked using known values for  $K_p$ ,  $T_1$ ,  $T_2$ ,  $T_3$  and calculating  $A_2$ ,  $A_1$ ,  $A_0$ ,  $B_1$ , and  $B_0$ . These numbers were then compared to the numbers obtained using the discretize command found in  $MATRIX_x$ . The results are identical. This serves to confirm that Equations 114, 117, and 121 are indeed correct. Given the values of  $A_2$ ,  $A_1$ ,  $A_0$ ,  $B_1$ ,  $B_0$  from identification using the RLS algorithm it remains to relate these coefficients back to the pilot model parameters. The following set of equations will accomplish this.

The quadratic equation may be used to solve Equations 121d and 121e simultaneously for  $r_4$  and  $r_5$ .

$$\begin{aligned} \text{Let} \quad a &= 1 \\ b &= B_1 \\ c &= B_0 \end{aligned}$$

$$r_5 = \frac{-b + \sqrt{b^2 - 4ac}}{2a} \quad (122)$$

$$r_4 = -B_1 - r_5 \quad (123)$$

The above values of  $r_4$  and  $r_5$  can be substituted into Equations 121a through 121c. Equations 121a through 121c can be written in matrix form as

$$\begin{bmatrix} 1 & 1 & 1 \\ -r_4 - r_5 & -1 - r_5 & -1 - r_4 \\ r_4 + r_5 & r_5 & r_4 \end{bmatrix} \begin{bmatrix} r_1 \\ r_2 \\ r_3 \end{bmatrix} = \begin{bmatrix} \lambda_2 \\ \lambda_1 \\ \lambda_0 \end{bmatrix} \quad (123a)$$

solving for  $r_1$ ,  $r_2$  and  $r_3$  and three.

$$\begin{bmatrix} r_1 \\ r_2 \\ r_3 \end{bmatrix} = \begin{bmatrix} 1 & 1 & 1 \\ -r_4 - r_5 & -1 - r_5 & -1 - r_4 \\ r_4 + r_5 & r_5 & r_4 \end{bmatrix}^{-1} \begin{bmatrix} \lambda_2 \\ \lambda_1 \\ \lambda_0 \end{bmatrix} \quad (123b)$$

and solving Equations 117 yield.

$$b_1 = - \frac{\ln(r_4)}{T}$$

$$b_2 = - \frac{\ln(r_5)}{T}$$

$$a_0 = b_1 b_2 r_1$$

Let

$$\begin{aligned} e_1 &= -a_0 - b_2(-b_2 + b_1)r_3 \\ e_2 &= -a_0 - b_1(-b_1 + b_2)r_2 \end{aligned}$$

then

$$\begin{bmatrix} b_2 & -b_2 \\ b_1^2 & -b_1 \end{bmatrix} \begin{bmatrix} a_1 \\ a_2 \end{bmatrix} = \begin{bmatrix} e_1 \\ e_2 \end{bmatrix}$$

$$\begin{bmatrix} a_1 \\ a_2 \end{bmatrix} = \begin{bmatrix} b_2 & -b_2 \\ b_1^2 & -b_1 \end{bmatrix}^{-1} \begin{bmatrix} e_1 \\ e_2 \end{bmatrix}$$

now use Equations 114 to relate  $a_2$ ,  $a_1$ ,  $a_0$ ,  $b_1$ ,  $b_2$  to the pilot model parameters.

$$\tau_1 = - \frac{a_2 b_1}{a_0}$$

$$\tau_2 = \frac{1}{b_2}$$

$$\tau_3 = \frac{1}{b_1}$$

$$K_p = \frac{a_0}{b_1 b_2}$$

There are a total of nine discretizations done in this section. Each discretization provides equations for going from the continuous representation of a transfer function to its discrete representation and back. For  $G_{p1}$  all 4 methods are used. For  $G_{p2}$  only Tustin's bilinear rule is used. For  $G_{p4}$  all 4 methods are used, the coefficients to the discrete transfer functions will be determined from the time histories obtained from the realtime pilot-in-the-loop simulation discussed in the technical background section. These numerical values for the discrete pilot model coefficients will be used in conjunction with the equations developed in this section to determine the continuous pilot model parameters  $K_p$ ,  $\tau_1$ ,  $\tau_2$ , and  $\tau_3$ . Three FORTRAN programs were written for this purpose. The accuracy of these programs were checked by calculating the values of the discrete coefficients from known values of  $K_p$ ,  $\tau_1$ ,  $\tau_2$ , and  $\tau_3$ . These values of the discrete coefficients were then used to calculate the

values of  $K_p$ ,  $\tau_1$ ,  $\tau_2$  and  $\tau_3$  from the equations developed in this section. In each case the equations worked correctly. In the cases where the quadratic equation was used to evaluate a parameter only 1 solution to the quadratic equation produced the correct result. The solution to the quadratic equation that produced the correct result for the test case is the one that will be used when the programs are used to solve for pilot model parameters from discrete coefficients obtained from applying the RLS algorithm to the realtime simulation data.

## V. Neal Smith Theory

Neal-Smith Theory is used to predict the pilot compensation required for a specific aircraft and bandwidth criterion. The bandwidth criterion selected is somewhat arbitrary. Neal-Smith Theory will be applied to the aircraft model of Equation 1 over a range of bandwidth. The bandwidth used in the analysis will range from 2.5 to 4.0 radians per second. This will provide a range of pilot model parameters to be expected from the identifications obtained from the realtime simulation data.

Neal-Smith theory is applied in the same manner as was demonstrated in the closed-loop simulation section. In this section it is repeated for several values of bandwidth.

The pilot model used is given in Equation 7. The aircraft model used is given in Equation 1. Equation 1 is the F-15 pitch transfer function with no time delay. Figure 28 is a Nichols Chart for the pilot/aircraft system optimized for a bandwidth of 2.5 radians per second. The circles on the plot are spaced at intervals of .5 radians per second. The circle that represents 2.5 radians per second is as close as it will come to both standards of performance. Figure 29 is a Nichols Chart for the

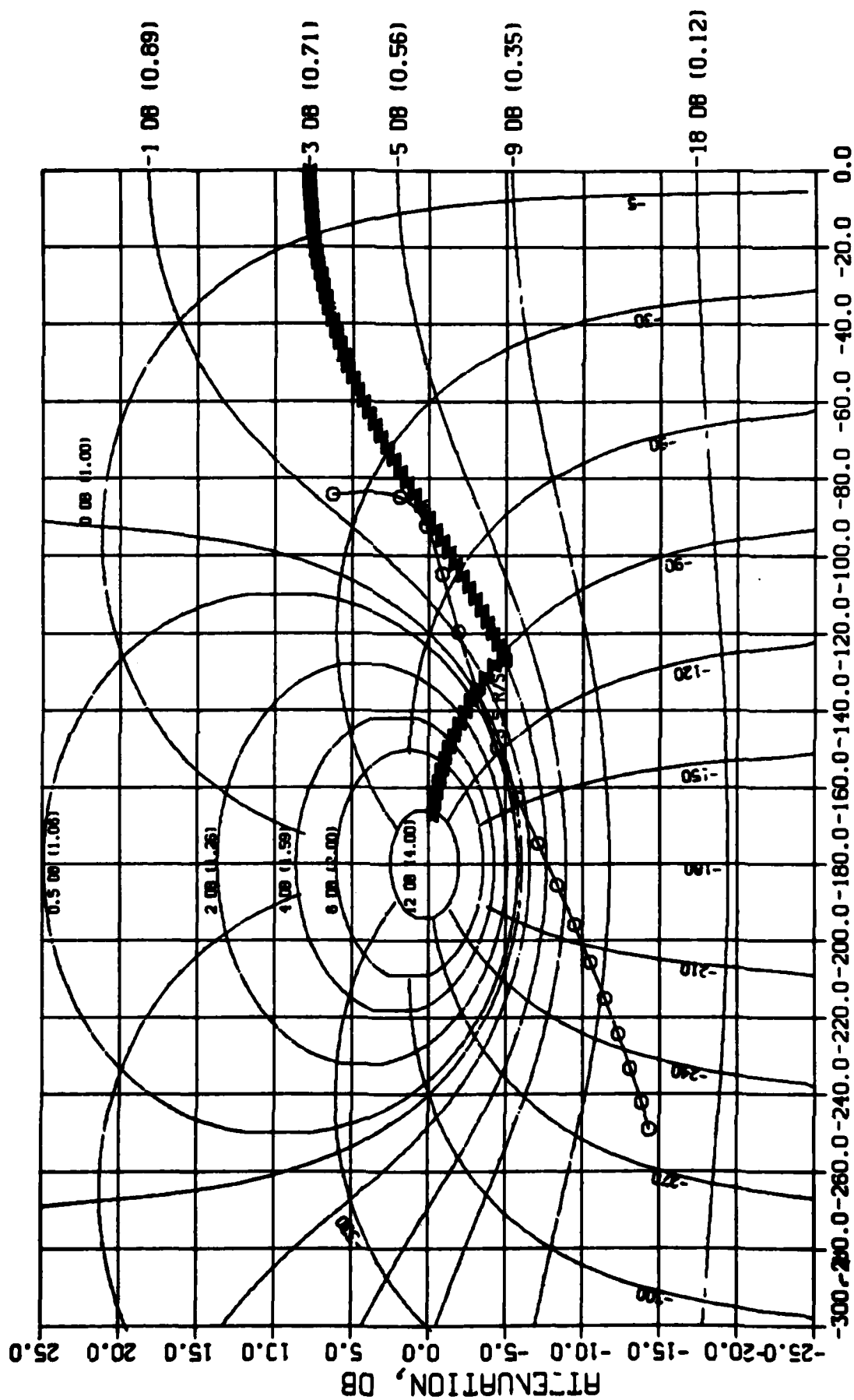
**Foot**



-95-



# NICHOLS CHART



PHASE ANGLE, DEG

pilot/aircraft system optimized for a bandwidth of 3.0 radians per second. The Neal-Smith analysis is done again for 3.5 and 4.0 radians per second. The results of all four optimizations are presented in table 3.

$\omega_{Bw}$	$K_p$	$\tau_1$	$\tau_2$
2.5	7.0323	.1200	.01
3.0	7.4728	.1933	.01
3.5	6.6464	.3571	.01
4.0	4.8417	.6252	.01

Optimal Pilot Models Calculated Over  
a Range of Bandwidth Criterion

Table 3

## VI. Identifications

### Analysis

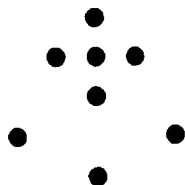
The aircraft model longitudinal dynamics are represented by Equations 1 and 2. The aircrafts time delay is represented by Equations 4, 5 and 6. Aircraft of different time delays are modeled by multiplying Equations 4, 5 or 6 by Equations 1 and 2. These different aircraft are then flown at the light bank and time histories are generated for identification. In this section, 4 different runs are examined in great detail. Table 4 describes the aircraft and the light switching sequence used for each run.

Run	A/C Time Delay (Sec)	Light Sequence		
		Segment		
		1	2	3
1	.0	4	6	8
2	.0	8	6	8
4	.1	4	6	8
5	.2	8	6	8

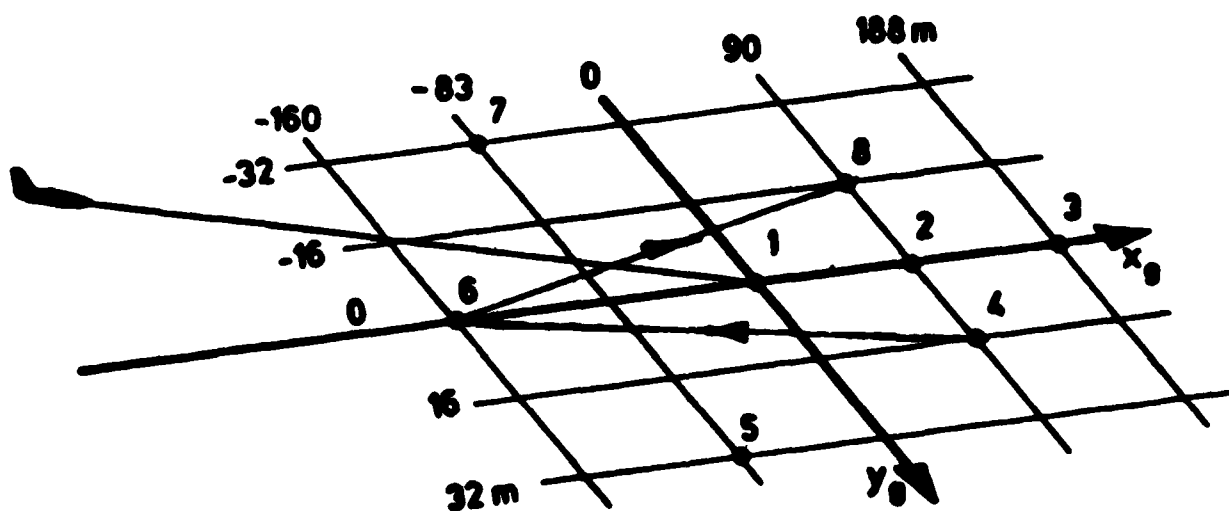
Description of Test Runs

Table 4

Run 4 and run 5 are included for comparison with run 1 and run 2. The light sequence for a particular run can be seen by comparing the sequences in Table 4 to the light bank in Figure 30.



View of Ground Targets from the Cockpit



Target Light Configuration

Figure 20

These sequences were chosen because they approximate a purely longitudinal task. Data for other sequences is available but contains segments of purely lateral switching which is not needed for identification of the longitudinal pilot model. The runs described in Table 4 were chosen because aircraft of different time delays were flown at the same light sequences. This will allow direct comparison of pilot model parameters for aircraft of different time delay that are performing the same task. Neal-Smith Theory predicts an increase in pilot lead and a decrease in pilot lag when the aircraft time delay is increased.

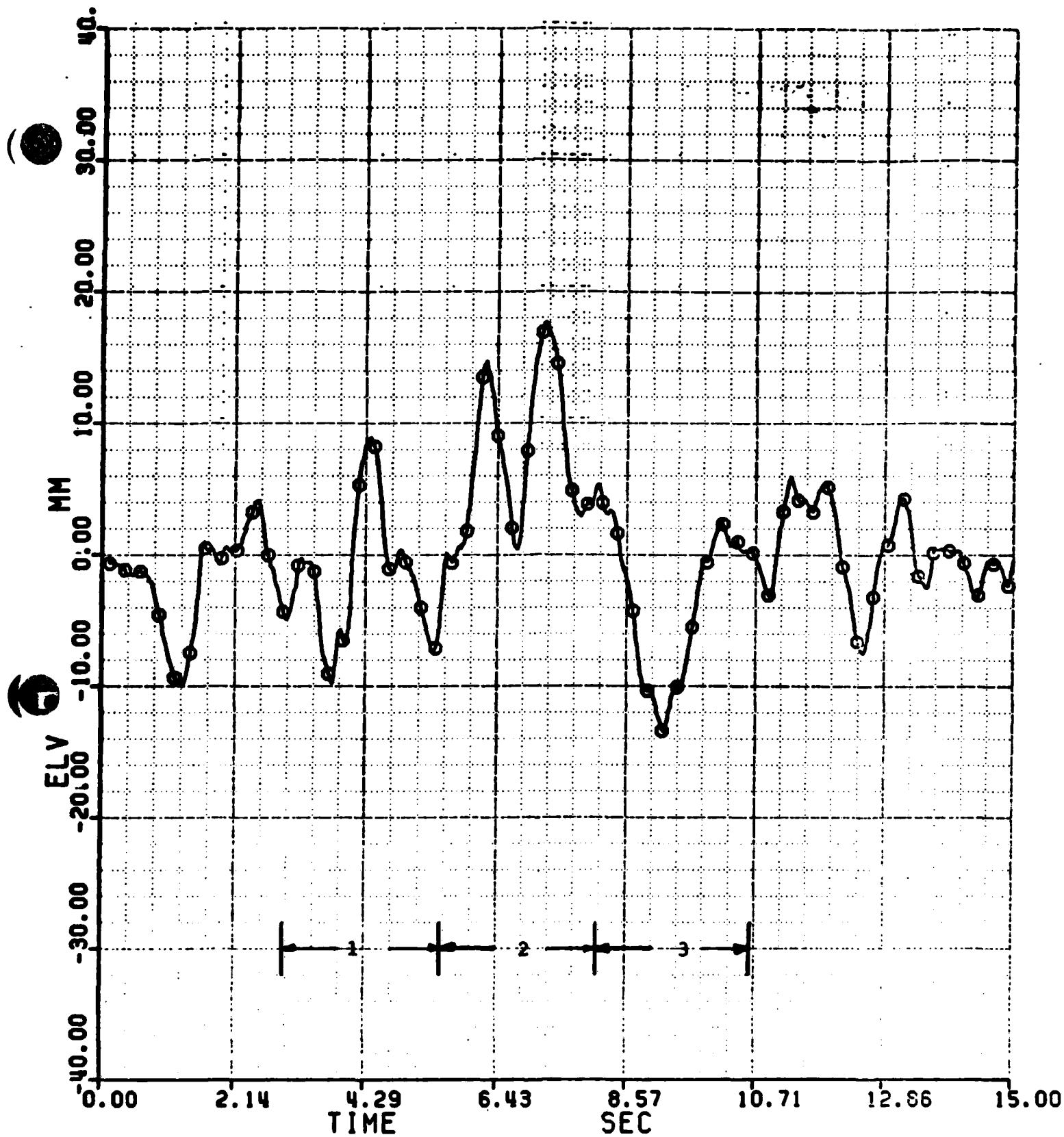
Runs 1 and 2 both employ the aircraft with zero time delay. Runs 1 and 2 will be used as a basis of comparison for Runs 4 and 5. Run 4 employs the aircraft with 100 milli-seconds of time delay and Run 5 employs the aircraft with 200 milli-seconds of time delay. Run 1 and run 4 were conducted using the same light sequence. Run 2 and run 5 were also conducted using the same light sequence. In order to apply the RLS algorithm it was necessary to break the data up into 3 segments for each run. Each segment corresponds to the time period where the pilot is attempting to minimize the pipper errors to a particular light. Each time the light is switched a separate identification was done on that segment of the data. The

segments are labeled 1, 2 and 3 as shown in Table 4. The identification was done in this manner so that the RLS algorithm would not be used on data with large discontinuities in the pipper errors. Breaking up the data into separate segments will also allow for direct comparison of the pilot model parameter identified for a particular segment.

An alternate method for taking into account the pilot time delay will also be used. Since pilot model 1 provides no means of identifying the pilot delay, the data streams will be shifted in time before application of the RLS algorithm in order to account for the delay in pilot output. Two different pilot time delays will be examined,  $T = .1s$  and  $T = .2s$ . A pilot delay of  $T = .3s$  was also tried but the fiterr became much greater and the values of  $\tau_1$  and  $\tau_2$  became unrealistic. Figures 31 through 38 are time histories of the control stick input and pipper errors for each run. The longitudinal control stick deflections are labeled ELV and are given in milli-meters. The longitudinal pipper errors are labeled TPIERRY and are given in milli-radians.

#### Identifications

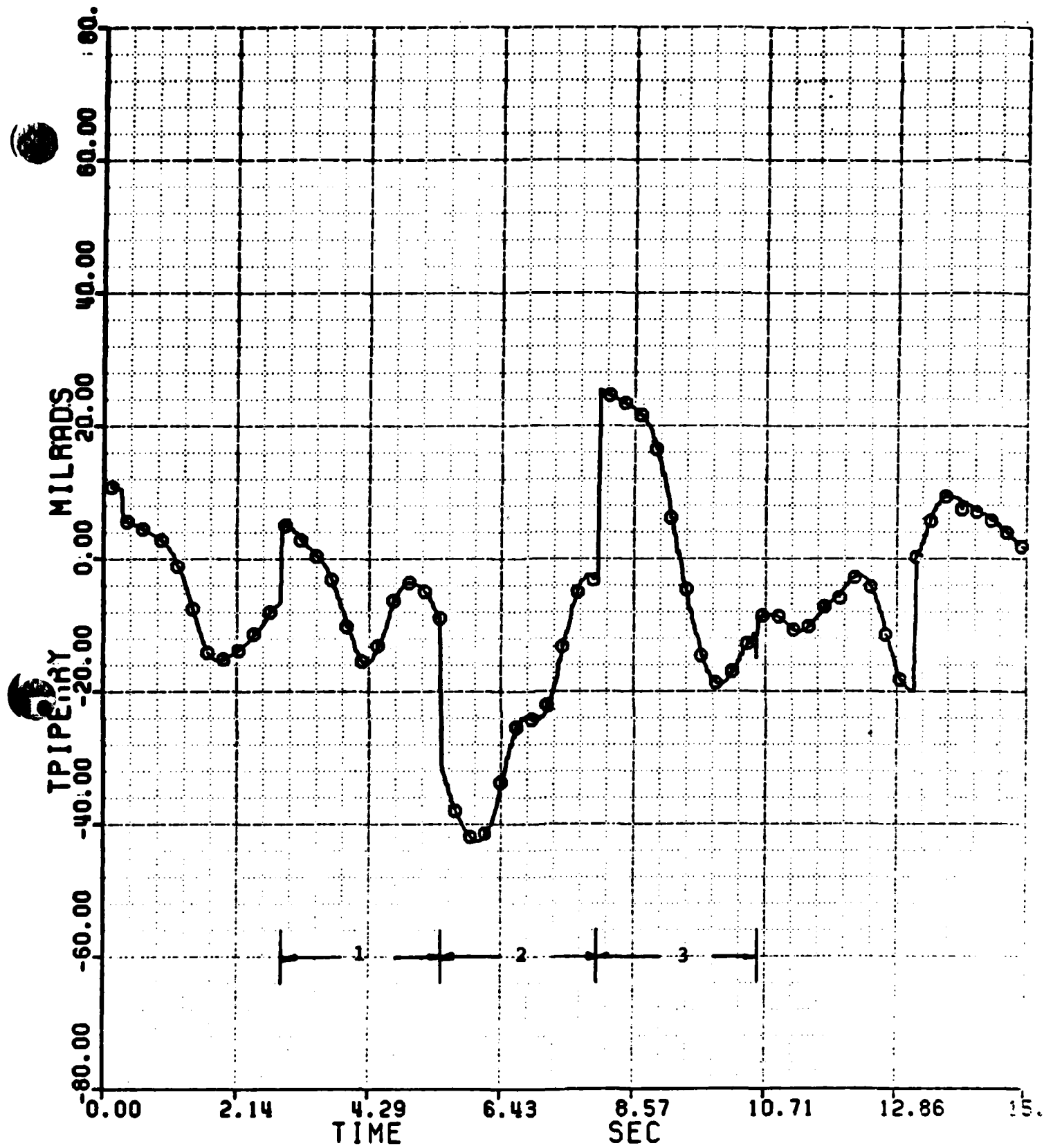
The pilot model parameters identified using pilot model 1 with no representation for the time delay are contained in table 5 through 10. Also contained in table



Longitudinal Control Stick Deflection

Run 1

Figure 31

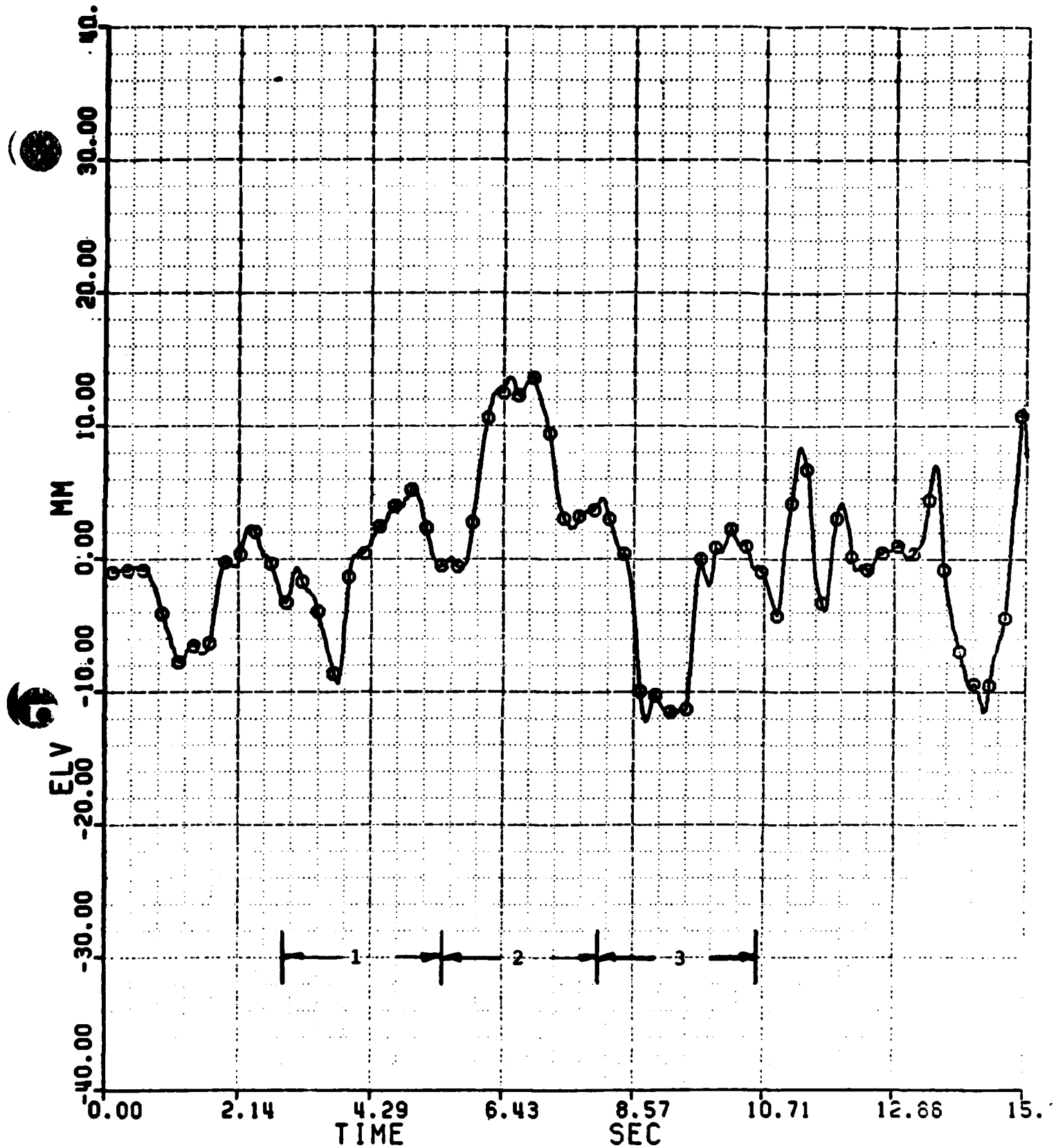


Longitudinal Pipper Error

Run 1

Figure 32

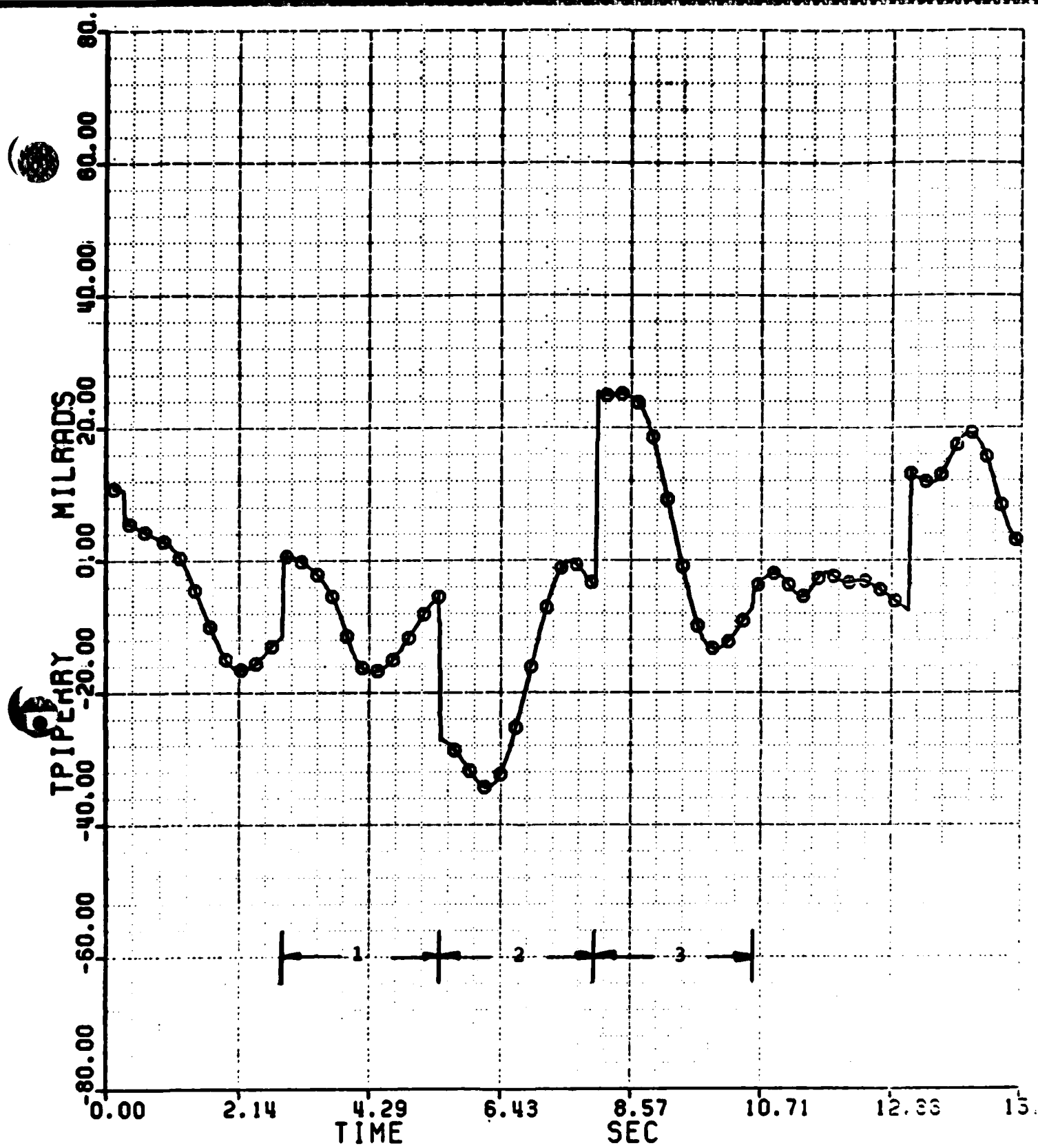




Longitudinal Control Stick Deflection

Run 2

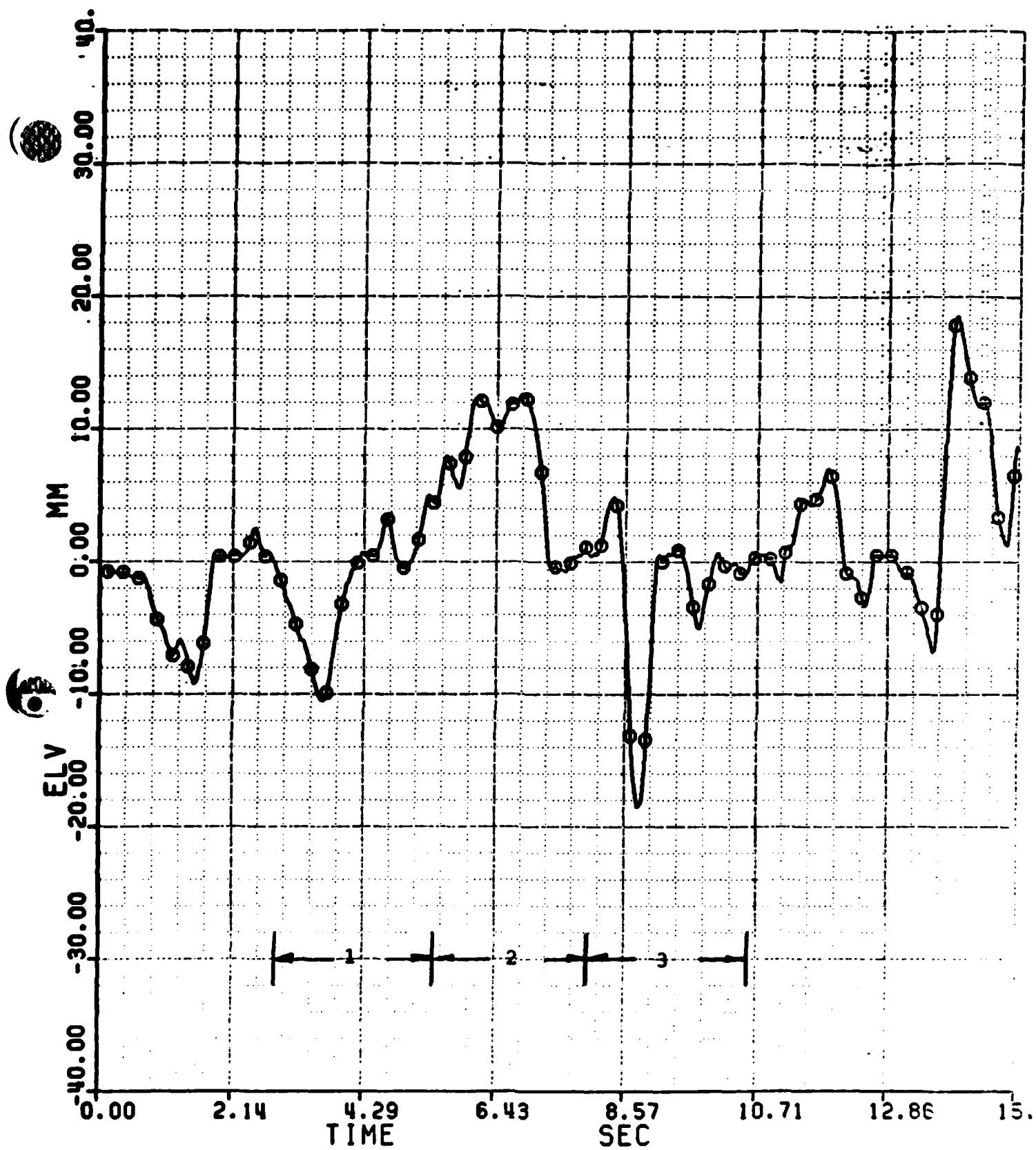
Figure 33



Longitudinal Pipper Error

Run 2

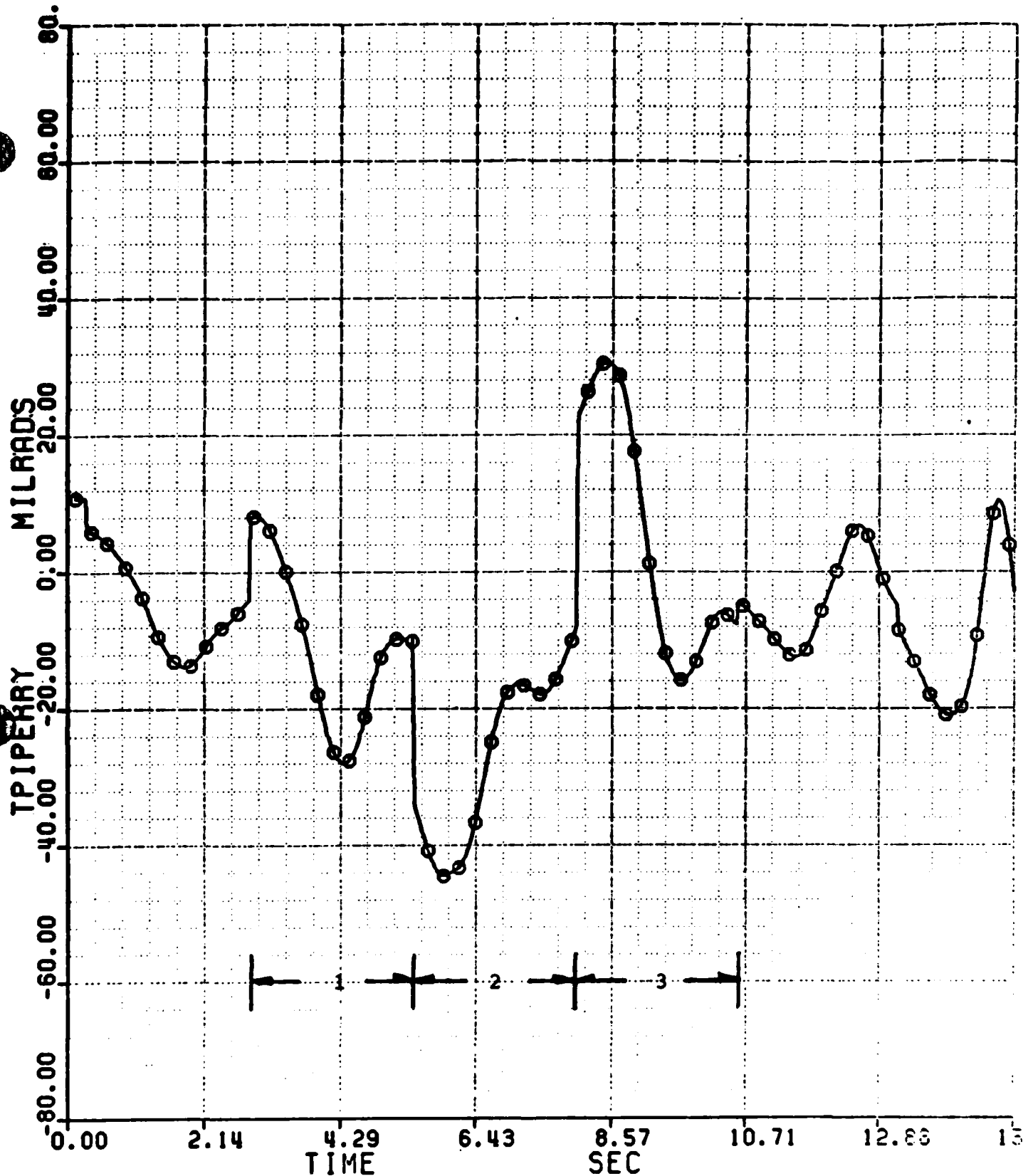
Figure 34



Longitudinal Control Stick Deflection

Run 4

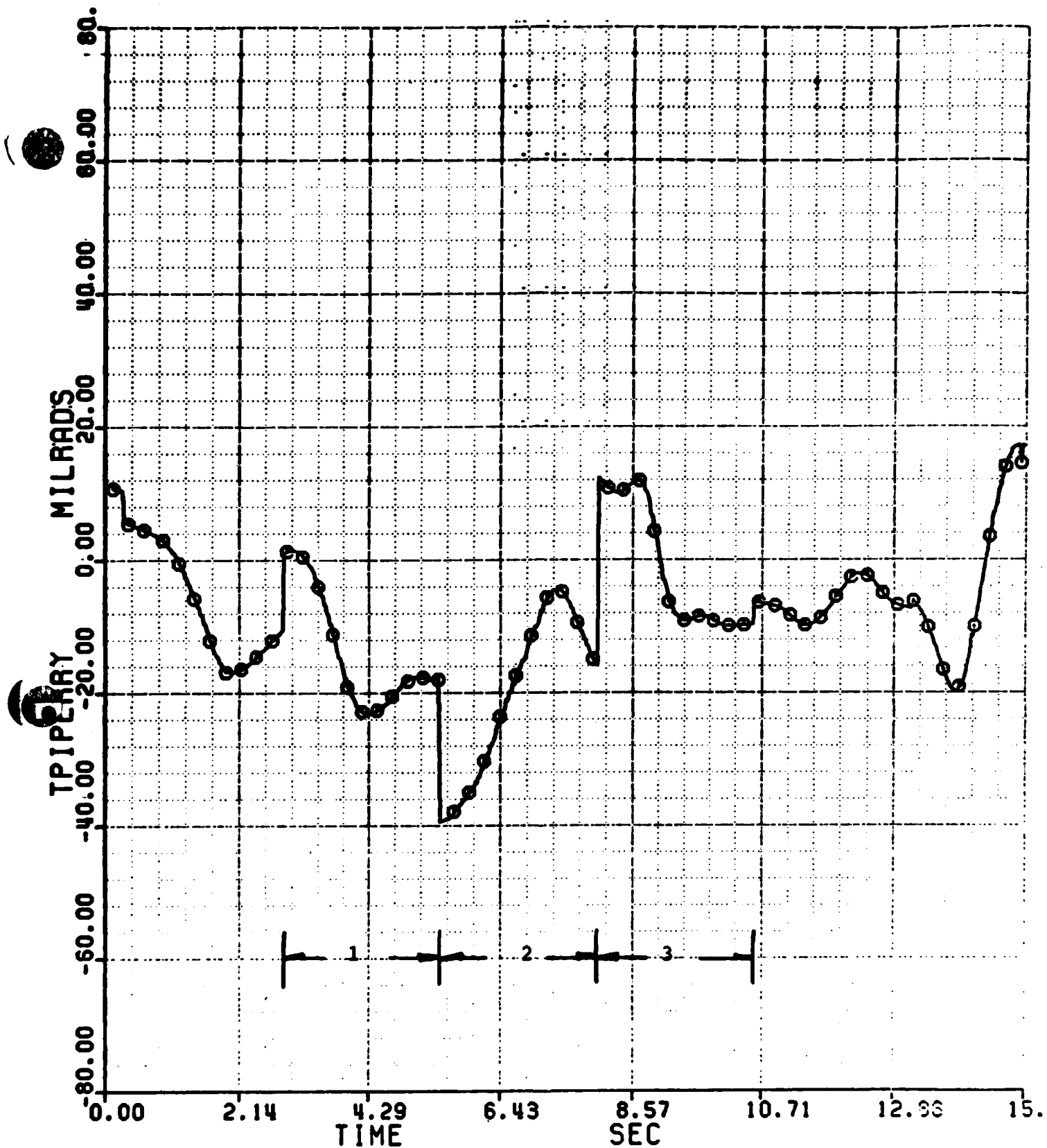
Figure 35



Longitudinal Pipper Errors

Run 5

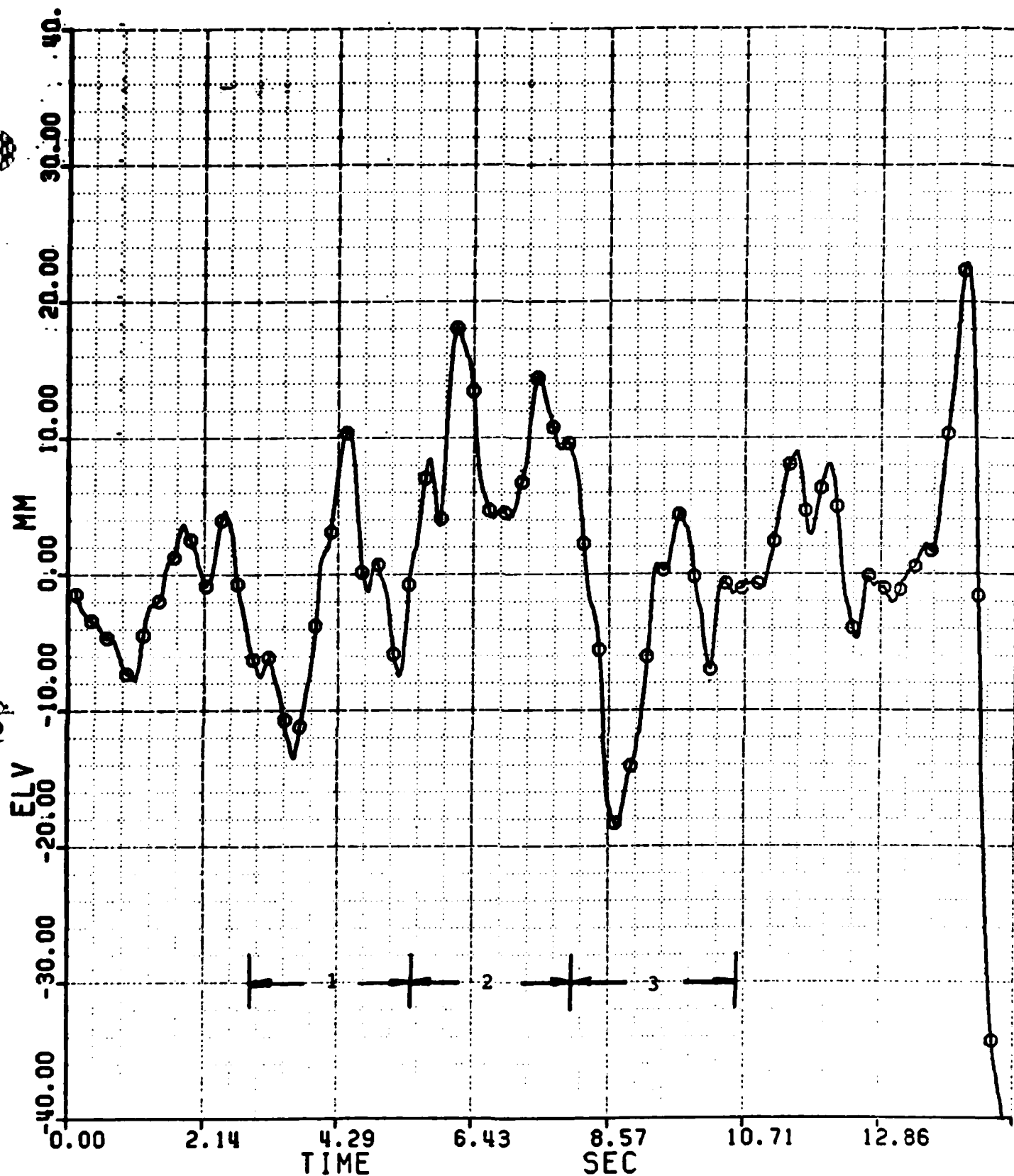
Figure 38



Longitudinal Pipper Error

Run 4

Figure 36



Longitudinal Control Stick Deflection

Run 5

Figure 37

5 through 10 are the pilot model parameters identified when the data streams are shifted to account for the pilot delay. Pilot time delays of .1 seconds and .2 seconds are represented. The identification using Pilot 2 are contained in Table 11 and the identifications using Pilot 4 are contained in Table 12 and Table 13.

In Table 5 through Table 13, the following abbreviations are used:

- FRR - Forward rectangular rule
- BRR - Backward rectangular rule
- TUST - Tustin's bilinear rule
- ZOH - Zero order hold

Pilot #1 Segment #1

	Run #1			Run #4		
	$K_D$	$\tau_1$	$\tau_2$	$K_D$	$\tau_1$	$\tau_2$
No data shift						
FRR	57.96	.1607	1.6778	47.24	.2607	1.5924
BRR	57.96	.1357	1.6528	47.24	.2357	1.5674
TUST	57.96	.1482	1.6653	47.24	.2482	1.5799
ZOH	57.96	.1595	1.6653	47.24	.2587	1.5798

Data Shifted for pilot delay of .1s

FRR	41.49	.5742	1.9084	1.88	6.1888	-.6394
BRR	41.49	.5742	1.8834	1.88	6.1638	-.6644
TUST	41.49	.5617	1.8959	1.88	6.1763	-.6519
ZOH	41.49	.5704	1.8959	1.88	6.3090	-.6518

Data shifted for pilot delay of .2s

FRR	22.95	1.2017	3.0120	Numerical difficulty due to the closeness of the discrete coefficients.
BRR	22.95	1.1767	2.9870	
TUST	22.95	1.1892	2.9995	
ZOH	22.95	1.1967	2.9995	

Pilot model parameters identified for Run 1 and Run 4 (Segment 1)

Table 5.



Pilot #1 Segment #2

	Run #1			Run #4		
	$K_D$	$\tau_1$	$\tau_2$	$K_D$	$\tau_1$	$\tau_2$
No data shift						
FRR	10.11	-.5869	.3771	8.92	-.6225	.3264
BRR	10.11	-.6119	.3521	8.92	-.6475	.3014
TUST	10.11	-.5994	.3646	8.92	-.6350	.3139
ZOH	10.11	-.5673	.3644	8.92	-.5983	.3137

Data Shifted for pilot delay of .1s

FRR	9.56	-.0336	.9225	11.49	.0006	.6281
BRR	9.56	-.0586	.8975	11.49	-.0244	.6031
TUST	9.56	-.0461	.9100	11.49	-.0119	.6156
ZOH	9.56	-.0331	.9100	11.49	.0005	.6156

Data shifted for pilot delay of .2s

FRR	9.26	.0457	1.1261	10.71	-.0100	.4836
BRR	9.26	.0207	1.1011	10.71	-.0350	.4586
TUST	9.26	.0332	1.1136	10.71	-.0225	.4711
ZOH	9.26	.0452	1.1136	10.71	-.0097	.4709

Pilot model parameters identified for Run 1 and Run 4 (Segment 2)

Table 6.

Pilot #1 Segment #3

	Run #1			Run #4		
No data shift	$K_D$	$\tau_1$	$\tau_2$	$K_D$	$\tau_1$	$\tau_2$
FRR	10.8	-.4988	.7310	9.40	-.4900	.4744
BRR	10.8	-.5238	.7060	9.40	-.5150	.4494
TUST	10.8	-.5113	.7185	9.40	-.5025	.4619
ZOH	10.8	-.4902	.7184	9.40	-.4770	.4618

Data Shifted for pilot delay of .1s

FRR	14.57	-.2298	.7102	12.97	-.1493	.5365
BRR	14.57	-.2548	.6852	12.97	-.1743	.5115
TUST	14.57	-.2423	.6977	12.97	-.1618	.5240
ZOH	14.57	-.2258	.6977	12.97	-.2458	.5239

Data shifted for pilot delay of .2s

FRR	14.79	-.1320	.7246	12.53	-.0780	.4873
BRR	14.79	-.1570	.6996	12.53	-.1030	.4623
TUST	14.79	-.1445	.7121	12.53	-.0905	.4748
ZOH	14.79	-.1297	.7121	12.53	-.0759	.4747

Pilot model parameters identified for Run 1 and Run 4 (Segment 3)

Table 7.

Pilot #1 Segment #1

	Run #2			Run #5		
	$K_D$	$\tau_1$	$\tau_2$	$K_D$	$\tau_1$	$\tau_2$
No data shift						
FRR	8.12	.8209	-.9294	2.62	5.6927	-.8306
BRR	8.12	.7959	-.9544	2.62	5.6677	-.8556
TUST	8.12	.8084	-.9419	2.62	5.6802	-.8431
ZOH	8.12	.8319	-.9418	2.62	5.7779	-.8430

Data Shifted for pilot delay of .1s

FRR	6.46	1.4589	-1.0776	10.75	-8.4349	-.9294
BRR	6.46	1.4339	-1.1026	10.75	-8.4599	-.9544
TUST	6.46	1.4464	-1.0901	10.75	-8.4474	-.9419
ZOH	6.46	1.4758	-1.0900	10.75	-8.5479	-.9418

Data shifted for pilot delay of .2s

FRR	7.42	1.5991	-1.2825	7.94	-3.9000	-1.5625
BRR	7.42	1.5741	-1.3071	7.94	-3.9250	-1.5875
TUST	7.42	1.5866	-1.2946	7.94	-3.9125	-1.5757
ZOH	7.42	1.6147	-1.2945	7.94	-3.9311	-1.5750

Pilot model parameters identified for Run 2 and Run 5 (Segment 1)

Table 8.

Pilot #1 Segment #2

	Run #2			Run #5		
No data shift	$K_D$	$\tau_1$	$\tau_2$	$K_D$	$\tau_1$	$\tau_2$
FRR	12.04	.2158	.9259	10.75	.0666	.9615
BRR	12.04	.1908	.9009	10.75	.0416	.8365
TUST	12.04	.2033	.9134	10.75	.0541	.9490
ZOH	12.04	.2129	.9134	10.75	.0657	.9490

Data Shifted for pilot delay of .1s

FRR	11.95	.3404	.9804	10.65	.2419	1.2626
BRR	11.95	.3154	.9554	10.65	.2169	1.2376
TUST	11.95	.3279	.9679	10.65	.2294	1.2501
ZOH	11.95	.3361	.9678	10.65	.2395	1.2501

Data shifted for pilot delay of .2s

FRR	11.44	.4552	1.0730	11.15	1.3132	3.0488
BRR	11.44	.4302	1.0480	11.15	1.2882	3.0238
TUST	11.44	.4427	1.0605	11.15	1.3007	3.0363
ZOH	11.44	.4499	1.0604	11.15	1.3078	3.0363

Pilot model parameters identified for Run 2 and Run 5 (Segment 2)

Table 9.

Pilot #1 Segment #3

	Run #2			Run #5		
	$K_D$	$\tau_1$	$\tau_2$	$K_D$	$\tau_1$	$\tau_2$
No data shift						
FRR	37.4	.1382	1.9685	11.86	-.2245	.3592
BRR	37.4	.1132	1.9435	11.86	-.2495	.3342
TUST	37.4	.1257	1.9560	11.86	-.2370	.3467
ZOH	37.4	.1374	1.9560	11.86	-.2166	.3425

Data Shifted for pilot delay of .1s

FRR	18.58	.1741	1.6778	10.65	.2419	1.2626
BRR	18.58	.1491	1.6528	10.65	.2169	1.2376
TUST	18.58	.1616	1.6653	10.65	.2294	1.2501
ZOH	18.58	.1728	1.6653	10.65	.2395	1.2501

Data shifted for pilot delay of .2s

FRR	4.72	-1.0063	1.9380	12.15	-.1272	.4424
BRR	4.72	-1.0313	1.9130	12.15	-.1522	.4214
TUST	4.72	-1.0188	1.9255	12.15	-.1397	.4339
ZOH	4.72	-.9497	1.9255	12.15	-.1236	.4338

Pilot model parameters identified for Run 2 and Run 5 (Segment 3)

Table 10.

Pilot #2  
Run #1

<u>Segment</u>	<u><math>K_D</math></u>	<u><math>\tau_1</math></u>	<u><math>\tau_2</math></u>	<u><math>\tau_3</math></u>
1	-.0080	3.3769	-0.0267	-0.0480
2	-.0316	.1388	-0.0266	.1060
3	-.0409	.0310	- .0274	.3991

Run #2

<u>Segment</u>	<u><math>K_D</math></u>	<u><math>\tau_1</math></u>	<u><math>\tau_2</math></u>	<u><math>\tau_3</math></u>
1	-.0112	4.714	-0.0272	-0.0009
2	-	-	-	-
3	-.0105	0.0359	-0.0255	0.2718

Pilot Model parameters identified using pilot  
model 2 for Run 1 and Run 2.

(Tustin's bilinear rule)

Table 11

Pilot #4  
Run #1

Segment #1

	$\underline{K_D}$	$\underline{\tau_1}$	$\underline{\tau_2}$	$\underline{\tau_3}$
FRR	4.0	-.2731	.1190	.7503
BRR	4.0	.0355	4.1837	-3.3644
TUST	.1572	3.3768	.8923	-0.0480
ZOH	4.0	5.5281	.1060	.7377

Segment #2

	$\underline{K_D}$	$\underline{\tau_1}$	$\underline{\tau_2}$	$\underline{\tau_3}$
FRR	-	-	-	-
BRR	6.4	-.1985	.4126	-.1263
TUST	.2573	.1388	.1253	.1860
ZOH	-	-	-	-

Segment #3

	$\underline{K_D}$	$\underline{\tau_1}$	$\underline{\tau_2}$	$\underline{\tau_3}$
FRR	9.46	.0360	.0923	.4670
BRR	9.46	-.4116	.5278	-.0185
TUST	.3724	.0310	.1352	.3991
ZOH	9.46	-.2685	.0791	.4544

Pilot Model parameters identified using pilot model 4 for Run 1

Table 12

Pilot #4

Run #2

Segment #1

	<u>K<sub>D</sub></u>	<u>τ<sub>1</sub></u>	<u>τ<sub>2</sub></u>	<u>τ<sub>3</sub></u>
FRR	-2.2281	-.8781	-.5057	.0723
BRR	-2.2281	-.0116	4.2180	-4.7015
TUST	.0877	4.7141	-.4576	-0.0009
ZOH	-2.2281	.6599	.0589	-0.5181

Segment #3

	<u>K<sub>D</sub></u>	<u>τ<sub>1</sub></u>	<u>τ<sub>2</sub></u>	<u>τ<sub>3</sub></u>
FRR	-	-	-	-
BRR	1.7294	-.2843	.0478	-.0234
TUST	.0681	.0359	-.2223	.2718
ZOH	-	-	-	-

Pilot Model parameters identified using pilot model 4 for Run 2

Table 13



## Discussion of Results

The section will discuss the identifications of Table 5 through Table 13 and their relationship to the pilot ratings.

Neal-Smith Theory predicts that as the aircraft time delay increases the pilot must compensate for this by adding more lead. Adding more lead required a higher work load and a higher work load leads to higher pilot ratings on the Cooper-Harper rating scale. This was seen to be the case for the aircraft flown in this test. The higher the time delay added to the aircraft model the worse the pilot ratings became. This is a well known fact in flying qualities research and was expected.

The exact pilot model parameters predicted by Neal-Smith were not identified. This may have been due in part to the error bias introduced by the pointing accuracies of the terrain board camera. This may also have been due to the fact that the pilot's attention was diverted to the lateral task. However, if the pilot model parameters identified in run 1 and run 2 are established as a baseline of comparison for run 4 and run 5 some interesting trends can be seen. Since it is not clear at what frequency the pilot is operating, the lead and lag will be examined to determine trends in pilot

compensation rather than calculate the pilot angle at some arbitrary frequency.

Neal-Smith Theory predicts an increase in the pilot compensation to compensate for aircraft time delay. An increase in pilot lead and a decrease in pilot lag will yield an increase in the angle of total pilot compensation. This can be seen to be the case when examining the pilot model parameters identified in Table 5 through Table 7. Pilot model 1 is used in each case. The aircraft in run 1 has no delay while the aircraft in run 4 has a 100 milli-sec delay. Both are flown at the same light sequence. If the values of lead and lag calculated in run 1 are used as a basis of comparison for run 4 it can be seen that the pilot lead increases and the pilot lag decreases in each of the 3 segments. It can also be seen that the pilot lead increase and the pilot lag decreases when the data is shifted by .1 seconds and .2 seconds to make up for pilot delay. The fact that the pilot will increase lead compensation and decrease lag compensation for an increase in the angle of total pilot compensation can be seen in Table 5 through Table 7. All discretization techniques provided similar results for pilot model 1. No technique appeared to be superior to any other.

Table 8 through Table 10 provide a similar comparison for run 2 and run 5. When comparing run 2 and run 5 it can

be seen that in segment 1 and 2 the pilot lead decrease and the pilot lag increase. This is not what is expected to be the case. However, segment 3 yields the expected results. This cannot be explained by the Neal-Smith Theory. It could be explained by an unusually quick gross acquisition leaving the pilot an unusually large amount of time to apply lag compensation for good steady state accuracy.

With the exception of segments 1 and 2 of runs 2 and 5, Table 5 through Table 10 show an increase in the total pilot angle contribution that is predicted by Neal-Smith Theory.

Table 11 presents the pilot model parameters identified for pilot model 2. The discretization techniques used on pilot model 2 is the Tustin's bilinear rule. The identifications gave negative values for  $K_p$  and  $\tau_3$ . For this reason it was excluded from further consideration.

Table 12 and Table 13 give the pilot model parameters identified for pilot model 3. The same problem exist as for pilot model 2. The inaccuracies in  $\tau_3$ , the pilot delay exclude the model from further consideration.

#### Pilot Comments

Pilot comments and Cooper-Harper ratings were recorded during testing. Runs 1 and 2 were flown using

the aircraft with zero time delay. The pilot describe the aircraft with zero time delay as follows.

"...did not use roll much, slight pitch bobble in fine tracking, it gets a pilot rating of 3 in pitch and a level 1 all around..." (12)

The pilot gave the aircraft with zero time delay a Copper-Harper rating of three which is from Figure 2, level 1 flying qualities.

After flying a few runs with the aircraft with a time delay of 100 milli-seconds the pilot was asked to give his ratings. His response was:

" gross acquisition acceptable, fine tracking is annoying...it gets a pilot rating of 5 in both axis..." (12)

From Figure (2) it can be seen that a Copper-Harper rating of 5 corresponds to level 2 flying qualities.

The aircraft with a time delay of 200 milli-seconds was flown and received the following pilot comments.

"...definitely has problems, unpredictable, pilot rating of 7 in pitch, same problem as before, small bobble not really a pilot induced oscillation..."(12)

A Cooper-Harper rating of 7 corresponds to level 3 flying qualities.

One may conclude from the pilot comments that the aircraft flown in run 1 and run 2 is a level 1 aircraft. The aircraft flown in run 4 is a level 2 aircraft and the aircraft flown in run 5 is a level 3 aircraft.

## VII. Conclusions and Recommendations

### Conclusions

Neal-Smith Theory accurately predicts the increase in pilot compensation for aircraft of increasing time delay. This was seen by comparison of run 1 to run 4 and run 2 to run 5. Pilot model 1 provided the most accurate results. Modeling of the pilot time delay proved to be difficult and unnecessary. Inaccuracies in the pilot delay identified will throw off the other terms in the identification. Shifting the data is the best way to eliminate pilot delay from the data. For low order transfer functions all methods of discretization provided similar results although the frequency domain plots indicate that Tustin's bilinear rule was the best. Therefore, the simplest method could be used without any loss in accuracy.

### Recommendations

One well known method of discretization pole-zero mapping was not attempted in this work. The pole-zero mapping technique maps a pole or zero in the  $s$ -plane directly into the  $z$ -plane. This method could be used and compared to the results obtained by the other methods.

The data used for the identifications in this work was not obtained for a purely longitudinal task. The

pilots attention was inevitably diverted from time to time on minimizing lateral pipper errors. The longitudinal pipper errors are never completely zero. This was not taken into account in this work. Lateral pilot dynamics should be taken into account. There is a need to determine when the pilots attention becomes diverted to the lateral task.

Since the human pilot is inconsistent a statistical approach could be taken were the parameters are averaged over many runs where the pilot is flying the same task.

It would also be helpful to know the sensitivity of the RLS algorithm to noise and pilot remnants when trying to identify the pilot delay. A closed loop simulation could be used to generate synthetic data for this purpose.

Matrix<sub>x</sub> cannot identify an improper transfer function. This made the use of a lead only pilot model impossible. Further investigation into the lead only pilot model could be useful.

**Appendix A**

**SIMULATION PROGRAM IDENT**



PROGRAM IDENT

DIMENSION THETAC(0:1100),E(-1:1100),DELP(-2:1100),THETA(-3:1100),  
EBIAS(0:1100), DELPR(0:1100),PSI(3,1100)  
LOGICAL FIRST  
INITIALIZATION

E(-1)= 0.  
DELP(-2)=0.  
DELP(-1)=0.  
THETA(-3)=0.  
THETA(-2)=0.  
THETA(-1)=0.

DO 30 J=1,3  
DO 30 I=1,1100  
PSI(I,J)=0.

30 CONTINUE

DO 10 I=0,1100  
E(I)= 0.  
EBIAS(I)=0.  
DELP(I)=0.  
DELPR(I)=0.  
THETA(I)=0.  
THETAC(I)=0.

10 CONTINUE

C SET INPUT VARIABLE TIME HISTORY ( REFERENCE NEAL-SMITH PG 23 )

DO 11 J=0,1100  
IF(J.GE. 00 .AND.J.LT.50 ) THETAC(J)= 0.0  
IF(J.GE. 50 .AND.J.LT.100 ) THETAC(J)= -1.0  
IF(J.GE.100 .AND.J.LT.170 ) THETAC(J)= -2.0  
IF(J.GE.170 .AND.J.LT.190 ) THETAC(J)= 0.0  
IF(J.GE.190 .AND.J.LT.230 ) THETAC(J)= -1.0  
IF(J.GE.230 .AND.J.LT.300 ) THETAC(J)= 0.0  
IF(J.GE.300 .AND.J.LT.340 ) THETAC(J)= 4.0  
IF(J.GE.340 .AND.J.LT.410 ) THETAC(J)= 1.5  
IF(J.GE.410 .AND.J.LT.420 ) THETAC(J)= -1.0  
IF(J.GE.420 .AND.J.LT.440 ) THETAC(J)= -1.5  
IF(J.GE.440 .AND.J.LT.500 ) THETAC(J)= -2.0  
IF(J.GE.500 .AND.J.LT.560 ) THETAC(J)= 0.0  
IF(J.GE.560 .AND.J.LT.590 ) THETAC(J)= -2.5  
IF(J.GE.590 .AND.J.LT.610 ) THETAC(J)= 0.0  
IF(J.GE.610 .AND.J.LT.630 ) THETAC(J)= 3.0  
IF(J.GE.630 .AND.J.LT.720 ) THETAC(J)= 0.0  
IF(J.GE.720 .AND.J.LT.770 ) THETAC(J)= 5.0  
IF(J.GE.770 .AND.J.LT.880 ) THETAC(J)= 3.0  
IF(J.GE.880 .AND.J.LT.910 ) THETAC(J)= 4.0  
IF(J.GE.910 .AND.J.LT.960 ) THETAC(J)= -1.0  
IF(J.GE.960 .AND.J.LT.980 ) THETAC(J)= -1.5  
IF(J.GE.980 .AND.J.LT.1000) THETAC(J)= -2.0  
IF(J.GE.1000.AND.J.LT.1010) THETAC(J)= -1.0  
IF(J.GE.1010.AND.J.LT.1020) THETAC(J)= -0.5  
IF(J.GE.1020) THETAC(J)= 0.0

11 CONTINUE

C CALCULATE COEFFICIENTS FOR THE OPTIMUM PILOT MODEL

```

TAU= .1
TAULAG = .3
TAU1=.1933
TAU2=.01
TAU3=TAULAG/2.
RKF=7.4728
RKF=.2942

```

```

DENOM = ( TAU2 * TAU3 )
AO = RKF/DENOM
A1 = RKF * ( TAU1 - TAU3 ) / DENOM
A2 = -RKF * ( TAU1 * TAU3 ) / DENOM
BO = 1./DENOM
B1 = ( TAU2 + TAU3 ) / DENOM

```

```

DENOM2 = ( 1./(TAU*TAU) + B1/TAU + BO )

```

```

AAO= ( A2/(TAU*TAU) + A1/TAU + AO )/DENOM2
AA1= ( -2.*A2/(TAU*TAU) - A1/TAU )/DENOM2
AA2= ( A2/(TAU*TAU) )/DENOM2
BE1= ( 2./(TAU*TAU) + B1/TAU )/DENOM2
BB2= (-1./(TAU*TAU) )/DENOM2

```

```

C PRINT OUT COEFFICIENTS FOR PILOT MODEL

```

```

PRINT *, ' '
PRINT *, 'TAU = ',TAU
PRINT *, 'TAU1 = ',TAU1
PRINT *, 'TAU2 = ',TAU2
PRINT *, 'TAU3 = ',TAU3
PRINT *, 'RKF = ',RKF
PRINT *, 'AO = ',AO
PRINT *, 'A1 = ',A1
PRINT *, 'A2 = ',A2
PRINT *, 'BO = ',BO
PRINT *, 'B1 = ',B1
PRINT *, 'AAO = ',AAO
PRINT *, 'AA1 = ',AA1
PRINT *, 'AA2 = ',AA2
PRINT *, 'BE1 = ',BE1
PRINT *, 'BB2 = ',BB2
PRINT *, ' '

```

```

C CALCULATE COEFFICIENTS FOR THE AIRCRAFT MODEL

```

```

RMVTINCH=.03937
RINCHTMM=25.4

```

```

C0=0.0
C1=9.0
C2=4.2
D0=1.1376*RINCHTMM
D1=.948*RINCHTMM

```

```

DENOM= (1./TAU**3. + C2/TAU**2. + C1/TAU + C0 )
CC1= -( -3./TAU**3. -2.*C2/TAU**2. -C1/TAU )/DENOM
CC2= -( 3./TAU**3. + C2/TAU**2. )/DENOM
CC3= ( 1./TAU**3. )/DENOM

```

```

DDO= ( D1/TAU + D0 )/DENOM
DD1= ( -D1/TAU )/DENOM

```

C PRINT OUT COEFFICIENTS FOR THE AIRCRAFT MODEL

```

PRINT *, ' '
PRINT *, 'C0' = ',C0
PRINT *, 'C1' = ',C1
PRINT *, 'C2' = ',C2
PRINT *, 'D0' = ',D0
PRINT *, 'D1' = ',D1
PRINT *, 'CC1' = ',CC1
PRINT *, 'CC2' = ',CC2
PRINT *, 'CC3' = ',CC3
PRINT *, 'CC0' = ',CC0
PRINT *, 'CD1' = ',CD1
PRINT *, ' '

```

C OPEN FILES FOR DATA STORAGE

```

OPEN(2,FILE='E.',STATUS='NEW')
OPEN(3,FILE='DELP.',STATUS='NEW')
OPEN(4,FILE='OUTDAT.',STATUS='NEW')
WRITE(4,1012)
WRITE(4,1013)
WRITE(4,1012)

```

```

1012 FORMAT(1X,' ')
1013 FORMAT(5X,' DELP(DEG) ',5X,' DELP(IN) ',5X,' THETA(DEG) ',5X)

```

C OPERATE LOOP

```

FIRST=.TRUE.

```

```

DO 20 K=1,1100

```

```

    E(K)=THETAC(K)-THETA(K-1)

```

```

    DELP(K)=.12*DELP(K-2)+.1*DELP(K-1)

```

```

    +.12*E(K-2)+.1*E(K-1)+.1*E(K)

```

```

    U=DELP(K-1)

```

```

    CALL F15(U,Y,FIRST)

```

```

    THETA(K)=Y

```

```

    PRINT *, 'E = ',DELP= ',THETA= ',E(K),DELP(K),THETA(K),THETAC(K)

```

```

    WRITE(4,1011)E(K),DELP(K),THETA(K),THETAC(K)

```

```

1011 FORMAT(1X,F12.4,5X,F12.4,5X,F12.4,5X,F12.5)

```

C WRITE(2,1010)E(K)

C WRITE(3,1010)DELP(K)

```

1010 FORMAT(=14.4)

```

```

20 CONTINUE

```

```

CLOSE(2)

```

```

CLOSE(3)

```

```

END

```

```

SUBROUTINE F15(U,Y,FIRST)

```

```

DIMENSION AT(3,3),BT(3),CT(2),XT(3),XT0(3)

```

```

LOGICAL FIRST

```

```

IF(FIRST)THEN

```

```

    FIRST=.FALSE.

```

```

    AT(1,1)= .9999

```

```

    AT(1,2)=.0999

```

```

    AT(1,3)=.0043

```

AT(2,1)=0.  
AT(2,2)=-.9613  
AT(2,3)=.0E04  
AT(3,1)=0.  
AT(3,2)=-.7240  
AT(3,3)=.6235

BT(1)=.00016777  
BT(2)=.00430000  
BT(3)=.08040000

CT(1)=1.1376 \*25.4  
CT(2)=.9460 \* 25.4  
CT(3)= 0.

XT0(1)=0.  
XT0(2)=0.  
XT0(3)=0.

XT(1)=0.  
XT(2)=0.  
XT(3)=0.

END IF

DO 25 I=1,3  
XT(I)=0.

25 CONTINUE

DO 10 I=1,3

DO 15 J=1,3

TEMP=AT(I,J)\*XT0(J)

XT(I)=XT(I)+TEMP

15 CONTINUE

XT(I)=XT(I)+BT(I)\*CT(I)

10 CONTINUE

Y=0.

DO 20 I=1,3

XT0(I)=XT(I)

YT=CT(I)\*XT(I)

Y=Y+YT

20 CONTINUE

RETURN

END

SIMULATION DATA (E. DELP. THETA. THETAC)

ERROR(DEG)	DELTA(IN)	THETA(DEG)	THETAC( DEG)
0.0000	0.0000	0.0000	0.00000
0.0000	0.0000	0.0000	0.00000
0.0000	0.0000	0.0000	0.00000
0.0000	0.0000	0.0000	0.00000
0.0000	0.0000	0.0000	0.00000
0.0000	0.0000	0.0000	0.00000
0.0000	0.0000	0.0000	0.00000
0.0000	0.0000	0.0000	0.00000
0.0000	0.0000	0.0000	0.00000
0.0000	0.0000	0.0000	0.00000
0.0000	0.0000	0.0000	0.00000
0.0000	0.0000	0.0000	0.00000
0.0000	0.0000	0.0000	0.00000
0.0000	0.0000	0.0000	0.00000
0.0000	0.0000	0.0000	0.00000
0.0000	0.0000	0.0000	0.00000
0.0000	0.0000	0.0000	0.00000
0.0000	0.0000	0.0000	0.00000
0.0000	0.0000	0.0000	0.00000
0.0000	0.0000	0.0000	0.00000
0.0000	0.0000	0.0000	0.00000
0.0000	0.0000	0.0000	0.00000
0.0000	0.0000	0.0000	0.00000
0.0000	0.0000	0.0000	0.00000
0.0000	0.0000	0.0000	0.00000
0.0000	0.0000	0.0000	0.00000
0.0000	0.0000	0.0000	0.00000
0.0000	0.0000	0.0000	0.00000
0.0000	0.0000	0.0000	0.00000
0.0000	0.0000	0.0000	0.00000
0.0000	0.0000	0.0000	0.00000
0.0000	0.0000	0.0000	0.00000
0.0000	0.0000	0.0000	0.00000
0.0000	0.0000	0.0000	0.00000
0.0000	0.0000	0.0000	0.00000
0.0000	0.0000	0.0000	0.00000
0.0000	0.0000	0.0000	0.00000
0.0000	0.0000	0.0000	0.00000
0.0000	0.0000	0.0000	0.00000
-1.0000	0.1559	0.0000	-1.00000
-1.0000	-0.3088	0.0170	-1.00000
-1.0170	-0.3262	-0.0204	-1.00000
-0.9796	-0.3285	-0.0490	-1.00000
-0.9510	-0.3069	-0.0762	-1.00000
-0.9238	-0.2912	-0.0954	-1.00000
-0.9046	-0.2779	-0.1145	-1.00000
-0.8855	-0.2699	-0.1293	-1.00000

-0.8707	-0.2625	-0.1455	-1.00000
-0.8545	-0.2577	-0.1591	-1.00000
-0.8409	-0.2523	-0.1743	-1.00000
-0.8257	-0.2484	-0.1874	-1.00000
-0.8126	-0.2435	-0.2020	-1.00000
-0.7980	-0.2396	-0.2147	-1.00000
-0.7853	-0.2353	-0.2288	-1.00000
-0.7712	-0.2317	-0.2412	-1.00000
-0.7588	-0.2274	-0.2547	-1.00000
-0.7453	-0.2239	-0.2668	-1.00000
-0.7332	-0.2197	-0.2797	-1.00000
-0.7203	-0.2163	-0.2914	-1.00000
-0.7086	-0.2124	-0.3039	-1.00000
-0.6961	-0.2090	-0.3153	-1.00000
-0.6847	-0.2052	-0.3273	-1.00000
-0.6727	-0.2020	-0.3383	-1.00000
-0.6617	-0.1984	-0.3498	-1.00000
-0.6502	-0.1952	-0.3605	-1.00000
-0.6393	-0.1917	-0.3716	-1.00000
-0.6284	-0.1886	-0.3820	-1.00000
-0.6180	-0.1853	-0.3927	-1.00000
-0.6073	-0.1823	-0.4028	-1.00000
-0.5972	-0.1791	-0.4131	-1.00000
-0.5869	-0.1762	-0.4228	-1.00000
-0.5772	-0.1731	-0.4327	-1.00000
-0.5673	-0.1703	-0.4421	-1.00000
-0.5579	-0.1673	-0.4517	-1.00000
-0.5483	-0.1646	-0.4608	-1.00000
-0.5392	-0.1617	-0.4700	-1.00000
-0.5300	-0.1590	-0.4798	-1.00000
-0.5212	-0.1563	-0.4877	-1.00000
-0.5123	-0.1537	-0.4963	-1.00000
-0.5037	-0.1511	-0.5048	-1.00000
-0.4952	-0.1486	-0.5131	-1.00000
-0.4869	-0.1460	-0.5214	-1.00000
-0.4788	-0.1436	-0.5293	-1.00000
-0.4707	-0.1412	-0.5373	-1.00000
-0.4627	-0.1388	-0.5450	-1.00000
-0.4550	-0.1364	-0.5527	-1.00000
-0.4475	-0.1342	-0.5602	-1.00000
-0.4398	-0.1319	-0.5676	-1.00000
-0.4324	-0.1297	-0.5748	-1.00000
-1.4252	-0.0294	-0.5820	-2.00000
-1.4130	-0.4342	-0.5719	-2.00000
-1.4281	-0.4495	-0.6163	-2.00000
-1.3837	-0.4487	-0.6516	-2.00000
-1.3484	-0.4260	-0.6855	-2.00000
-1.3143	-0.4064	-0.7112	-2.00000
-1.2883	-0.3931	-0.7367	-2.00000
-1.2633	-0.3832	-0.7578	-2.00000
-1.2422	-0.3739	-0.7903	-2.00000
-1.2197	-0.3673	-0.7999	-2.00000
-1.2001	-0.3600	-0.8211	-2.00000
-1.1789	-0.3542	-0.8401	-2.00000
-1.1599	-0.3477	-0.8605	-2.00000
-1.1395	-0.3423	-0.8789	-2.00000
-1.1211	-0.3360	-0.8985	-2.00000
-1.1013	-0.3308	-0.9165	-2.00000
-1.0833	-0.3248	-0.9353	-2.00000
-1.0647	-0.3197	-0.9527	-2.00000

-1.0473	-0.3139	-0.9709	-2.00000
-1.0291	-0.3090	-0.9877	-2.00000
-1.0123	-0.3034	-1.0052	-2.00000
-0.9948	-0.2986	-1.0216	-2.00000
-0.9784	-0.2933	-1.0384	-2.00000
-0.9616	-0.2886	-1.0542	-2.00000
-0.9458	-0.2835	-1.0705	-2.00000
-0.9295	-0.2790	-1.0858	-2.00000
-0.9142	-0.2741	-1.1014	-2.00000
-0.8986	-0.2697	-1.1162	-2.00000
-0.8838	-0.2650	-1.1313	-2.00000
-0.8687	-0.2607	-1.1457	-2.00000
-0.8543	-0.2562	-1.1602	-2.00000
-0.8398	-0.2520	-1.1741	-2.00000
-0.8259	-0.2476	-1.1881	-2.00000
-0.8115	-0.2436	-1.2015	-2.00000
-0.7985	-0.2394	-1.2150	-2.00000
-0.7850	-0.2355	-1.2280	-2.00000
-0.7720	-0.2315	-1.2411	-2.00000
-0.7589	-0.2277	-1.2536	-2.00000
-0.7464	-0.2238	-1.2662	-2.00000
-0.7333	-0.2201	-1.2783	-2.00000
-0.7217	-0.2164	-1.2905	-2.00000
-0.7095	-0.2128	-1.3022	-2.00000
-0.6973	-0.2092	-1.3139	-2.00000
-0.6851	-0.2058	-1.3253	-2.00000
-0.6747	-0.2023	-1.3366	-2.00000
-0.6634	-0.1990	-1.3475	-2.00000
-0.6525	-0.1956	-1.3585	-2.00000
-0.6415	-0.1924	-1.3691	-2.00000
-0.6309	-0.1892	-1.3796	-2.00000
-0.6204	-0.1861	-1.3898	-2.00000
-0.6102	-0.1830	-1.4000	-2.00000
-0.6000	-0.1800	-1.4099	-2.00000
-0.5901	-0.1769	-1.4197	-2.00000
-0.5803	-0.1740	-1.4293	-2.00000
-0.5707	-0.1711	-1.4387	-2.00000
-0.5613	-0.1683	-1.4480	-2.00000
-0.5520	-0.1655	-1.4571	-2.00000
-0.5429	-0.1628	-1.4661	-2.00000
-0.5339	-0.1601	-1.4749	-2.00000
-0.5251	-0.1575	-1.4835	-2.00000
-0.5165	-0.1549	-1.4920	-2.00000
-0.5080	-0.1523	-1.5004	-2.00000
-0.4996	-0.1498	-1.5086	-2.00000
-0.4914	-0.1473	-1.5166	-2.00000
-0.4834	-0.1448	-1.5246	-2.00000
-0.4754	-0.1425	-1.5324	-2.00000
-0.4676	-0.1402	-1.5400	-2.00000
-0.4600	-0.1379	-1.5476	-2.00000
-0.4524	-0.1356	-1.5550	-2.00000
-0.4450	-0.1334	-1.5622	-2.00000
1.5622	-0.4450	-1.5694	0.00000
1.5694	0.4835	-1.6104	0.00000
1.6104	0.5254	-1.5425	0.00000
1.5425	0.5321	-1.4920	0.00000
1.4920	0.4908	-1.4444	0.00000
1.4444	0.4615	-1.4124	0.00000
1.4124	0.4369	-1.3808	0.00000
1.3808	0.4228	-1.3575	0.00000



1.3575	0.4099	-1.3313	0.00000
1.3313	0.4022	-1.3103	0.00000
1.3103	0.3931	-1.2858	0.00000
1.2858	0.3872	-1.2655	0.00000
1.2655	0.3792	-1.2422	0.00000
1.2422	0.3736	-1.2223	0.00000
1.2223	0.3662	-1.1999	0.00000
1.1999	0.3502	-1.1805	0.00000
1.1805	0.3537	-1.1590	0.00000
1.1590	0.3484	-1.1401	0.00000
1.1401	0.3417	-1.1194	0.00000
1.1194	0.3354	-1.1011	0.00000
0.1011	0.4569	-1.0912	-1.00000
0.0812	0.0151	-1.0464	-1.00000
0.0464	-0.0074	-1.0648	-1.00000
0.0648	-0.0147	-1.0761	-1.00000
0.0761	0.0011	-1.0949	-1.00000
0.0849	0.0112	-1.0873	-1.00000
0.0873	0.0195	-1.0887	-1.00000
0.0887	0.0227	-1.0872	-1.00000
0.0872	0.0249	-1.0865	-1.00000
0.0865	0.0249	-1.0943	-1.00000
0.0843	0.0252	-1.0831	-1.00000
0.0831	0.0246	-1.0810	-1.00000
0.0810	0.0246	-1.0798	-1.00000
0.0798	0.0237	-1.0778	-1.00000
0.0778	0.0236	-1.0766	-1.00000
0.0766	0.0229	-1.0747	-1.00000
0.0747	0.0226	-1.0735	-1.00000
0.0735	0.0220	-1.0718	-1.00000
0.0718	0.0217	-1.0706	-1.00000
0.0706	0.0211	-1.0689	-1.00000
0.0689	0.0209	-1.0678	-1.00000
0.0678	0.0203	-1.0662	-1.00000
0.0662	0.0200	-1.0651	-1.00000
0.0651	0.0195	-1.0635	-1.00000
0.0635	0.0192	-1.0624	-1.00000
0.0624	0.0187	-1.0610	-1.00000
0.0610	0.0184	-1.0599	-1.00000
0.0599	0.0180	-1.0585	-1.00000
0.0585	0.0177	-1.0574	-1.00000
0.0574	0.0172	-1.0561	-1.00000
0.0561	0.0170	-1.0551	-1.00000
0.0551	0.0165	-1.0538	-1.00000
0.0538	0.0163	-1.0528	-1.00000
0.0528	0.0159	-1.0516	-1.00000
0.0516	0.0156	-1.0506	-1.00000
0.0506	0.0152	-1.0494	-1.00000
0.0494	0.0149	-1.0484	-1.00000
0.0484	0.0146	-1.0473	-1.00000
0.0473	0.0143	-1.0464	-1.00000
0.0464	0.0140	-1.0453	-1.00000
1.0453	-0.1432	-1.0444	0.00000
1.0444	0.3222	-1.0604	0.00000
1.0604	0.3393	-1.0221	0.00000
1.0221	0.3413	-0.9925	0.00000
0.9925	0.3194	-0.9645	0.00000
0.9645	0.3034	-0.9443	0.00000
0.9443	0.2899	-0.9244	0.00000
0.9244	0.2316	-0.9087	0.00000

0.9087	0.2739	-0.8916	0.00000
0.8916	0.2689	-0.8772	0.00000
0.8772	0.2632	-0.8612	0.00000
0.8612	0.2591	-0.8472	0.00000
0.8472	0.2540	-0.8319	0.00000
0.8319	0.2501	-0.8183	0.00000
0.8183	0.2453	-0.8035	0.00000
0.8035	0.2415	-0.7903	0.00000
0.7903	0.2369	-0.7761	0.00000
0.7761	0.2332	-0.7633	0.00000
0.7633	0.2289	-0.7496	0.00000
0.7496	0.2252	-0.7372	0.00000
0.7372	0.2210	-0.7240	0.00000
0.7240	0.2175	-0.7120	0.00000
0.7120	0.2135	-0.6993	0.00000
0.6993	0.2100	-0.6876	0.00000
0.6876	0.2062	-0.6754	0.00000
0.6754	0.2029	-0.6641	0.00000
0.6641	0.1992	-0.6524	0.00000
0.6524	0.1959	-0.6414	0.00000
0.6414	0.1924	-0.6301	0.00000
0.6301	0.1892	-0.6195	0.00000
0.6195	0.1859	-0.6086	0.00000
0.6086	0.1827	-0.5983	0.00000
0.5983	0.1795	-0.5878	0.00000
0.5878	0.1765	-0.5778	0.00000
0.5778	0.1733	-0.5677	0.00000
0.5677	0.1704	-0.5581	0.00000
0.5581	0.1674	-0.5483	0.00000
0.5483	0.1646	-0.5390	0.00000
0.5390	0.1617	-0.5296	0.00000
0.5296	0.1590	-0.5206	0.00000
0.5206	0.1562	-0.5115	0.00000
0.5115	0.1535	-0.5028	0.00000
0.5028	0.1508	-0.4940	0.00000
0.4940	0.1482	-0.4856	0.00000
0.4856	0.1457	-0.4771	0.00000
0.4771	0.1432	-0.4690	0.00000
0.4690	0.1407	-0.4608	0.00000
0.4608	0.1383	-0.4529	0.00000
0.4529	0.1259	-0.4451	0.00000
0.4451	0.1366	-0.4375	0.00000
0.4375	0.1313	-0.4299	0.00000
0.4299	0.1290	-0.4225	0.00000
0.4225	0.1268	-0.4152	0.00000
0.4152	0.1246	-0.4081	0.00000
0.4081	0.1225	-0.4010	0.00000
0.4010	0.1204	-0.3941	0.00000
0.3941	0.1183	-0.3873	0.00000
0.3873	0.1162	-0.3807	0.00000
0.3807	0.1142	-0.3741	0.00000
0.3741	0.1123	-0.3676	0.00000
0.3676	0.1103	-0.3613	0.00000
0.3613	0.1084	-0.3551	0.00000
0.3551	0.1066	-0.3489	0.00000
0.3489	0.1047	-0.3429	0.00000
0.3429	0.1029	-0.3370	0.00000
0.3370	0.1011	-0.3312	0.00000
0.3312	0.0994	-0.3255	0.00000
0.3255	0.0977	-0.3199	0.00000

0.3199	0.0960	-0.3144	0.00000
0.3144	0.0944	-0.3090	0.00000
4.3090	-0.5348	-0.3036	4.00000
4.3036	1.3262	-0.3664	4.00000
4.3664	1.3944	-0.2116	4.00000
4.2110	1.4020	-0.0921	4.00000
4.0921	1.3133	0.0215	4.00000
3.9785	1.2495	0.1034	4.00000
3.8966	1.1951	0.1843	4.00000
3.8157	1.1617	0.2482	4.00000
3.7518	1.1306	0.3178	4.00000
3.6822	1.1102	0.3766	4.00000
3.6234	1.0870	0.4420	4.00000
3.5580	1.0701	0.4988	4.00000
3.5012	1.0493	0.5614	4.00000
3.4380	1.0234	0.6168	4.00000
3.3832	1.0139	0.6770	4.00000
3.3230	0.9983	0.7309	4.00000
3.2691	0.9797	0.7888	4.00000
3.2112	0.9644	0.8411	4.00000
3.1509	0.9469	0.8968	4.00000
3.1032	0.9320	0.9476	4.00000
3.0524	0.9149	1.0011	4.00000
2.9957	0.9005	1.0504	4.00000
2.9496	0.8842	1.1019	4.00000
2.8981	0.8702	1.1497	4.00000
2.8503	0.8545	1.1993	4.00000
2.8007	0.8403	1.2456	4.00000
2.7544	0.8258	1.2934	4.00000
2.7060	0.8125	1.3382	4.00000
2.6613	0.7981	1.3842	4.00000
2.6155	0.7852	1.4276	4.00000
2.5724	0.7713	1.4720	4.00000
2.5230	0.7564	1.5140	4.00000
2.4860	0.7435	1.5567	4.00000
2.4433	0.7333	1.5974	4.00000
2.4026	0.7205	1.6386	4.00000
2.3614	0.7057	1.6780	4.00000
2.3220	0.6962	1.7177	4.00000
2.2823	0.6849	1.7553	4.00000
2.2442	0.6730	1.7941	4.00000
2.2059	0.6615	1.8309	4.00000
-0.3309	1.0427	1.8679	1.50000
-0.3579	-0.1322	1.9450	1.50000
-0.4460	-0.1858	1.8891	1.50000
-0.3681	-0.2028	1.8510	1.50000
-0.3510	-0.1593	1.8175	1.50000
-0.3175	-0.1303	1.8026	1.50000
-0.3026	-0.1077	1.7883	1.50000
-0.2683	-0.0970	1.7834	1.50000
-0.2834	-0.0983	1.7749	1.50000
-0.2749	-0.0859	1.7721	1.50000
-0.2721	-0.0817	1.7649	1.50000
-0.2649	-0.0811	1.7622	1.50000
-0.2622	-0.0792	1.7556	1.50000
-0.2556	-0.0778	1.7527	1.50000
-0.2527	-0.0752	1.7465	1.50000
-0.2465	-0.0749	1.7435	1.50000
-0.2435	-0.0725	1.7376	1.50000
-0.2376	-0.0721	1.7345	1.50000

-0.2345	-0.0699	1.7290	1.50000
-0.2290	-0.0694	1.7258	1.50000
-0.2258	-0.0674	1.7206	1.50000
-0.2206	-0.0668	1.7175	1.50000
-0.2175	-0.0649	1.7125	1.50000
-0.2125	-0.0643	1.7094	1.50000
-0.2094	-0.0626	1.7047	1.50000
-0.2047	-0.0619	1.7016	1.50000
-0.2016	-0.0603	1.6972	1.50000
-0.1972	-0.0596	1.6941	1.50000
-0.1941	-0.0581	1.6899	1.50000
-0.1899	-0.0573	1.6868	1.50000
-0.1868	-0.0559	1.6828	1.50000
-0.1828	-0.0552	1.6798	1.50000
-0.1798	-0.0539	1.6760	1.50000
-0.1760	-0.0531	1.6730	1.50000
-0.1730	-0.0519	1.6694	1.50000
-0.1694	-0.0511	1.6665	1.50000
-0.1665	-0.0499	1.6630	1.50000
-0.1630	-0.0492	1.6602	1.50000
-0.1602	-0.0481	1.6569	1.50000
-0.1569	-0.0472	1.6541	1.50000
-0.1541	-0.0462	1.6510	1.50000
-0.1510	-0.0455	1.6483	1.50000
-0.1483	-0.0445	1.6452	1.50000
-0.1452	-0.0435	1.6426	1.50000
-0.1426	-0.0428	1.6397	1.50000
-0.1397	-0.0421	1.6371	1.50000
-0.1371	-0.0412	1.6343	1.50000
-0.1343	-0.0405	1.6318	1.50000
-0.1318	-0.0396	1.6291	1.50000
-0.1291	-0.0389	1.6267	1.50000
-0.1267	-0.0381	1.6241	1.50000
-0.1241	-0.0374	1.6218	1.50000
-0.1218	-0.0366	1.6193	1.50000
-0.1193	-0.0359	1.6170	1.50000
-0.1170	-0.0352	1.6146	1.50000
-0.1146	-0.0345	1.6124	1.50000
-0.1124	-0.0338	1.6101	1.50000
-0.1101	-0.0332	1.6080	1.50000
-0.1080	-0.0325	1.6058	1.50000
-0.1058	-0.0319	1.6037	1.50000
-0.1037	-0.0312	1.6016	1.50000
-0.1016	-0.0306	1.5995	1.50000
-0.0995	-0.0300	1.5975	1.50000
-0.0975	-0.0294	1.5956	1.50000
-0.0956	-0.0289	1.5936	1.50000
-0.0936	-0.0282	1.5917	1.50000
-0.0917	-0.0276	1.5898	1.50000
-0.0898	-0.0271	1.5880	1.50000
-0.0880	-0.0265	1.5861	1.50000
-0.0861	-0.0260	1.5844	1.50000
-2.5844	0.3568	1.5826	-1.00000
-2.5826	-0.7968	1.6234	-1.00000
-2.6234	-0.8399	1.5281	-1.00000
-2.5281	-0.9451	1.4550	-1.00000
-2.4550	-0.7905	1.3854	-1.00000
-2.3854	-0.7509	1.3357	-1.00000
-2.3357	-0.7171	1.2865	-1.00000
-2.2865	-0.6967	1.2480	-1.00000

-2.2490	-0.5776	1.2058	-1.00000
-2.2056	-0.5553	1.1705	-1.00000
-2.6705	-0.5727	1.1309	-1.50000
-2.6309	-0.7954	1.1052	-1.50000
-2.6052	-0.7916	1.0486	-1.50000
-2.5466	-0.7831	1.0010	-1.50000
-2.5010	-0.7605	0.9510	-1.50000
-2.4510	-0.7433	0.9089	-1.50000
-2.4089	-0.7254	0.8644	-1.50000
-2.3644	-0.7123	0.8255	-1.50000
-2.3255	-0.6978	0.7837	-1.50000
-2.2837	-0.6865	0.7463	-1.50000
-2.2463	-0.6735	0.7063	-1.50000
-2.2063	-0.6629	0.6701	-1.50000
-2.1701	-0.6506	0.6317	-1.50000
-2.1317	-0.6403	0.5965	-1.50000
-2.0965	-0.6285	0.5595	-1.50000
-2.0595	-0.6185	0.5254	-1.50000
-2.0254	-0.6073	0.4898	-1.50000
-1.9895	-0.5975	0.4567	-1.50000
-1.9567	-0.5867	0.4224	-1.50000
-1.9224	-0.5772	0.3904	-1.50000
-2.3904	-0.4984	0.3574	-2.00000
-2.3574	-0.7120	0.3348	-2.00000
-2.3348	-0.7108	0.2843	-2.00000
-2.2643	-0.7030	0.2400	-2.00000
-2.2400	-0.6826	0.1957	-2.00000
-2.1957	-0.6651	0.1570	-2.00000
-2.1570	-0.6502	0.1180	-2.00000
-2.1180	-0.6373	0.0824	-2.00000
-2.0824	-0.6252	0.0458	-2.00000
-2.0458	-0.6147	0.0118	-2.00000
-2.0118	-0.6034	-0.0223	-2.00000
-1.9757	-0.5926	-0.0562	-2.00000
-1.9435	-0.5823	-0.0899	-2.00000
-1.9101	-0.5734	-0.1215	-2.00000
-1.8762	-0.5633	-0.1544	-2.00000
-1.8436	-0.5540	-0.1852	-2.00000
-1.8143	-0.5443	-0.2166	-2.00000
-1.7834	-0.5353	-0.2465	-2.00000
-1.7535	-0.5259	-0.2767	-2.00000
-1.7233	-0.5172	-0.3056	-2.00000
-1.6944	-0.5082	-0.3348	-2.00000
-1.6652	-0.4993	-0.3628	-2.00000
-1.6372	-0.4911	-0.3909	-2.00000
-1.6091	-0.4829	-0.4179	-2.00000
-1.5821	-0.4745	-0.4451	-2.00000
-1.5549	-0.4666	-0.4712	-2.00000
-1.5288	-0.4585	-0.4974	-2.00000
-1.5026	-0.4509	-0.5227	-2.00000
-1.4773	-0.4431	-0.5480	-2.00000
-1.4520	-0.4357	-0.5724	-2.00000
-1.4276	-0.4282	-0.5968	-2.00000
-1.4032	-0.4211	-0.6204	-2.00000
-1.3796	-0.4139	-0.6439	-2.00000
-1.3561	-0.4069	-0.6668	-2.00000
-1.3332	-0.3999	-0.6895	-2.00000
-1.3105	-0.3932	-0.7115	-2.00000
-1.2885	-0.3865	-0.7335	-2.00000
-1.2665	-0.3800	-0.7548	-2.00000

-1.2452	-0.3735	-0.7759	-2.00000
-1.2241	-0.3673	-0.7966	-2.00000
-1.2034	-0.3610	-0.8170	-2.00000
-1.1830	-0.3549	-0.8369	-2.00000
-1.1631	-0.3489	-0.8566	-2.00000
-1.1434	-0.3430	-0.8759	-2.00000
-1.1241	-0.3372	-0.8949	-2.00000
-1.1051	-0.3315	-0.9135	-2.00000
-1.0865	-0.3259	-0.9319	-2.00000
-1.0681	-0.3204	-0.9499	-2.00000
-1.0502	-0.3150	-0.9676	-2.00000
-1.0324	-0.3097	-0.9849	-2.00000
-1.0151	-0.3045	-1.0021	-2.00000
-0.9979	-0.2994	-1.0188	-2.00000
-0.9812	-0.2943	-1.0354	-2.00000
-0.9646	-0.2894	-1.0516	-2.00000
-0.9484	-0.2845	-1.0675	-2.00000
-0.9325	-0.2797	-1.0832	-2.00000
-0.9163	-0.2750	-1.0986	-2.00000
-0.9014	-0.2704	-1.1137	-2.00000
-0.8863	-0.2659	-1.1286	-2.00000
-0.8714	-0.2614	-1.1432	-2.00000
1.1432	-0.2570	-1.1576	0.00000
1.1576	0.2649	-1.2057	0.00000
1.2057	0.4040	-1.1448	0.00000
1.1448	0.4127	-1.1012	0.00000
1.1012	0.3735	-1.0603	0.00000
1.0603	0.3462	-1.0349	0.00000
1.0349	0.3236	-1.0098	0.00000
1.0098	0.3115	-0.9929	0.00000
0.9929	0.3004	-0.9730	0.00000
0.9730	0.2947	-0.9581	0.00000
0.9581	0.2875	-0.9398	0.00000
0.9398	0.2833	-0.9254	0.00000
0.9254	0.2772	-0.9079	0.00000
0.9079	0.2733	-0.8938	0.00000
0.8938	0.2676	-0.8771	0.00000
0.8771	0.2639	-0.8633	0.00000
0.8633	0.2585	-0.8472	0.00000
0.8472	0.2548	-0.8337	0.00000
0.8337	0.2497	-0.8183	0.00000
0.8183	0.2461	-0.8052	0.00000
0.8052	0.2412	-0.7904	0.00000
0.7904	0.2376	-0.7776	0.00000
0.7776	0.2320	-0.7634	0.00000
0.7634	0.2295	-0.7510	0.00000
0.7510	0.2251	-0.7374	0.00000
0.7374	0.2216	-0.7253	0.00000
0.7253	0.2174	-0.7122	0.00000
0.7122	0.2140	-0.7005	0.00000
0.7005	0.2100	-0.6879	0.00000
0.6879	0.2067	-0.6765	0.00000
0.6765	0.2029	-0.6644	0.00000
0.6644	0.1996	-0.6534	0.00000
0.6534	0.1959	-0.6417	0.00000
0.6417	0.1928	-0.6310	0.00000
0.6310	0.1892	-0.6198	0.00000
0.6198	0.1862	-0.6094	0.00000
0.6094	0.1828	-0.5987	0.00000
0.5987	0.1798	-0.5886	0.00000

0.5886	0.1765	-0.5782	0.00000
0.5782	0.1736	-0.5685	0.00000
0.5685	0.1705	-0.5585	0.00000
0.5585	0.1677	-0.5490	0.00000
0.5490	0.1647	-0.5394	0.00000
0.5394	0.1620	-0.5302	0.00000
0.5302	0.1591	-0.5210	0.00000
0.5210	0.1564	-0.5121	0.00000
0.5121	0.1536	-0.5032	0.00000
0.5032	0.1511	-0.4946	0.00000
0.4946	0.1484	-0.4860	0.00000
0.4860	0.1459	-0.4777	0.00000
0.4777	0.1433	-0.4694	0.00000
0.4694	0.1409	-0.4614	0.00000
0.4614	0.1384	-0.4533	0.00000
0.4533	0.1361	-0.4456	0.00000
0.4456	0.1337	-0.4379	0.00000
0.4379	0.1314	-0.4304	0.00000
0.4304	0.1291	-0.4229	0.00000
0.4229	0.1269	-0.4157	0.00000
0.4157	0.1247	-0.4084	0.00000
0.4084	0.1226	-0.4014	0.00000
-2.0986	0.5127	-0.3945	-2.50000
-2.1055	-0.6535	-0.3452	-2.50000
-2.1548	-0.6992	-0.4321	-2.50000
-2.0579	-0.7069	-0.4970	-2.50000
-2.0030	-0.6547	-0.5584	-2.50000
-1.9416	-0.6176	-0.6003	-2.50000
-1.8997	-0.5362	-0.6416	-2.50000
-1.8584	-0.5621	-0.6725	-2.50000
-1.8275	-0.5514	-0.7070	-2.50000
-1.7930	-0.5413	-0.7350	-2.50000
-1.7650	-0.5294	-0.7672	-2.50000
-1.7326	-0.5214	-0.7943	-2.50000
-1.7057	-0.5110	-0.8251	-2.50000
-1.6749	-0.5035	-0.8516	-2.50000
-1.6484	-0.4938	-0.8812	-2.50000
-1.6183	-0.4865	-0.9069	-2.50000
-1.5921	-0.4772	-0.9354	-2.50000
-1.5646	-0.4701	-0.9605	-2.50000
-1.5395	-0.4613	-0.9878	-2.50000
-1.5122	-0.4543	-1.0121	-2.50000
-1.4879	-0.4458	-1.0384	-2.50000
-1.4616	-0.4390	-1.0621	-2.50000
-1.4379	-0.4309	-1.0873	-2.50000
-1.4127	-0.4242	-1.1103	-2.50000
-1.3897	-0.4165	-1.1345	-2.50000
-1.3655	-0.4100	-1.1568	-2.50000
-1.3432	-0.4026	-1.1801	-2.50000
-1.3199	-0.3962	-1.2018	-2.50000
-1.2982	-0.3892	-1.2242	-2.50000
-1.2758	-0.3830	-1.2452	-2.50000
1.2452	-0.7684	-1.2668	0.00000
1.2668	0.4018	-1.3296	0.00000
1.3296	0.4519	-1.2569	0.00000
1.2569	0.4634	-1.2050	0.00000
1.2050	0.4156	-1.1572	0.00000
1.1572	0.3822	-1.1281	0.00000
1.1281	0.3549	-1.0999	0.00000
1.0999	0.3404	-1.0812	0.00000

1.0812	0.3277	-1.0593	0.00000
1.0593	0.3212	-1.0432	0.00000
1.0432	0.3131	-1.0232	0.00000
1.0232	0.3086	-1.0076	0.00000
1.0076	0.3018	-0.9885	0.00000
0.9885	0.2977	-0.9733	0.00000
0.9733	0.2914	-0.9549	0.00000
0.9549	0.2874	-0.9400	0.00000
0.9400	0.2815	-0.9224	0.00000
0.9224	0.2775	-0.9078	0.00000
0.9078	0.2719	-0.8910	0.00000
0.8910	0.2679	-0.8767	0.00000
3.8767	-0.2080	-0.8606	3.00000
3.8606	1.1351	-0.8977	3.00000
3.8977	1.2323	-0.7700	3.00000
3.7700	1.2352	-0.6706	3.00000
3.6706	1.1656	-0.5744	3.00000
3.5744	1.1149	-0.5034	3.00000
3.5034	1.0704	-0.4321	3.00000
3.4321	1.0427	-0.3749	3.00000
3.3749	1.0161	-0.3125	3.00000
3.3125	0.9982	-0.2554	3.00000
3.2554	0.9776	-0.2006	3.00000
3.2006	0.9625	-0.1492	3.00000
3.1492	0.9439	-0.0928	3.00000
3.0928	0.9295	-0.0428	3.00000
3.0428	0.9119	0.0114	3.00000
2.9836	0.8979	0.0600	3.00000
2.9400	0.8811	0.1122	3.00000
2.8878	0.8674	0.1594	3.00000
2.8406	0.8514	0.2095	3.00000
2.7909	0.8331	0.2554	3.00000
-0.2554	1.2934	0.3036	0.00000
-0.3036	-0.1165	0.3991	0.00000
-0.3991	-0.1824	0.3332	0.00000
-0.3332	-0.2031	0.2905	0.00000
-0.2905	-0.1523	0.2537	0.00000
-0.2537	-0.1177	0.2377	0.00000
-0.2377	-0.0913	0.2237	0.00000
-0.2237	-0.0793	0.2197	0.00000
-0.2197	-0.0700	0.2124	0.00000
-0.2124	-0.0674	0.2109	0.00000
-0.2109	-0.0635	0.2052	0.00000
-0.2052	-0.0632	0.2038	0.00000
-0.2038	-0.0606	0.1986	0.00000
-0.1986	-0.0606	0.1969	0.00000
-0.1969	-0.0584	0.1920	0.00000
-0.1920	-0.0584	0.1902	0.00000
-0.1902	-0.0565	0.1856	0.00000
-0.1856	-0.0562	0.1836	0.00000
-0.1836	-0.0546	0.1793	0.00000
-0.1793	-0.0544	0.1773	0.00000
-0.1773	-0.0527	0.1733	0.00000
-0.1733	-0.0525	0.1712	0.00000
-0.1712	-0.0510	0.1674	0.00000
-0.1674	-0.0506	0.1653	0.00000
-0.1653	-0.0493	0.1617	0.00000
-0.1617	-0.0489	0.1596	0.00000
-0.1596	-0.0476	0.1562	0.00000
-0.1562	-0.0472	0.1541	0.00000



-0.1541	-0.0460	0.1509	0.00000
-0.1509	-0.0455	0.1489	0.00000
-0.1488	-0.0444	0.1458	0.00000
-0.1455	-0.0440	0.1437	0.00000
-0.1437	-0.0429	0.1408	0.00000
-0.1408	-0.0424	0.1388	0.00000
-0.1388	-0.0415	0.1361	0.00000
-0.1361	-0.0410	0.1340	0.00000
-0.1340	-0.0401	0.1314	0.00000
-0.1314	-0.0396	0.1294	0.00000
-0.1294	-0.0387	0.1269	0.00000
-0.1269	-0.0382	0.1250	0.00000
-0.1250	-0.0374	0.1226	0.00000
-0.1226	-0.0369	0.1207	0.00000
-0.1207	-0.0361	0.1194	0.00000
-0.1194	-0.0356	0.1166	0.00000
-0.1166	-0.0349	0.1144	0.00000
-0.1144	-0.0344	0.1126	0.00000
-0.1126	-0.0337	0.1105	0.00000
-0.1105	-0.0332	0.1087	0.00000
-0.1087	-0.0326	0.1067	0.00000
-0.1067	-0.0321	0.1050	0.00000
-0.1050	-0.0315	0.1031	0.00000
-0.1031	-0.0310	0.1014	0.00000
-0.1014	-0.0304	0.0996	0.00000
-0.0996	-0.0299	0.0979	0.00000
-0.0979	-0.0294	0.0962	0.00000
-0.0962	-0.0289	0.0946	0.00000
-0.0946	-0.0284	0.0929	0.00000
-0.0929	-0.0279	0.0913	0.00000
-0.0913	-0.0274	0.0897	0.00000
-0.0897	-0.0269	0.0882	0.00000
-0.0882	-0.0265	0.0867	0.00000
-0.0867	-0.0260	0.0852	0.00000
-0.0852	-0.0255	0.0837	0.00000
-0.0837	-0.0251	0.0823	0.00000
-0.0823	-0.0247	0.0808	0.00000
-0.0808	-0.0243	0.0795	0.00000
-0.0795	-0.0238	0.0781	0.00000
-0.0781	-0.0234	0.0768	0.00000
-0.0768	-0.0230	0.0754	0.00000
-0.0754	-0.0226	0.0741	0.00000
-0.0741	-0.0222	0.0728	0.00000
-0.0728	-0.0219	0.0716	0.00000
-0.0716	-0.0215	0.0703	0.00000
-0.0703	-0.0211	0.0692	0.00000
-0.0692	-0.0207	0.0679	0.00000
-0.0679	-0.0204	0.0668	0.00000
-0.0668	-0.0200	0.0656	0.00000
-0.0656	-0.0197	0.0645	0.00000
-0.0645	-0.0194	0.0634	0.00000
-0.0634	-0.0190	0.0623	0.00000
-0.0623	-0.0187	0.0612	0.00000
-0.0612	-0.0184	0.0602	0.00000
-0.0602	-0.0181	0.0591	0.00000
-0.0591	-0.0177	0.0581	0.00000
-0.0581	-0.0174	0.0571	0.00000
-0.0571	-0.0171	0.0561	0.00000
-0.0561	-0.0168	0.0552	0.00000
-0.0552	-0.0166	0.0542	0.00000

-0.0542	-0.0163	0.0533	0.00000
-0.0533	-0.0160	0.0524	0.00000
4.9476	-0.8002	0.0514	5.00000
4.5456	1.5285	-0.0345	5.00000
5.0345	1.6159	0.1518	5.00000
4.8482	1.6275	0.2940	5.00000
4.7060	1.5195	0.4289	5.00000
4.5711	1.4416	0.5244	5.00000
4.4756	1.3753	0.6187	5.00000
4.3813	1.3356	0.6919	5.00000
4.3081	1.2987	0.7723	5.00000
4.2277	1.2752	0.8353	5.00000
4.1607	1.2491	0.9147	5.00000
4.0853	1.2289	0.9794	5.00000
4.0206	1.2048	1.0516	5.00000
3.9484	1.1858	1.1148	5.00000
3.8852	1.1641	1.1842	5.00000
3.8158	1.1465	1.2456	5.00000
3.7544	1.1250	1.3123	5.00000
3.6677	1.1078	1.3721	5.00000
3.6279	1.0872	1.4362	5.00000
3.5638	1.0704	1.4942	5.00000
3.5058	1.0507	1.5558	5.00000
3.4442	1.0343	1.6121	5.00000
3.3879	1.0155	1.6714	5.00000
3.3288	0.9995	1.7260	5.00000
3.2740	0.9814	1.7831	5.00000
3.2169	0.9659	1.8360	5.00000
3.1640	0.9485	1.8910	5.00000
3.1090	0.9323	1.9423	5.00000
3.0577	0.9167	1.9952	5.00000
3.0048	0.9020	2.0448	5.00000
2.9552	0.8860	2.0958	5.00000
2.9042	0.8717	2.1439	5.00000
2.8561	0.8564	2.1930	5.00000
2.8070	0.8425	2.2356	5.00000
2.7604	0.8277	2.2869	5.00000
2.7131	0.8142	2.3320	5.00000
2.6680	0.8000	2.3776	5.00000
2.6244	0.7870	2.4212	5.00000
2.5785	0.7733	2.4652	5.00000
2.5343	0.7606	2.5074	5.00000
2.4926	0.7475	2.5498	5.00000
2.4502	0.7352	2.5906	5.00000
2.4094	0.7225	2.6316	5.00000
2.3684	0.7106	2.6710	5.00000
2.3290	0.6984	2.7105	5.00000
2.2895	0.6869	2.7486	5.00000
2.2514	0.6752	2.7867	5.00000
2.2133	0.6640	2.8236	5.00000
2.1764	0.6527	2.8604	5.00000
2.1396	0.6419	2.8960	5.00000
0.1040	0.6448	2.9315	3.00000
0.0685	0.0030	3.0000	3.00000
0.0000	-0.0424	2.9594	3.00000
0.0406	-0.0571	2.9354	3.00000
0.0646	-0.0239	2.9142	3.00000
0.0858	-0.0024	2.9078	3.00000
0.0922	0.0144	2.9017	3.00000
0.0923	0.0209	2.9032	3.00000

0.0968	0.0263	2.9015	3.00000
0.0985	0.0267	2.9044	3.00000
0.0956	0.0235	2.9037	3.00000
0.0963	0.0275	2.9066	3.00000
0.0934	0.0234	2.9061	3.00000
0.0939	0.0272	2.9066	3.00000
0.0914	0.0278	2.9083	3.00000
0.0917	0.0257	2.9105	3.00000
0.0895	0.0272	2.9103	3.00000
0.0897	0.0262	2.9123	3.00000
0.0877	0.0266	2.9123	3.00000
0.0877	0.0257	2.9141	3.00000
0.0859	0.0260	2.9141	3.00000
0.0859	0.0252	2.9152	3.00000
0.0842	0.0254	2.9159	3.00000
0.0841	0.0247	2.9174	3.00000
0.0826	0.0249	2.9177	3.00000
0.0823	0.0242	2.9190	3.00000
0.0810	0.0243	2.9193	3.00000
0.0807	0.0234	2.9206	3.00000
0.0794	0.0234	2.9209	3.00000
0.0791	0.0233	2.9221	3.00000
0.0779	0.0234	2.9224	3.00000
0.0776	0.0224	2.9235	3.00000
0.0765	0.0220	2.9239	3.00000
0.0761	0.0225	2.9249	3.00000
0.0751	0.0225	2.9254	3.00000
0.0748	0.0221	2.9263	3.00000
0.0737	0.0220	2.9267	3.00000
0.0733	0.0217	2.9276	3.00000
0.0724	0.0216	2.9281	3.00000
0.0719	0.0213	2.9289	3.00000
0.0711	0.0212	2.9293	3.00000
0.0707	0.0209	2.9301	3.00000
0.0699	0.0208	2.9306	3.00000
0.0694	0.0204	2.9313	3.00000
0.0687	0.0205	2.9318	3.00000
0.0682	0.0202	2.9325	3.00000
0.0673	0.0201	2.9329	3.00000
0.0671	0.0196	2.9336	3.00000
0.0664	0.0196	2.9340	3.00000
0.0660	0.0195	2.9346	3.00000
0.0654	0.0194	2.9351	3.00000
0.0649	0.0192	2.9357	3.00000
0.0643	0.0191	2.9361	3.00000
0.0639	0.0189	2.9367	3.00000
0.0633	0.0189	2.9371	3.00000
0.0629	0.0186	2.9377	3.00000
0.0623	0.0185	2.9381	3.00000
0.0619	0.0184	2.9386	3.00000
0.0614	0.0182	2.9390	3.00000
0.0610	0.0181	2.9395	3.00000
0.0605	0.0180	2.9399	3.00000
0.0601	0.0178	2.9404	3.00000
0.0596	0.0177	2.9408	3.00000
0.0592	0.0176	2.9412	3.00000
0.0588	0.0174	2.9416	3.00000
0.0584	0.0173	2.9420	3.00000
0.0580	0.0172	2.9424	3.00000
0.0576	0.0171	2.9428	3.00000

0.0572	0.0170	2.9432	3.00000
0.0568	0.0169	2.9436	3.00000
0.0564	0.0167	2.9439	3.00000
0.0561	0.0166	2.9443	3.00000
0.0557	0.0165	2.9447	3.00000
0.0553	0.0164	2.9450	3.00000
0.0550	0.0163	2.9454	3.00000
0.0546	0.0162	2.9457	3.00000
0.0543	0.0161	2.9461	3.00000
0.0539	0.0160	2.9464	3.00000
0.0536	0.0159	2.9467	3.00000
0.0533	0.0158	2.9470	3.00000
0.0530	0.0157	2.9473	3.00000
0.0527	0.0156	2.9477	3.00000
0.0523	0.0155	2.9479	3.00000
0.0521	0.0154	2.9483	3.00000
0.0517	0.0153	2.9485	3.00000
0.0515	0.0152	2.9488	3.00000
0.0512	0.0152	2.9491	3.00000
0.0509	0.0151	2.9494	3.00000
0.0506	0.0150	2.9497	3.00000
0.0503	0.0149	2.9499	3.00000
0.0501	0.0148	2.9502	3.00000
0.0498	0.0147	2.9504	3.00000
0.0496	0.0147	2.9507	3.00000
0.0493	0.0146	2.9510	3.00000
0.0490	0.0145	2.9512	3.00000
0.0488	0.0144	2.9514	3.00000
0.0486	0.0144	2.9517	3.00000
0.0483	0.0143	2.9519	3.00000
0.0481	0.0142	2.9521	3.00000
0.0479	0.0142	2.9524	3.00000
0.0476	0.0141	2.9526	3.00000
0.0474	0.0140	2.9528	3.00000
0.0472	0.0140	2.9530	3.00000
0.0470	0.0139	2.9532	3.00000
0.0468	0.0139	2.9534	3.00000
0.0466	0.0138	2.9536	3.00000
0.0464	0.0137	2.9538	3.00000
0.0462	0.0137	2.9540	3.00000
0.0460	0.0136	2.9542	3.00000
0.0458	0.0135	2.9544	3.00000
1.0456	0.0134	2.9546	4.00000
1.0454	0.0132	2.9378	4.00000
1.0622	0.0339	2.9754	4.00000
1.0246	0.0341	3.0042	4.00000
0.9958	0.0320	3.0315	4.00000
0.9685	0.0304	3.0509	4.00000
0.9491	0.0291	3.0701	4.00000
0.9299	0.0283	3.0851	4.00000
0.9149	0.0275	3.1015	4.00000
0.8985	0.0270	3.1152	4.00000
0.8848	0.0265	3.1306	4.00000
0.8694	0.0261	3.1438	4.00000
0.8562	0.0256	3.1586	4.00000
0.8414	0.0252	3.1715	4.00000
0.8265	0.0248	3.1856	4.00000
0.8144	0.0244	3.1982	4.00000
0.8018	0.0240	3.2118	4.00000
0.7892	0.0236	3.2241	4.00000

0.7759	0.2324	3.2371	4.00000
0.7629	0.2229	3.2490	4.00000
0.7510	0.2249	3.2616	4.00000
0.7384	0.2215	3.2731	4.00000
0.7269	0.2177	3.2852	4.00000
0.7148	0.2144	3.2964	4.00000
0.7036	0.2107	3.3080	4.00000
0.6920	0.2075	3.3189	4.00000
0.6811	0.2040	3.3301	4.00000
0.6699	0.2009	3.3406	4.00000
0.6594	0.1975	3.3514	4.00000
0.6486	0.1945	3.3615	4.00000
-4.3615	0.9757	3.3719	-1.00000
-4.3719	-1.3556	3.4668	-1.00000
-4.4668	-1.4459	3.2897	-1.00000
-4.2397	-1.4601	3.1562	-1.00000
-4.1562	-1.2549	3.0301	-1.00000
-4.0301	-1.2795	2.9430	-1.00000
-3.9430	-1.2158	2.8572	-1.00000
-3.8572	-1.1755	2.7921	-1.00000
-3.7921	-1.1442	2.7199	-1.00000
-3.7199	-1.1230	2.6607	-1.00000
-3.6607	-1.0984	2.5933	-1.00000
-3.5933	-1.0815	2.5361	-1.00000
-3.5361	-1.0599	2.4716	-1.00000
-3.4716	-1.0439	2.4158	-1.00000
-3.4158	-1.0236	2.3537	-1.00000
-3.3537	-1.0091	2.2994	-1.00000
-3.2994	-0.9888	2.2398	-1.00000
-3.2398	-0.9726	2.1869	-1.00000
-3.1869	-0.9552	2.1297	-1.00000
-3.1297	-0.9403	2.0783	-1.00000
-3.0783	-0.9227	2.0232	-1.00000
-3.0232	-0.9082	1.9733	-1.00000
-2.9733	-0.8914	1.9204	-1.00000
-2.9204	-0.8772	1.8720	-1.00000
-2.8720	-0.8611	1.8211	-1.00000
-2.8211	-0.8473	1.7742	-1.00000
-2.7742	-0.8316	1.7252	-1.00000
-2.7252	-0.8164	1.6797	-1.00000
-2.6797	-0.8036	1.6325	-1.00000
-2.6325	-0.7905	1.5884	-1.00000
-2.5884	-0.7763	1.5430	-1.00000
-2.5430	-0.7636	1.5003	-1.00000
-2.5003	-0.7499	1.4566	-1.00000
-2.4566	-0.7376	1.4152	-1.00000
-2.4152	-0.7244	1.3731	-1.00000
-2.3731	-0.7124	1.3330	-1.00000
-2.3330	-0.6998	1.2924	-1.00000
-2.2924	-0.6882	1.2537	-1.00000
-2.2537	-0.6760	1.2145	-1.00000
-2.2145	-0.6648	1.1770	-1.00000
-2.1770	-0.6531	1.1392	-1.00000
-2.1392	-0.6421	1.1030	-1.00000
-2.1030	-0.6309	1.0665	-1.00000
-2.0665	-0.6203	1.0315	-1.00000
-2.0315	-0.6094	0.9963	-1.00000
-1.9963	-0.5992	0.9624	-1.00000
-1.9624	-0.5887	0.9285	-1.00000
-1.9285	-0.5739	0.8958	-1.00000

-1.8958	-0.5657	0.8630	-1.00000
-1.8630	-0.5592	0.8313	-1.00000
-2.3313	-0.4710	0.7998	-1.50000
-2.2998	-0.6945	0.7776	-1.50000
-2.2776	-0.6939	0.7285	-1.50000
-2.2285	-0.6861	0.6846	-1.50000
-2.1846	-0.6662	0.6416	-1.50000
-2.1416	-0.6497	0.6033	-1.50000
-2.1033	-0.6343	0.5654	-1.50000
-2.0654	-0.6219	0.5304	-1.50000
-2.0304	-0.6098	0.4949	-1.50000
-1.9949	-0.5993	0.4614	-1.50000
-1.9614	-0.5885	0.4273	-1.50000
-1.9273	-0.5787	0.3949	-1.50000
-1.8949	-0.5684	0.3621	-1.50000
-1.8621	-0.5590	0.3308	-1.50000
-1.8308	-0.5491	0.2991	-1.50000
-1.7991	-0.5400	0.2688	-1.50000
-1.7688	-0.5306	0.2382	-1.50000
-1.7382	-0.5217	0.2089	-1.50000
-1.7089	-0.5126	0.1795	-1.50000
-1.6795	-0.5041	0.1511	-1.50000
-2.1511	-0.4168	0.1227	-2.00000
-2.1227	-0.6414	0.1038	-2.00000
-2.1038	-0.6416	0.0576	-2.00000
-2.0576	-0.6349	0.0168	-2.00000
-2.0168	-0.6158	-0.0232	-2.00000
-1.9768	-0.6002	-0.0585	-2.00000
-1.9415	-0.5857	-0.0935	-2.00000
-1.9065	-0.5742	-0.1257	-2.00000
-1.8743	-0.5629	-0.1585	-2.00000
-1.8415	-0.5532	-0.1892	-2.00000
-1.8108	-0.5432	-0.2206	-2.00000
-1.7794	-0.5343	-0.2503	-2.00000
-1.7497	-0.5243	-0.2805	-2.00000
-1.7195	-0.5152	-0.3093	-2.00000
-1.6907	-0.5071	-0.3385	-2.00000
-1.6615	-0.4987	-0.3663	-2.00000
-1.6337	-0.4900	-0.3944	-2.00000
-1.6056	-0.4819	-0.4213	-2.00000
-1.5787	-0.4735	-0.4485	-2.00000
-1.5515	-0.4656	-0.4745	-2.00000
-0.5255	-0.6144	-0.5007	-1.00000
-0.4993	-0.1412	-0.5429	-1.00000
-0.4571	-0.1159	-0.5307	-1.00000
-0.4593	-0.1063	-0.5264	-1.00000
-0.4736	-0.1204	-0.5237	-1.00000
-0.4763	-0.1290	-0.5279	-1.00000
-0.4721	-0.1350	-0.5324	-1.00000
-0.4676	-0.1361	-0.5404	-1.00000
-0.4596	-0.1366	-0.5468	-1.00000
-0.4532	-0.1347	-0.5553	-1.00000
0.0553	-0.2118	-0.5619	-0.50000
0.0619	0.0236	-0.5786	-0.50000
0.0786	0.0339	-0.5664	-0.50000
0.0664	0.0376	-0.5599	-0.50000
0.0599	0.0285	-0.5527	-0.50000
0.0527	0.0232	-0.5505	-0.50000
0.0505	0.0182	-0.5472	-0.50000
0.0472	0.0165	-0.5469	-0.50000

0.0469	0.0145	-0.5448	-0.50000
0.0448	0.0144	-0.5448	-0.50000
0.5448	-0.0652	-0.5431	0.00000
0.5431	0.1679	-0.5516	0.00000
0.5516	0.1758	-0.5313	0.00000
0.5313	0.1771	-0.5169	0.00000
0.5169	0.1656	-0.5019	0.00000
0.5019	0.1579	-0.4921	0.00000
0.4921	0.1507	-0.4812	0.00000
0.4812	0.1468	-0.4736	0.00000
0.4736	0.1425	-0.4642	0.00000
0.4642	0.1402	-0.4571	0.00000
0.4571	0.1370	-0.4484	0.00000
0.4484	0.1351	-0.4415	0.00000
0.4415	0.1322	-0.4332	0.00000
0.4332	0.1304	-0.4264	0.00000
0.4264	0.1277	-0.4184	0.00000
0.4184	0.1259	-0.4118	0.00000
0.4118	0.1233	-0.4042	0.00000
0.4042	0.1215	-0.3977	0.00000
0.3977	0.1191	-0.3904	0.00000
0.3904	0.1174	-0.3841	0.00000
0.3841	0.1151	-0.3771	0.00000
0.3771	0.1133	-0.3709	0.00000
0.3709	0.1112	-0.3642	0.00000
0.3642	0.1095	-0.3582	0.00000
0.3582	0.1074	-0.3518	0.00000
0.3518	0.1057	-0.3460	0.00000
0.3460	0.1037	-0.3398	0.00000
0.3398	0.1021	-0.3341	0.00000
0.3341	0.1002	-0.3282	0.00000
0.3282	0.0986	-0.3227	0.00000
0.3227	0.0969	-0.3170	0.00000
0.3170	0.0952	-0.3117	0.00000
0.3117	0.0935	-0.3061	0.00000
0.3061	0.0919	-0.3010	0.00000
0.3010	0.0903	-0.2957	0.00000
0.2957	0.0888	-0.2907	0.00000
0.2907	0.0872	-0.2856	0.00000
0.2856	0.0858	-0.2808	0.00000
0.2808	0.0842	-0.2758	0.00000
0.2758	0.0825	-0.2712	0.00000
0.2712	0.0813	-0.2664	0.00000
0.2664	0.0800	-0.2619	0.00000
0.2619	0.0786	-0.2573	0.00000
0.2573	0.0772	-0.2530	0.00000
0.2530	0.0759	-0.2485	0.00000
0.2485	0.0746	-0.2443	0.00000
0.2443	0.0732	-0.2400	0.00000
0.2400	0.0721	-0.2360	0.00000
0.2360	0.0708	-0.2319	0.00000
0.2318	0.0696	-0.2279	0.00000
0.2279	0.0684	-0.2239	0.00000
0.2239	0.0672	-0.2201	0.00000
0.2201	0.0660	-0.2163	0.00000
0.2163	0.0649	-0.2126	0.00000
0.2126	0.0638	-0.2089	0.00000
0.2089	0.0627	-0.2053	0.00000
0.2053	0.0616	-0.2017	0.00000
0.2017	0.0606	-0.1983	0.00000

0.1983	0.0595	-0.1948	0.00000
0.1948	0.0585	-0.1915	0.00000
0.1915	0.0575	-0.1882	0.00000
0.1882	0.0565	-0.1850	0.00000
0.1850	0.0555	-0.1818	0.00000
0.1818	0.0546	-0.1786	0.00000
0.1786	0.0534	-0.1755	0.00000
0.1755	0.0527	-0.1725	0.00000
0.1725	0.0518	-0.1696	0.00000
0.1696	0.0509	-0.1666	0.00000
0.1666	0.0500	-0.1638	0.00000
0.1638	0.0491	-0.1609	0.00000
0.1609	0.0482	-0.1592	0.00000
0.1582	0.0475	-0.1554	0.00000
0.1554	0.0466	-0.1528	0.00000
0.1528	0.0458	-0.1501	0.00000
0.1501	0.0451	-0.1475	0.00000
0.1475	0.0443	-0.1450	0.00000
0.1450	0.0435	-0.1425	0.00000
0.1425	0.0427	-0.1400	0.00000
0.1400	0.0420	-0.1376	0.00000
0.1376	0.0413	-0.1353	0.00000
0.1352	0.0406	-0.1329	0.00000



**Appendix B**

**PROGRAM BASE**

PROGRAM BASE

LOGICAL FIRST, DELAY  
CHARACTER\*6 ANSWER

WRITE(\*, 201)  
FORMAT(1X, 'PILOT NUMBER (S, 1, 2, 3, 4, N)')

202 READ (\*, 202), ANSWER  
FORMAT(A6)

A=1.4445  
B=7.4726  
C=.01  
J=1.0  
E=.3  
F=.15

AC= A\*C  
AD= A\*D  
AE= A\*E  
AF= A\*F  
BC= C\*C  
BD= B\*D  
BE= B\*E  
BF= B\*F  
CE= C\*E  
DE= D\*E  
CF= C\*F  
FC= F\*C  
FE= F\*E

RTDEG=7.3  
FIRST=.TRUE.  
DELAY=.FALSE.

OPEN(2, FILE='BASE.DAT', STATUS='OLD')  
WRITE(2, 101)  
WRITE(2, 103)

DO 100 I=1, 100

XJ=I/10.  
PHI=E\*XJ  
PHID=PHI\*RTDEG  
CP=CCS(PHI)  
SP=SIN(PHI)  
DENOM= C\*C\*XJ\*XJ+D\*D

IF(ANSWER.EQ.'B') THEN  
IF(FIRST)WRITE(\*, 301)  
FORMAT(1X, 'BASELINE')

301

XR=((AC-EC)\*XJ\*SP+(AC\*XJ\*XD+ED)\*CP)/DENOM  
XI=((AC-EC)\*XJ\*CP-(AC\*XJ\*XD+ED)\*SP)/DENOM

XMGT=SQRT(XR\*\*2.+XI\*\*2.)  
XPHT=ATAN2(XI, XR)

GOTO 401

```

302 ELSE IF(ANSWER.EQ.'1') THEN
    IF(FIRST)WRITE(*,302)
    FORMAT(1X,'PILOT 1')

    XRN=B
    XIN=A*X0

    XRD=D
    XID=C*X0

303 ELSE IF(ANSWER.EQ.'2') THEN
    IF(FIRST)WRITE(*,303)
    FORMAT(1X,'PILOT 2')

    XRN=(A*B*X0*X0+B)
    XIN=(A-B*B)*X0

    XRD=D
    XID=C*X0

304 ELSE IF(ANSWER.EQ.'3') THEN
    IF(FIRST)WRITE(*,304)
    FORMAT(1X,'PILOT 3')

    XRN=B
    XIN=A*X0

    XRD=D-C*B*X0*X0
    XID=(C+D)*X0

    ELSE IF(ANSWER.EQ.'4') THEN
    IF(FIRST)WRITE(*,305)
    FORMAT(1X,'PILOT 4')

    XRN=A*B*X0*X0+B
    XIN=(A-B*B)*X0

    XRD=D-F*C*X0*X0
    XID=(C+D*B)*X0

306 ELSE IF(ANSWER.EQ.'N') THEN
    IF(FIRST) THEN
    WRITE(*,306)
    FORMAT(1X,'NICHOLS PLOT DATA')
    DELAY=.TRUE.
    END IF

```

C OPTIMUM PILOT MODEL AT OMEGA = 2

C  $XRN = -135.9 * X0 * X0 + 250.1$

C  $XIN = 272.7 * X0$

C  $XRD = X0 * X0 * X0 * X0 - 429. * X0 * X0$

C  $XID = -104.2 * X0 * X0 * X0 + 299.9 * X0$

C BASELINE AIRCRAFT AND TIME DELAY

C  $XRN = 1.1376$

C  $XIN = .943 * X0$

```

C      XRD = -4.2*X0*XC
C      XID = 9.*X0 - XC*X0*X0

C      OPTIMUM PILOT MODEL AT OMEGA = 4

      RNO = 550.5
      RN1 = 503.2
      RN2 = 286.9

      RD4 = 1.
      RD3 = 104.2
      RD2 = 429.0
      RD1 = 899.8

      XRN = RNO - RN2*X0*X0
      XIN = RN1 *X0

      XRD = XC**4 - RD2*XC**2
      XID = RD1*XC - RD3*XC**3

      END IF

      XMGTN = SQRT( XPA**2.+XIN**2)
      XPHTN = ATAN2(XIN,XRN)
      XPHND = XPHTN*RTDEG

      XMGTD = SQRT( XAD**2.+XID**2)
      XPHTD = ATAN2(XID,XRD)
      XPHDD = XPHTD*RTDEG

      XMGT= XMGTN/XMGTD
      XPHT= XPHTN - XPHTD
      IF(DELAY) XPHT=XPHT-PHI

401  CONTINUE
      IF(FIRST) FIRST=.FALSE.
      XMG=20.*LOG10(XMGT)
      XPH=XPHT*RTDEG
      IF(ANSWER.EQ.'N')THEN
      IF(XPH.GT.0.) XPH=XPH-360.
      END IF

      WRITE(2,105) X0,XMG,XPH,XRN,XIN,XPHND,XRD,XID,XPHDD,PHI
      WRITE(*,102) X0,XMG,XPH

100  CONTINUE
      CLOSE(2)
101  FORMAT(7X,' OMEGA ',5X,' MAG(DEG)',2X,' PHASE (DEG) ',2X,' XRN ',
.2X,' XIN ',2X,' NUM ',2X,' XRD ',2X,' XID ',2X,' DEN ',2X,' PHI ')
102  FORMAT(1X,5F14.4)
105  FORMAT(1X,10F10.2)
103  FORMAT(1X)

      END

```

**FREQUENCY RESPONSE OF OPTIMAL PILOT MODEL  
USING THE ACTUAL TIME DELAY**

OMEGA	MAGNITUDE (DB)	PHASE (DEG)
0.0000	17.4697	0.0000
0.1000	17.4713	-0.6688
0.2000	17.4761	-1.3385
0.3000	17.4842	-2.0098
0.4000	17.4955	-2.6835
0.5000	17.5099	-3.3606
0.6000	17.5275	-4.0417
0.7000	17.5483	-4.7276
0.8000	17.5720	-5.4191
0.9000	17.5988	-6.1169
1.0000	17.6285	-6.8218
1.1000	17.6612	-7.5343
1.2000	17.6966	-8.2552
1.3000	17.7349	-8.9850
1.4000	17.7758	-9.7243
1.5000	17.8193	-10.4736
1.6000	17.8653	-11.2336
1.7000	17.9138	-12.0045
1.8000	17.9646	-12.7870
1.9000	18.0176	-13.5812
2.0000	18.0729	-14.3877
2.1000	18.1302	-15.2067
2.2000	18.1895	-16.0385
2.3000	18.2507	-16.8833
2.4000	18.3137	-17.7415
2.5000	18.3785	-18.6130
2.6000	18.4448	-19.4982
2.7000	18.5127	-20.3971
2.8000	18.5821	-21.3097
2.9000	18.6528	-22.2363
3.0000	18.7248	-23.1767
3.1000	18.7979	-24.1310
3.2000	18.8723	-25.0992
3.3000	18.9476	-26.0813
3.4000	19.0239	-27.0771
3.5000	19.1011	-28.0867
3.6000	19.1791	-29.1099
3.7000	19.2579	-30.1466
3.8000	19.3374	-31.1968
3.9000	19.4174	-32.2602
4.0000	19.4981	-33.3367
4.1000	19.5792	-34.4261
4.2000	19.6608	-35.5284
4.3000	19.7428	-36.6433
4.4000	19.8251	-37.7706
4.5000	19.9077	-38.9102
4.6000	19.9906	-40.0619
4.7000	20.0737	-41.2254
4.8000	20.1569	-42.4006
4.9000	20.2402	-43.5873
5.0000	20.3237	-44.7852
5.1000	20.4072	-45.9942
5.2000	20.4907	-47.2140
5.3000	20.5742	-48.4445
5.4000	20.6576	-49.6854
5.5000	20.7410	-50.9365
5.6000	20.8242	-52.1977
5.7000	20.9074	-53.4687

5.8000	20.9903	-54.7493
5.9000	21.0732	-56.0394
6.0000	21.1558	-57.3386
6.1000	21.2382	-58.6469
6.2000	21.3204	-59.9640
6.3000	21.4023	-61.2897
6.4000	21.4839	-62.6239
6.5000	21.5653	-63.9664
6.6000	21.6464	-65.3169
6.7000	21.7272	-66.6754
6.8000	21.8077	-68.0415
6.9000	21.8879	-69.4153
7.0000	21.9677	-70.7964
7.1000	22.0472	-72.1848
7.2000	22.1263	-73.5802
7.3000	22.2050	-74.9825
7.4000	22.2834	-76.3915
7.5000	22.3614	-77.8072
7.6000	22.4391	-79.2292
7.7000	22.5163	-80.6576
7.8000	22.5932	-82.0922
7.9000	22.6697	-83.5327
8.0000	22.7457	-84.9792
8.1000	22.8214	-86.4314
8.2000	22.8967	-87.8892
8.3000	22.9715	-89.3525
8.4000	23.0460	-90.8212
8.5000	23.1200	-92.2951
8.6000	23.1936	-93.7741
8.7000	23.2668	-95.2582
8.8000	23.3396	-96.7472
8.9000	23.4120	-98.2409
9.0000	23.4840	-99.7394
9.1000	23.5556	-101.2424
9.2000	23.6267	-102.7499
9.3000	23.6974	-104.2619
9.4000	23.7678	-105.7780
9.5000	23.8377	-107.2984
9.6000	23.9072	-108.8229
9.7000	23.9762	-110.3514
9.8000	24.0449	-111.8839
9.9000	24.1132	-113.4202
10.0000	24.1811	-114.9602



-  
**LIST OF REFERENCES**

- 1 Koehler, Ruthard DIPL.-ING, Buchacker, Ernst Dr.-ING,  
A Flight Test Method for Pilot/Aircraft Analysis.  
Flight Mechanics Branch, Institut FUR Flugmechanik  
Der DFVLR.
  
- 2 Enright, Randall M. Predicting Pilot Opinion -  
Ratings of Flying Qualities of Highly Control-  
Augmented Aircraft Using an Optimal Pilot Model.  
MS Thesis AFIT/GAE/AA/80D-3. School of Engineering, Air  
Force Institute of Technology (AFIT), Wright-Patterson  
AFB, Oh., December 1980.
  
- 3 Neal, Peter T. Smith, Rogers E., An In-Flight  
Investigation to Develop Control System Design  
Criteria for Fighter Airplanes. AFFDL-TR-70-74,  
Volume I, Wright-Patterson Air Force Base, Ohio: Air  
Force Flight Dynamics Laboratory, December 1970.
  
- 4 George, Frank L., Outline: A Classical Control  
Theory Pilot Model. AFWAL/FIGC Wright-Patterson  
AFB, Ohio.
  
- 5 Ogata, Katsuhiko Modern Control Engineering.  
Englewood Cliffs, N.J., Prentice-Hall, Inc.,  
1970.
  
- 6 Franklin, Gene F., Powell, David J. Digital  
Control of Dynamic Systems. TJ216.F72 1980.
  
- 7 Ogata, Katsuhilo, Discrete Time Control Systems.  
Prentice-Hall, Inc., 1987.
  
- 8 MATRIX<sub>x</sub> Users Manual.
  
- 9 Reid, Gary J., Linear System Fundamentals.  
Continuous and Discrete. Classic and Modern. McGraw-  
Hill, Inc., 1983.

10 Hess, R.A., Mnich, M.A., "Identification of Pilot-Vehicle Dynamics from In-Flight Tracking Data," Journal of Guidance and Control, Vol. 9, No. 4, July-August 1986.

11 Biezd, D.J., Sturmer, S.R., Test Pilot Evaluation of the Closed-Loop "Grate" Flight Test Technique, August 1986.

12 Biezd, D.J., Pilot Comments Recorder During Grate Simulation Testing.

13 Total, Interactive Software Package, AFIT.

**Vita:- Michael J. Rosenbleeth**

Michael J. Rosenbleeth was born in Vineland, New Jersey on November 20, 1955. He graduated high school in 1974 from Clay High School in Oregon, Ohio. In December of 1976 he enlisted in the United States Air Force. Three cold years were spent in the missile fields of North Dakota before being accepted into the Airmen's Education and Commissioning Program. In December of 1982 he received a Bachelor of Science degree in Aerospace Engineering from Texas A&M University, and a commission as a Second Lieutenant. Upon commissioning he was assigned to the Air Force Wright Aeronautical Laboratory, Flight Dynamics Laboratory where he worked for three years as a Simulation Development Engineer. In 1986, he was selected for Admission to the Air Force Institute of Technology, which he entered in June of that year. He graduated with the Master of Science degree in Aeronautical Engineering, specializing in Stability and Control, in December 1987.

This thesis was typed by Miss Shirley Miller.

## REPORT DOCUMENTATION PAGE

Form Approved  
OMB No. 0704-0188

## 1a. REPORT SECURITY CLASSIFICATION

Unclassified

## 1b. RESTRICTIVE MARKINGS

## 2a. SECURITY CLASSIFICATION AUTHORITY

## 2b. DECLASSIFICATION/DOWNGRADING SCHEDULE

## 3. DISTRIBUTION/AVAILABILITY OF REPORT

Approved for Public Release;  
Distribution Unlimited

## 4. PERFORMING ORGANIZATION REPORT NUMBER(S)

AFIT/GAE/AA/87D-19

## 5. MONITORING ORGANIZATION REPORT NUMBER(S)

Air Force Institute of Technology (AFIT/ENA)

## 6a. NAME OF PERFORMING ORGANIZATION

Air Force Institute of Technology (if applicable)  
(AFIT-ENA)WPAFB, OH 45433

## 6b. OFFICE SYMBOL

(if applicable)

## 7a. NAME OF MONITORING ORGANIZATION

## 6c. ADDRESS (City, State, and ZIP Code)

## 7b. ADDRESS (City, State, and ZIP Code)

## 8a. NAME OF FUNDING/SPONSORING ORGANIZATION

NASA/DRYDEN

## 8b. OFFICE SYMBOL

(if applicable)

## 9. PROCUREMENT INSTRUMENT IDENTIFICATION NUMBER

## 8c. ADDRESS (City, State, and ZIP Code)

## 10. SOURCE OF FUNDING NUMBERS

PROGRAM  
ELEMENT NO.PROJECT  
NO.TASK  
NO.WORK UNIT  
ACCESSION NO.

## 11. TITLE (Include Security Classification)

Realtime Pilot Model Parameter Identification

Approved for Release: LAW AFR 190-17  
 LYNN E. WILSON 31 Dec 87  
 Dean for Research and Professional Development  
 Air Force Institute of Technology (AFIT)  
 Wright-Patterson AFB OH 45433

## 12. PERSONAL AUTHOR(S)

Michael J. Rosenbleeth, Captain, USAF

## 13a. TYPE OF REPORT

MS Thesis

## 13b. TIME COVERED

FROM May 86 TO Dec 87

## 14. DATE OF REPORT (Year, Month, Day)

87 Dec 19

## 15. PAGE COUNT

63

## 16. SUPPLEMENTARY NOTATION

## 17. COSATI CODES

FIELD

GROUP

SUB-GROUP

01

04

## 18. SUBJECT TERMS (Continue on reverse if necessary and identify by block number)

Pilot Modeling

Identification

Flying Qualities, Discretization Techniques

## 19. ABSTRACT (Continue on reverse if necessary and identify by block number)

An air to ground test technique was simulated on the Flight Dynamics Laboratory's LAMARS simulation system. Data was recorded on longitudinal stick deflection and longitudinal pipper errors. The data was used to identify pilot model parameters using the Recursive Least Squares (RLS) Algorithm. Several different pilot models and discretization techniques are used to determine which method is best suited to this task. Neal-Smith Theory is used to predict a range of pilot model parameters to be expected from RLS identification. Pilot model parameters are identified using three aircraft with different time delays. The identified pilot model parameters and pilot ratings are compared to see if a correlation exist. The specific values of pilot model parameters predicted by Neal-Smith Theory were not identified. However, trends in the pilot model parameters predicted by Neal-Smith Theory, for aircraft of increasing time delay, can be observed in the identifications.

## 20. DISTRIBUTION/AVAILABILITY OF ABSTRACT

☒ UNCLASSIFIED/UNLIMITED ☐ SAME AS RPT. ☒ DTIC USERS

## 21. ABSTRACT SECURITY CLASSIFICATION

Unclassified

## 22a. NAME OF RESPONSIBLE INDIVIDUAL

Michael J. Rosenbleeth

## 22b. TELEPHONE (Include Area Code)

(513) 429-5853

## 22c. OFFICE SYMBOL

AFIT/ENA

END

FILMED

MARCH, 19 88

DTIC